A TALE OF TWO:

RECONSTRUCTING CLIMATE FROM TREE-RINGS OF THE NORTH AEGEAN, AD 1089-1989,

AND

LATE PLEISTOCENE TO PRESENT:

DENDROCHRONOLOGY IN UPSTATE NEW YORK

A Dissertation

Presented to the Faculty of the Graduate School

of Cornell University

In Partial Fulfillment of the Requirements for the Degree of

Doctor of Philosophy

by

Carol Bliss Griggs

May 2006

A TALE OF TWO: RECONSTRUCTING CLIMATE FROM TREE-RINGS OF THE NORTH AEGEAN, AD 1089-1989, AND LATE PLEISTOCENE TO PRESENT: DENDROCHRONOLOGY IN UPSTATE NEW YORK

Carol Bliss Griggs, Ph.D.

Cornell University 2006

In the first two chapters, oak samples from the north Aegean (39-42ºN, 22-37ºE) are used in dendroclimatological research. In the first chapter, the precipitation of May and June is shown to be the primary limiting factor in annual ring growth and is reconstructed from a tree-ring chronology of historic building and modern forest samples, AD 1089 to 1989. Removing all but the high-frequency variability plus normalizing the oak data sets gives an accurate regional precipitation reconstruction.

The low-frequency variance in the same chronology filtered with a 24-kernel Gaussian filter explains 91.6% of the variance in the filtered North Atlantic Oscillation (NAO) May index, 1915-1967, but not before that period. In the second chapter, the oak chronology is divided into three grids, west to east. The May NAO is recorded in the western grid chronology from 1833-1967. Using the similarities and differences in the three grids' filtered oak chronologies over time as indicators of the effect of the May NAO on the region, the low-frequency May NAO is reconstructed for AD 1181 to 1967.

The third and fourth chapters examine the tree-ring record of samples collected in New York State (41-45ºN, 73-80ºW). Over 30 tree-ring chronologies that represent various windows of time from 15,000 years ago to the present have been constructed from tree-ring measurements of wood collected from six modern woodlands, seven historical structures and timbers, and eight river, stream, and pond sediments. Chapter 3 focuses on the oldest samples dating from the late Pleistocene Epoch, including wood sections found in three mastodon excavations in New York State. The oldest

wood macrofossils are spruce and their respective radiocarbon dates reflect the southeast to northwest retreat of the ice sheet and subsequent migration of arboreal species across New York State.

Chapter four is a compendium of the collected wood samples from the Holocene Epoch. Regional modern and historic chronologies date from AD 1625 to 2004 for oak, AD 1593 to 2003 for hemlock, and AD 1681 to 1848 for pine. Floating chronologies date throughout the Holocene, from *ca.* 9500 BC to the mid-fourteenth century AD.

BIOGRAPHICAL SKETCH

Carol Bliss Griggs graduated from Cornell University in 1977 with B.A. in Anthropology and Archaeology. She worked for the Aegean Dendrochronology Project at Cornell University as its first supervisor from 1978 to 1979, then returned to school at the University of Maine at Orono. She graduated from there in 1983 with an M.S. in Quaternary Studies, an interdisciplinary study including Archaeology, Geology and Paleoecology. Her thesis title is "The Impact of Environment on Tree-Ring Growth in One Climate Region in Maine."

After a short hiatus from tree-ring research, including marrying William Griggs in 1985, she returned to the Aegean Dendrochronology Project in 1986 and worked as a Research Support Specialist from 1986 to 1992. In 1992 her daughter Katie was born, allowing another hiatus of 5 years of fun with a growing child. In 1998 she returned to work at the ADP, which in 1991 had become the Malcolm and Carolyn Wiener Laboratory for Dendrochronology of the Aegean and Near East.

In 1999 she participated in the first excavation of one of the three mastodon sites included in this research and became fascinated with the quantities of wood that were found along with the bones and other material. The collection and early radiocarbon dates of the samples pulled her in 2001 into working towards her Ph.D. in Geology with the use of that recovered wood plus all the archives of the ADP.

This work is dedicated to my family: husband Bill and daughter Katie who have coped with great patience, encouragement, and support through the days, weeks, months, and years involved in this research. Stepsons Tom, Mike, and Fran, and all their respective families are also thanked for their continuing encouragement. I especially thank my parents, Jane and Ted Bliss, for their never-ending moral support.

Appreciation and gratitude are due to many, many, other people. One group includes my fellow grad students, and the faculty and staff of the Department of Earth and Atmospheric Sciences at Cornell. In particular many thanks are due to Warrren Allmon for his advice, enthusiasm for my research, and for taking the position of my advisor and committee chairman in lieu of Art Bloom. Thanks are due also to John Chiment and Joan Ramage who got me started in the mastodon wood collection and for John's help with many collecting trips at a moment's notice. To Art Bloom, who put me on the Quaternary path many years ago, I give thanks for all his advice, support, and editing. We still need to get out and collect more wood from Coy Glen, Art! And finally to Art DeGaetano, an advisor and mentor of the dendroclimatological aspect of this research. He has been an immense help in guiding me along the rigorous path of proving speculations. I trust that our collaboration will continue.

A second group is the Aegean Dendrochronology Project director, personnel, and students. Director Peter Kuniholm has played a major part in my life from my initial dendrochronological training in my undergraduate years, through quasi-continual support at the lab, and always as an advisor and mentor. The ADP is his baby and his collection and direction of the archival of the tree-ring

samples is outstanding. It has been a joy for me to help the project grow. Many thanks also go to Mary Jaye Bruce, Maryanne Newton, and all the ADP research supervisors and students that have measured and analyzed the tree-ring data over the years. Also thanks go to Bernd Kromer and Sahra Talamo for their radiocarbon analysis, and to Sturt Manning, on the brink of assuming the ADP's directorship, for his continuing encouragement.

ACKNOWLEDGMENTS

Chapters one and two:

The Malcolm and Carolyn Wiener Laboratory for Aegean and Near Eastern Dendrochronology at Cornell University is supported by the National Science Foundation, BCS-0314282 and SBR-9905389, the Malcolm H. Wiener Foundation, and individual Patrons of the Aegean Dendrochronology Project. Ed Cook and the Lamont-Doherty Tree-Ring Laboratory provided consultation; Keith Briffa, Mike Baillie, and Jon Pilcher all encouraged this research at its infancy. For climate data sets and answers to technical questions we acknowledge Mike Hulme, Phil Jones, and the Climatic Research Unit; Ramzi Touchan and associates; Rosanne D'Arrigo and Heidi Cullen; Ünal Akkemik and colleagues; Jim Hurrell, Stephen Gray and associates; Juerg Luterbacher, Eleni Xoplaki, and associates; and the National Oceanic and Atmospheric Administration. For the precipitation data, the gu23wld0098.dat (Version 1.0) was constructed and supplied by Dr. Mike Hulme at the Climatic Research Unit, University of East Anglia, Norwich, UK. Their work was supported by the UK Department of the Environment, Transport, and the Regions (Contract EPG 1/1/85).

Chapters three and four:

Acknowledgments are due to John Chiment, mastodon excavation crews, landowners, and many others for their help in collecting wood samples and for alerting me about old buildings and buried wood. They are also due to Drs. Art Bloom, Norton Miller, and Richard Laub for their comments and insight into the late Pleistocene Epoch in New York State. Radiocarbon dates were funded by the

Eppley Foundation and the Paleontological Research Institution and analyzed by Drs. Bernd Kromer and Sahra Talamo at the Heidelberg Laboratory, Heidelberg, Germany, and colleagues at the Beta Analytic Laboratory, Miami, Florida, USA. Thanks to the Malcolm and Carolyn Wiener Laboratory for Aegean and Near Eastern Dendrochronology, Cornell University, under the direction of Dr. Peter Kuniholm, for use of its tree-ring measurement equipment, analysis software, and the funding of one radiocarbon date.

TABLE OF CONTENTS

LIST OF FIGURES

LIST OF TABLES

CHAPTER ONE

A REGIONAL RECONSTRUCTION OF MAY-JUNE PRECIPITATION IN THE NORTH AEGEAN FROM OAK TREE RINGS, AD 1089-1989

by Carol Bliss Griggs, Arthur T. DeGaetano,[1] Peter Ian Kuniholm,[2] and Maryanne W. Newton[2]

SUMMARY

May-June precipitation is the primary limiting factor in annual tree-ring growth of the oaks of northeastern Greece and northwestern Turkey (39-42º N, 22-37º E). In a regional tree-ring chronology of historic building and modern forest samples, the May-June precipitation explains at least 40.6% of the variance for 1900-1985, and is here reconstructed from AD 1089 to 1989. The reconstruction is compared to existing precipitation reconstructions for Turkey. The mean temperature of May and June is also a growth-limiting factor due to its effect on the availability of precipitation to the trees, but is more difficult to calibrate and reconstruct accurately due to the trees' indirect response and the low number of long temperature records available for the interior of northwestern Turkey.

An analysis of various methods of manipulating oak tree-ring data for regional climate reconstruction shows that removing all but the high-frequency variability plus normalizing the oak data sets before combining them into a master chronology are optimal techniques for an accurate precipitation reconstruction of the entire area. However, these methods do remove the low-frequency signal and dampen some of the evidence of local extremes in May-June precipitation. This issue will be addressed in future research.

[1] Earth and Atmospheric Sciences, 1119 Bradfield Hall, Cornell University, Ithaca, NY 14853.
[2] The Malcolm and Carolyn Wiener Laboratory for Aegean and Near Eastern Dendrochronology, B48 Goldwin Smith Hall, Cornell University, Ithaca, NY, 14853.

INTRODUCTION

The common signal recorded in tree-ring patterns from Turkey, Greece, and surrounding countries is the basis for dating wood from historical and archaeological sites at the Malcolm and Carolyn Wiener Laboratory for Aegean and Near Eastern Dendrochronology at Cornell University. Analyses of an oak tree-ring chronology of forests and historic sites covering most of the 2nd millennium AD indicate that the primary growth-limiting climate factor recorded in their common signal is the total precipitation of May and June, the period in which most of the growing-season rainfall occurs in this region.

Oak tree-ring chronologies have been analyzed for possible climate signals over much of the temperate species' ranges in the northern hemisphere, but the oaks' growth response to limiting climate factors has been difficult to quantify.[3] The oaks in this study are growing in a sub-humid mesothermic climate[4] at the southern boundaries of the geographic ranges of the included forest species.[5] The limited precipitation of the growing season, and what is available to the trees from that amount, is critical to the oaks' cambial activity[6] and thus to the widths of the annual rings.

The use of historical and archaeological tree-ring data as paleoclimate proxy data is currently under intense scrutiny here and in other regions.[7] Two critical issues are that the samples were collected for a non-dendroclimatic purpose, and that there is generally no record of the source of the timber. The location of each sample on its parent tree, including compass direction and height on the bole, plus each tree's immediate environment are impossible to discern for the historic sites' timbers, and

[3] Pilcher 1995; Kelly et al., 2002; Wilson and Elling 2004; García-Suárez 2005.
[4] Zohary 1973, v.1.
[5] Davis 1982.
[6] Akkemik et al., 2005; Kramer and Kozlowski 1979.
[7] Wilson et al., 2004; Esper et al., 2002, 2003; Kelly et al., 2002.

only to a limited degree in the forest sites where we often have collected from stacks of freshly logged timber. The secure crossdating of the samples, both within and between sites, the number of samples, and the large area of the study region offset both issues and justify the use of our oak chronology as proxy data.[8]

Previous research using modern oak, pine, juniper, and cedar chronologies in the Mediterranean region has shown that wide (narrow) rings correspond to signature years of high (low) precipitation,[9] and that signature growth years correspond to persistent anomalies in atmospheric circulation patterns.[10] March to June precipitation has been reconstructed from a single site collection of oak samples in the north central region of Turkey, 1635-2000;[11] February through June precipitation has been reconstructed for Sivas, Turkey, 1628-1980 from chronologies of 5 different species from around Turkey including one that is used here;[12] and the May-June precipitation has been reconstructed for 1323-1998 from juniper and for 1776-1998 from juniper, pine, and cedar samples from southwestern Turkey.[13] Their reconstructions are compared to ours in the discussion section.

THE REGION

Geography and climate

The area of northeastern Greece and northwestern Turkey (39 to 42º N latitude 22 to 37º E longitude) was selected as the study region from the locations of seven sampled oak forest sites and the high number of oak samples collected from many buildings in that region (Figure 1.1; Table 1.1). The area was also subdivided into

[8] Fritts 1976; Cook and Kairiukstis 1989.
[9] Gassner and Christiansen-Weniger 1942.
[10] Hughes et al., 2001.
[11] Akkemik et al., 2005.
[12] D'Arrigo and Cullen 2001.
[13] Touchan et al., 2003.

three grids from west to east. The western grid is composed of the Thessaloniki-Larisa area east of the Pindus Mountains and extending eastward along the north side of the Aegean Sea (G1 at 22-26ºE); the center grid includes the east Aegean and Marmara Sea Transition regions, a more coastal environment (G2 at 26-32ºE); and the eastern grid is composed of the interior of the Black Sea ecoregion plus a small part of Inner Anatolia (G3 at 32-37ºE, Figure 1.2).[14] The entire area has very low summer precipitation (July-August) and during the rest of the year has fairly constant precipitation in the outer regions with the highest variation in the center grid where the winter months have the highest precipitation (Figure 1.2).

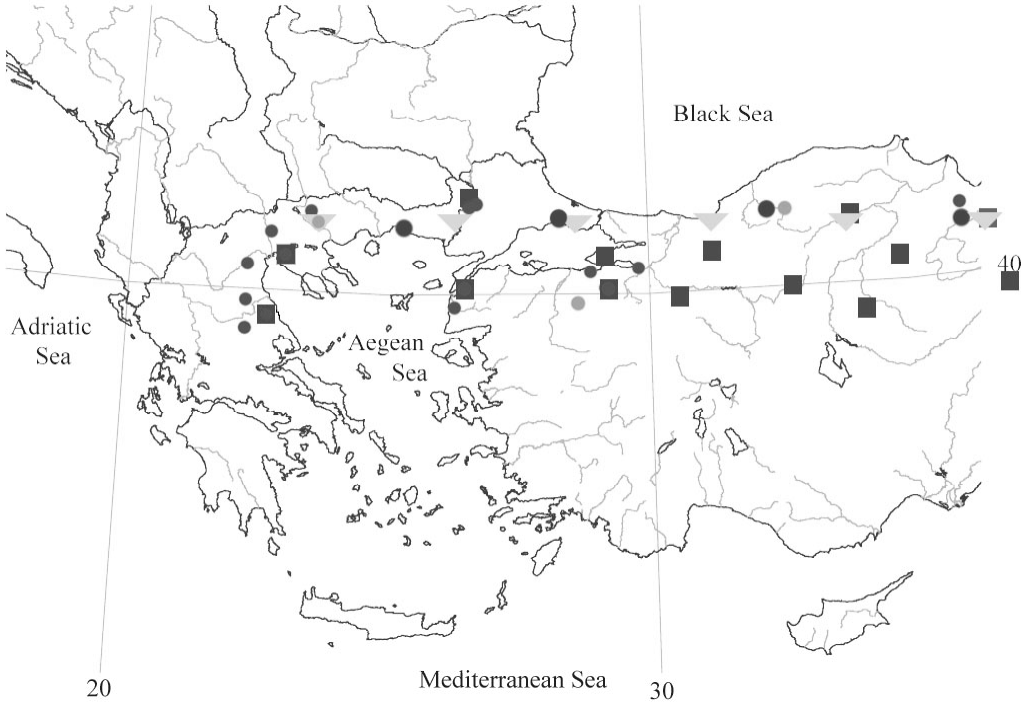

Figure 1.1. A map of the location of the forest (dark circles), historic sites (light circles), meteorological stations (squares) and centers of the CRU climate data grids (triangles) are shown here.

[14] Atalay 2002; Xoplaki 2002.

Table 1.1. The historic and forest site locations plus chronology dates, lengths, number of samples, and average correlation coefficients (*r*) between samples. (Continued on the next two pages.)

Grid	Lat °N	Long °E	Region or City	Site Name	Subdivision	Chronology Begins	Chronology Ends	Length	No. of samples	Average *r* values
	Greece									
	39.47	22.07	Karditsa	Palamas, Hg. Athanasios		1647	1809	163	13	0.393
	39.47	22.07	Elasson	Panaghia Olympiotissa		1214	1335	122	7	0.346
	40.52	22.18	Verroia	Holy Apostles (Old Metropolitan)		1758	1889	132	3	0.414
				Palatitsa, Hg. Demetrios		1628	1780	153	2	0.473
				Tou Christou		1240	1327	88	4	0.468
	39.72	22.73	Larisa	Aghia, Hg. Panteleimon		1358	1476	119	5	0.422
	40.62	22.92	Thessaloniki	Hg. Antonios		1570	1828	257	7	0.346
				Hg. Georgios (Rotonda)	Early	1207	1318	112	2	0.470
					Late	1662	1827	166	5	0.361
					Middle 1	1518	1588	71	2	0.484
					Middle 2	1350	1518	169	2	0.385
				Hg. Aikaterini		1155	1315	161	5	0.400
1				Hg. Demetrios		1337	1519	183	3	0.502
				Holy Apostles	Byzantine	1170	1329	160	6	0.433
					Turkish porch	1247	1490	244	3	0.380
				Heptapyrgion (Yedikule)		1373	1431	59	2	0.662
				Hg. Sophia		1355	1521	167	7	0.420
				Nikolaos Orphanos	Early	1257	1458	202	1	-----
					Late	1614	1811	198	2	0.341
				Nea Panaghia		1557	1832	276	26	0.276
				Frourio Vardari (Octagonal Tower)		1478	1597	120	14	0.331
				Metamorphosis Soter		1630	1773	144	3	0.359
				Vlatadon Monastery	Early	1199	1339	141	24	0.365
					Late	1557	1800	244	21	0.309
				White Tower	Early	1211	1535	325	11	0.272
					Late	1567	1847	281	14	0.345

Table 1.1 (Continued).

Grid	Lat °N	Long °E	Region or City	Site Name	Subdivision	Chronology Begins	Chronology Ends	Length	No. of samples	Average *r* values
1, cont.	41.22	23.37	Thrace	Sidherokastro		1207	1327	121	4	0.367
	41.08	23.52	Serres	Prodromos Monastery	Early	1199	1345	147	6	0.282
					Late	1377	1497	121	6	0.431
				Serres, Orestes Tower		1211	1323	113	3	0.413
				Serres, Mehmet Bey Mosque		1322	1489	168	7	0.503
				Serres, Zincirli Mosque		1406	1492	87	3	0.523
	40.47	23.57	Chalkidiki	Arnaia, Barbara, Koutri Chorafi Forest		1740	1979	240	10	0.296
	41.23	25.42	Livadia	Komotini, Paterma Forest		1840	1979	140	12	0.355
2	**Greece**									
	41.35	26.47	Didymoteichon	Didymoteichon, Vayazit Mosque		1186	1495	310	30	0.305
	41.38	26.60	Pythion	Pythion Castle		1209	1331	123	5	0.243
	Turkey									
	39.87	26.20	Çanakkale	Üvecik, Cezayirli Hasan Paşa Köşkü		1627	1782	156	5	0.416
	40.13	26.40		Kilid ul-Bahir Castle		1295	1462	168	21	0.311
	41.13	28.45	İstanbul	Belgrade Ormanı (forest)		1769	1985	217	26	0.319
	39.92	28.55	Bursa	Devecikonağı Forest		1773	1985	213	19	0.238
	40.38	28.78		Mudanya, Tirilye, Kemerli Kilise		1198	1336	139	8	0.306
	41.02	28.97	İstanbul	Kariye Camii	Late	1189	1308	120	12	0.372
				Beyoğlu, Karaköy Vapur İskelesi	Black Sea	1602	1852	251	4	0.234
					Thrace	1721	1857	137	8	0.354
				Ayasofya	Bannister	1394	1581	188	8	0.342
					NW Buttress	1188	1332	145	8	0.350
					Türbe	1356	1615	260	7	0.334
	40.18	29.07	Bursa	I. Murat Hüdavendiğâr Camii		1111	1384	274	7	0.359
	40.43	29.72	Bilecik	İznik, Elbeyli, Mara Camii		1398	1554	157	6	0.194
				İznik, Nilüfer İmareti		1136	1375	240	6	0.353
				İznik, Hg. Sophia		1081	1241	161	4	0.350
	40.23	30.00	Bilecik	Vezirhan		1526	1657	132	4	0.382

Table 1.1 (Continued).

Grid	Lat °N	Long °E	Region or City	Site Name	Site Division	Chronology Begins	Chronology Ends	Length	No. of samples	Average *r* values
	Turkey									
	41.20	32.28	Zonguldak	Yenice, Bakraz Forest		1623	1984	362	10	0.327
3	41.42	32.67		Karabük, Büyükdüz Forest		1699	1985	287	10	0.390
	41.08	36.05	Samsun	Kavak, Çakallı Forest		1835	1989	155	17	0.386
	41.08	36.15	Samsun	Kavak, Bekdemirköy, Cami		1089	1875	787	41	0.373
						Totals:		**10576**	**511**	
						Averages:		**189**	**9**	**0.370**

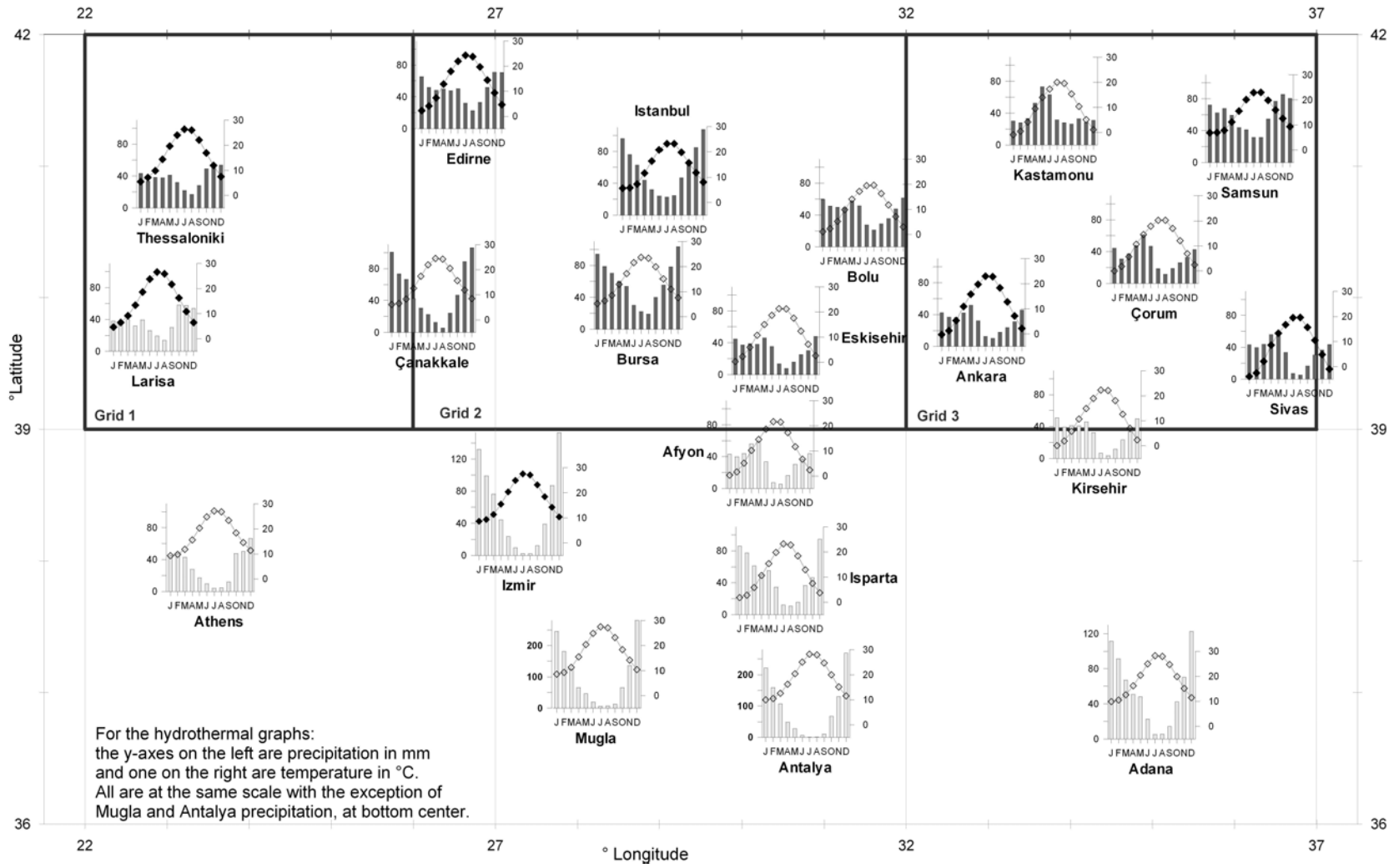

Figure 1.2. Hydrothermal graphs of the data from the meteorological stations. Filled bars and diamonds are the stations whose data are used here.

The May-June average precipitation ranges from 56 to 136mm (average 84mm), with an increase from west to east (Figure 1.2). The average values are smaller than the May-June precipitation immediately along the Black Sea coast (67 to 230mm, average 108mm) and higher than that along the Mediterranean coast (27 to 66mm, average 49mm).

DATA AND METHODS

The Tree-Ring Data

Our 511 tree-ring sections and cores come from seven modern forest and 49 historic building chronologies. The historic chronologies are from 38 buildings, eight of which have two or more building phases or different timber sources (Figure 1.3 and Table 1.1).[15] The ring counts of the historic segments range from 39 to 357 rings (average 116) and the forest segments from 61 to 362 rings (average 156). Site chronologies range from 59 to 787 (average 194) years in length (Figures 1.3 and 1.4).

There is no reliable way to distinguish oak species from wood anatomy alone.[16] Seven oak species were identified in five of the seven forests (Table 1.2). They are all deciduous oak species from the subgenus *Quercus* Oersted[17] and grow in Euxinian and sub-Euxinian mesic sites at elevations ranging from 20 to 1300 meters above sea level.[18] The southern boundaries of most of the included species' ranges are within the study region due to the sub-humid climate. This is a good indicator that the limited precipitation available to the trees is a major factor, overriding the issue that different species' limiting growth factors can be different climate parameters.[19]

[15] Kuniholm 2000, 1994a; Kuniholm and Striker 1987, 1983.
[16] Huber and von Jazewitsch 1956, p.29; Pilcher 1995.
[17] Schweingruber 1990.
[18] Davis 1982.
[19] Wilson and Elling 2004; Kelly et al., 2002; Baillie 1982, 1995.

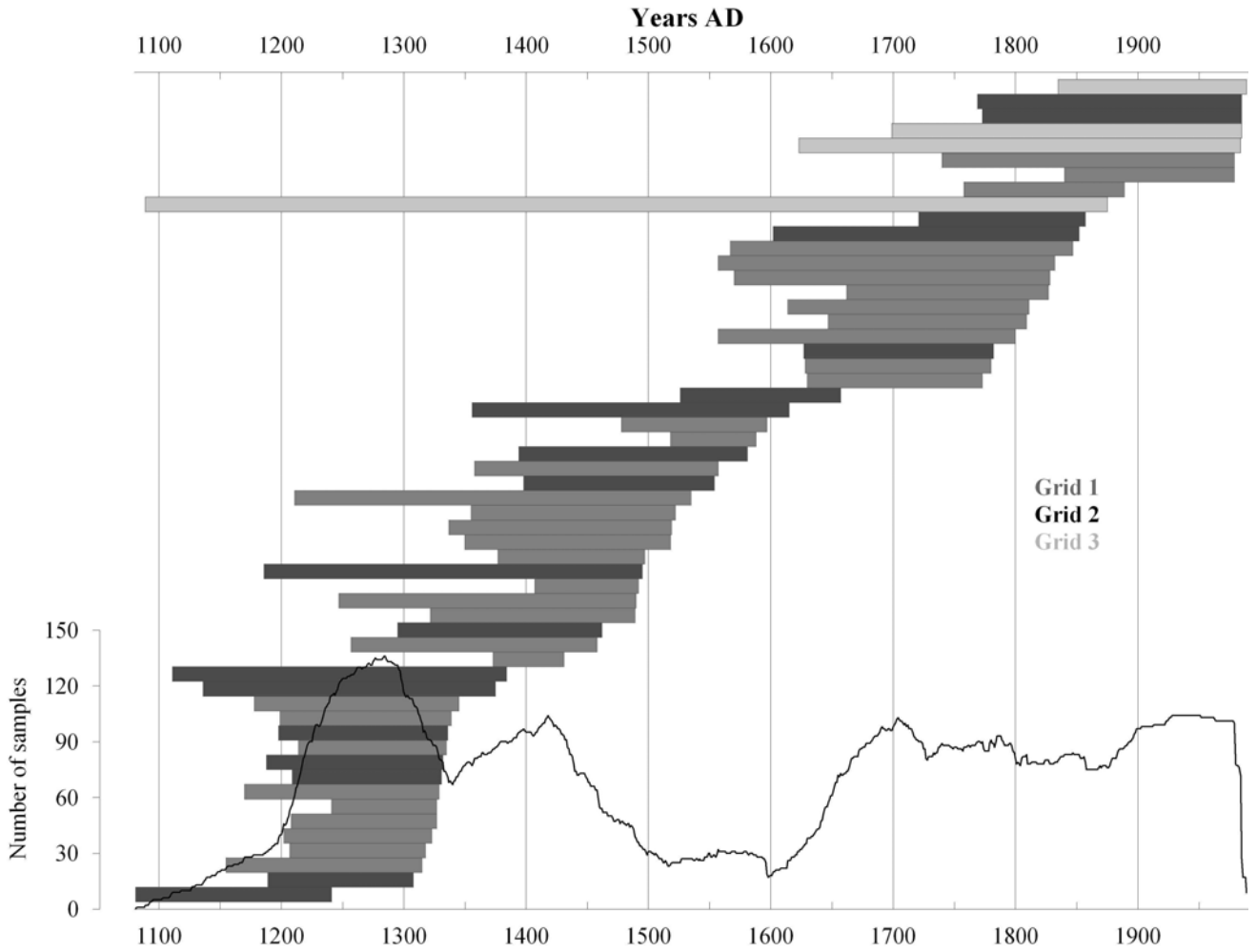

Figure 1.3. The historic and forest chronologies, their placement in the grids, and the number of samples over time. The grid locations of the forest and historic buildings are indicated by their colors. See Figure 1.1 and Table 1.1 for site locations.

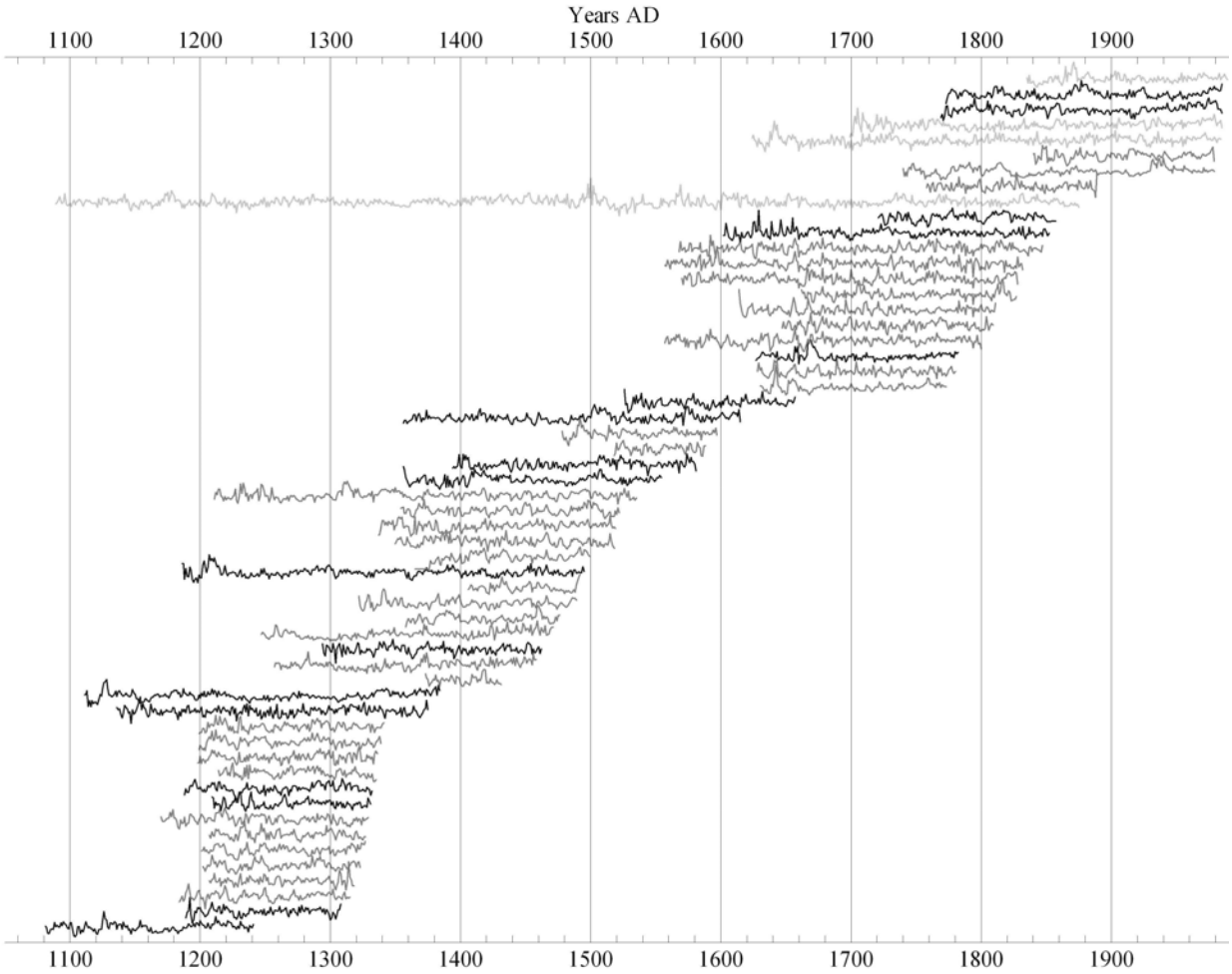

Figure 1.4. The time series of the 56 site chronologies used in the regional chronology and indicated in the bar graph in Figure 1.3. The medium gray lines are the chronologies from the Grid 1, the black lines from Grid 2, and the light gray lines from Grid 3.

Table 1.2. The oak species reported at five of the seven forest sites. All are deciduous, temperate-climate species (see text). *In both cases the foresters were using "macar meşesi," Hungarian oak, a common name of *Q. frainetto* (Davis 1982, Yaltırık 1984).

Grid	Lat N	Long E	Elev (m)	Region	Forest	*Quercus* species
1	40.47	23.57	600	Chalkidiki	Arnaia, Koutri Forest	*Q. frainetto (=Q. conferta*)
1	41.23	25.42	400-450	Paterma	Komotini, Livadia Forest	*Quercus sessiliflora* and *Q. robur*
2	41.13	28.45	70-140	İstanbul	Belgrade Forest	*"Q. hungarica"**
						Q. frainetto
						Q. petraea iberica (= *Q. dschoruchensis*)
2	39.92	28.55	550-950	Bursa	Devecikonağı Forest	*Q. petraea*
						Q. robur
						*"Q. hungarica"**
3	41.20	32.28	600-1100	Zonguldak	Yenice, Bakraz Forest	*Q. hartwissiana*
3	41.42	32.67	900	Zonguldak	Karabük, Büyükdüz Forest	*Q. petraea iberica* (= *Q. dschoruchensis*)
						Q. petraea petraea (= *Q. sessiliflora*)
3	41.08	36.05	500-750	Samsun	Kavak, Çakallı Forest	*Quercus* genus only

We assume that most of the historic samples' species are included in the forest species list. A secure crossdating between sites indicates that the historic sites' species contain the same common signal. The locations of the historic buildings, the secure crossdating between samples and chronologies, and the paucity or complete absence of oak samples from buildings outside the study area in southern Turkey imply that the timbers used in their construction were from local oaks, and that they are all mesothermic species.[20] If the samples are of different oak species, then those species' growth responses are very similar to the forest species' response, or the tree-ring patterns could not have been securely crossdated.

Oak ring-width variability is low relative to conifers and diffuse ring-porous angiosperms due to the minimum width of the necessary springwood vessels each year, approximately 0.30mm in our samples. The vessels grow before the new leaves open in the spring,[21] using the reserved material from the previous growth season to produce the needed cells. Thus the previous year's climate parameters are possible growth-limiting factors. Pilcher found that the spring temperature of the year-before-growth correlated significantly with the earlywood widths, but not high enough to reconstruct the temperature.[22] The part of the ring growth that varies the most is the latewood, growing after the leaves are established, generally from May through the summer for as long as the moisture is sufficient for secondary cambial activity.

Our data do not represent the full range of tree-ring widths in the oaks due to the requirement of at least 50 rings (estimated ring count) in each sample for secure crossdating purposes. Samples with fewer than 60 rings are not included here unless they contain unique signature patterns for particular years. Therefore samples with low ring count, generally due to large ring-widths over extended periods, are absent

[20] Davis 1982; Zohary 1973.
[21] Pilcher 1995.
[22] Pilcher and Gray 1982.

and our ring-width measurements are in the middle to low range of ring widths of all oak ring growth, similar to the ring-widths in the historic samples of Norway spruce noted in Wilson et al.[23]

The historic wood has no provenance other than the buildings' locations: in our regional context this is not important.[24] The buildings' locations and the more secure crossdating between site chronologies within each of the three grids imply that there was little or no transportation of oak timbers from very far outside the study region. In larger cities, such as Thessaloniki and Istanbul, transport may have been necessary at the times of extensive building, especially in the early 14th, late 15th to early 16th, and late 18th to early 19th centuries, but the correlations between the included chronologies of each city area do not indicate long-distance transport to any great extent. Oak forests are still located around the region today, albeit in smaller numbers. The dendrochronology of historic buildings such as Haghia Paraskevi, a Gothic (*i.e.* Frankish) church in Chalkis, Greece,[25] that was constructed of alpine larch is the exception that 'proves' the rule. Any chronology from such a building is not included in the regional chronology since it does not crossdate with the other local site chronologies.

At each forest site at least 10 sections were collected from forest timbers or stumps. At the historical sites, sections and cores were collected in whatever quantity was available. The sites' samples are combined into site chronologies (Table 1.1). Seven historical sites have more than one site chronology from different building phases. One other site with one building phase has possibly two species of oak and/or sources of timber represented in its samples, and its data were split into two site chronologies.

[23] Wilson et al., 2004.
[24] Kelly et al., 1989.
[25] Hammond 2005; Kuniholm 2004b.

Two or more radii are measured from samples with visible differences in ring widths around the circumference of a section or in radii on a core, otherwise one radius is measured. The rings of each radius are measured twice, in hundredths of millimeters. The two sets of measurements are then reconciled to at least 97% accuracy, with the same positive or negative signs in the differences between year-to-year ring widths.

For crossdating purposes, each site's samples are detrended with mainly negative exponential curves in order to preserve any long-term variance that samples have in common as well as their year-to year variance. In general detrending removes a tree's unique response to its environment and equalizes the variance in ring widths over its lifespan.[26] A site's detrended sample data are crossdated with each other using the Student's *t*-test, trend coefficients, and visual comparisons to establish each site chronology.[27] Each site chronology is then crossdated with other dated chronologies to determine its correct calendar dates. The average correlation coefficients (*r*) between the samples within each of the 56 site chronologies are listed in Table 1.1. Figure 1.3 shows the distribution of the site chronologies and sample numbers over time, and Figure 1.4 shows the site chronologies. Table 1.3 lists the average correlation coefficients between all samples, and between samples within and outside of each grid. Table 1.4 lists the correlation coefficients of each site chronology with the other site chronologies that share the same time period.

For a regional climate reconstruction, the oak ring-widths were detrended by fitting a cubic spline curve to each sample's raw measurements, which reduces low-frequency variance and enhances annual variance. The questions of what parameters to use in specifying the fit of the spline curve (minimum least-squares fit, or frequency

[26] Cook and Kairiukstis 1989; Cook and Peters 1997.
[27] Baillie and Pilcher 1973; Fritts 1976; Pohl 1995.

Table 1.3. Average correlation coefficients between the samples in each of the three grids (left); within the site chronologies from the same grids (center); and between samples from different site chronologies within the grids (right).

Average correlation coefficients between:	All samples within grids		Samples within sites		Samples outside sites	
	r	N	*r*	N	*r*	N
Grid 1	0.231	8118	0.399	1645	0.188	6473
Grid 2	0.190	5687	0.321	1341	0.149	4346
Grid 3	0.293	1333	0.379	644	0.213	689

Table 1.4. Average correlation coefficients (*r*) between site chronologies within the grids and between grids.

Between site chronologies	Average *r* -values	Count
within		
Grid 1	0.300	169
Grid 2	0.293	60
Grid 3	0.409	5
between		
G1 and G2	0.214	118
G2 and G3	0.259	30
G1 and G3	0.141	60
All correlations	0.246	442

response and wavelength of minimum rigidity), and whether the chosen parameter(s) should be the same for all the samples or determined by each sample's length and variance were addressed by Cook and Kairiukstis.[28] Smoothed cubic-spline curves were fitted by CORINA[29] using a minimum sum of residual variance of e^{-16} as the limit to the amount of variance explained by a curve fitted to each sample.[30] ARSTAN[31] was used to fit a spline curve with the minimum rigidity of 28 years, 50% frequency response to all the samples' measurements.

[28] Cook and Kairiukstis 1989, p. 112.
[29] software available at https://sourceforge.net/projects/corina/
[30] Cook and Peters 1997.
[31] Cook and Holmes 1999.

The mean sensitivity, a measure of the mean relative change in ring widths over time,[32] of the oak site chronologies ranges from 0.098 to 0.287 and their standard deviations range from 0.090 to 0.323, normal values for oak tree-ring data.[33] The data sets were combined into four different chronologies to test differences between the detrending methods, the effects of normalizing the data, and the results of averaging site chronologies versus sample data sets. One chronology is composed of ARSTAN-detrended sample data and the other three are constructed of CORINA-detrended data: one of the sample data, one of normalized sample data, and the other of the normalized site chronologies.

For an evaluation of what low-frequency variance is removed by detrending with the spline curves, the conservatively detrended sample data used for crossdating purposes were also built into site chronologies, and the chronologies were averaged into the low-frequency retained ("LFR") tree-ring chronologies for each grid and the total region.

Tests between the five methods' chronologies included each chronology's correlation coefficient and sign test with the May-June δP (Table 1.5). The sign test is the percentage of years when the two data sets both increase or decrease in value from year to year. Between the four cubic spline chronologies and the May-June δP (Table 1.5) there are no significant differences in the results of the methodology over the calibration years. The number of samples outweighs the importance of the methodology in this study, but the chronologies constructed of the normalized data sets correlate slightly higher with the MJ δP, which may indicate that normalization enhances the regional climate signal contained in the oak tree-ring chronology.

[32] Fritts 1976.
[33] Baillie and Pilcher 1973.

Table 1.5. The correlation coefficients and sign tests between the five method chronologies and MJ δP for 1931-1985, and 1900-1989. Any correlation below 0.632 explains less than 40%. The normalized site chronology has a slightly higher correlation with the May-June δP, but not significantly higher. The sign test is the percentage of the period that the signs, positive or negative, are the same in the differences between consecutive years' values in the tree-ring chronology and in the May-June precipitation anomalies.

Method	Correlation 1931-1985	Correlation 1900-1989	% sign agreement 1931-1985	% sign agreement 1900-1989
Cubic spline sample	0.775	0.618	0.852	0.730
Cubic spline norm samp	0.773	0.611	0.815	0.730
Cubic spline norm site	0.781	0.636	0.759	0.663
Arstan cubic spline samp	0.764	0.600	0.796	0.708
Low frequency retained	0.543	0.495	0.759	0.663

The low-frequency-retained chronology has the expected lower values of the correlation coefficient and the sign test with the May-June δP, but both are still statistically significant (Table 1.5). The differences between it and the cubic-spline chronology, and their record of the MJ δP are discussed below**.**

The process of using the minimum residual-fit curve for detrending each sample rather than a curve of the same wavelength and rigidity for detrending all samples (CORINA *vs*. ARSTAN; either can be done with ARSTAN) appears to produce optimal results (Table 1.5), but again it is an insignificant increase. Extensive testing with limited data sets is necessary to assess the methodological nuances better.

From these tests, we decided to use only one spline-curve method chronology for the May-June δP reconstruction and to compare it with the LFR chronology to determine what was removed by the detrending. Of the spline-curve chronologies, the normalized site chronology was chosen due to its high values but also so that the sites were equally weighted.

The temporal variance over each chronology was adjusted according to the number of samples and the average correlation coefficients between the data sets that are contained in each year.[34] This adjustment reduces the amplitude of variance in the periods of low sample count in the early years of the chronologies and to a lesser extent in the 15th through early 17th centuries. It also adds a small amount of amplitude to the last 100 years due to the increasing average biological age of the included tree rings. From the very small differences between values in the original and adjusted chronologies, it is evident that the number of samples is large enough for accurate values for most of its length. The only period that it is significantly adjusted is when the sample number is less than 25 and when the chronology is composed mostly of juvenile growth rings, and that occurs only in the first century, AD 1081-1168.

Climate Data

Monthly precipitation and temperature anomalies (δP and δT, respectively) were calculated from meteorological station data available at the National Climatic Data Center / National Oceanographic and Atmospheric Administration's website, http://www.ncdc.noaa.gov/oa/ncdc.html, on the Global Historical Climatology Network page. The 15 stations used here (Table 1.6, Figure 1.2) all contain monthly values for 1931-1985 data, 13 with long precipitation records and eight with long temperature records. Two stations contain a few missing values that were replaced with the averaged value from the two or three closest stations.

[34] Osborn et al., 1997; Briffa 1999.

Table 1.6. Meteorological stations, their locations, and the percent of the grids' area that is unique to each. The percent is equal to 100 times the weight used in calculating the respective grids' anomalies. The three grids' anomalies were averaged into the regional ADP precipitation and temperature anomaly data sets. Figure 2 includes hydrothermal graphs of each station. The Izmir(*) station is not in the study region but was added for latitudinal depth.

				Percent of ADP grid data represented by each station					
				Precipitation			Temperature		
Stations	Lat ºN	Long ºE	Alt m	G1	G2	G3	G1	G2	G3
GREECE									
Larisa	39.6	22.4	73				11.2		
Thessaloniki	40.6	23	30P, 4T	52.5			45.9		
TURKEY									
Çanakkale	40.1	26.4	3	30.4	9.6				
Edirne	41.7	26.6	48	17.1	6.2		33.3	9.2	
Izmir *	38.4	27.3	25				9.6	11.2	
Istanbul	41	29.1	40		23.7			59.6	
Bursa	40.2	29.1	100		22.1				
Eskisehir	39.8	30.6	783		17.1				
Bolu	40.7	31.6	742		20.0	5.8			
Ankara	40	32.9	894		1.3	18.4		20.0	53.8
Kastamonu	41.4	33.8	799			18.3			
Kirşehir	39.1	34.2	985			10.8			
Çorum	40.6	35	837			20.4			
Samsun	41.3	36.3	44			15.0			29.1
Sivas	39.8	37	1285			11.3			17.1

Gridded monthly precipitation and temperature data in eight 5º latitude by 5º longitude grids for the region 35˚-45˚ latitude and 20˚-40˚ longitude were downloaded from the Climate Research Unit (CRU) website http://www.cru.uea.ac.uk/ for comparison with our data. Precipitation data begin in 1900, an advantage over the station data discussed above, but the data of the 1900-1930 period still need to be used with caution, since the available data for that period are mainly from outside our

region with the grids' values interpolated from them.[35] Temperature data available from the same eight grids begin at dates ranging from the late 1800s up to 1927 and all end in 1998.

The station monthly precipitation data were converted to square roots in order to correct a slight skewedness and then anomalies were calculated by subtracting the monthly average, then dividing by the standard deviation of the period in common for each month, 1931-1985. The monthly temperature data were each converted to anomalies in ºC by subtracting the average of their monthly values for 1931-1985. Both sets' monthly values were then weighted using Thiessen polygons[36] over each of the three 3º latitude by 5º longitude grids in our region of study (Figure 1.2), with one outer station's temperature data added for latitudinal depth, and then averaged together for the region's anomalies.

Each CRU grid's precipitation data were also transformed using square roots, and both the CRU precipitation and temperature data were converted to anomalies in the same way as the ADP grids noted above. The data sets from the four grids in each 5º latitude segment (35-40ºN and 40-45°N) were averaged.

A comparison between the ADP and the CRU precipitation anomalies indicated that the CRU 40-45ºN latitude data sufficiently represent the precipitation anomalies of the study region ($r = 0.823$) despite the additional 3 degrees of latitude to the north. The correlation between the ADP δP and the CRU 35º-40°N latitude δP data is lower, at 0.706. The longer period of the CRU grids, plus their equally high correlation with the oak chronology justified the use of the CRU δP 40-45°N latitude data for this study, despite the caveat noted above. The CRU δT data, however, do not

[35] Hulme 1992, 1994; Hulme et al., 1998.
[36] Jones 1988; Jones and Hulme 1996.

significantly correlate with either the ADP δT data or the tree-ring chronologies; the station and ADP grid temperature anomalies were used here.

Calibration, verification, and reconstruction

Correlations between the chronologies and the monthly climate parameters of the year before growth and the year of growth were calculated for 1931-1985 (Figure 1.5). May and June precipitation is clearly the major growth-limiting factor with the precipitation of April in the year before growth plus the mean temperatures of May and June as other possible growth-limiting forces.

A regression analysis with the tree-ring chronology as the predictand and the May and June δP as the predictors give both approximately the same weight, thus both have about the same effect on the tree-ring growth in that period. Combining the two variables to use as a single predictor slightly increased the variance explained. Additions of the other significantly correlated parameters add small amounts to the variance explained, but not consistently over time.

The chronology was divided into three sequences for verification and calibration of the reconstructed values. One sequence consisted of 1941-1970 and a second segment included a split sequence of 1931-1940 and 1971-1985. The third sequence has the 1900-1930 period and was used for verification alone. For each sequence the chronology was used as the predictor to calculate the coefficients of a regression equation with the May-June precipitation anomalies as the predictand. The two regression equations were tested with the other sequence for verification. The coefficients for the final reconstruction equation were calculated from the values of 1931-1970 due to the reduced amount of available climate data prior to 1931 plus the reduced response in the 1971-1980 data (Figure 1.6). The two years of 1936 and 1947, whose values statistically had the most influence, were also removed for a better

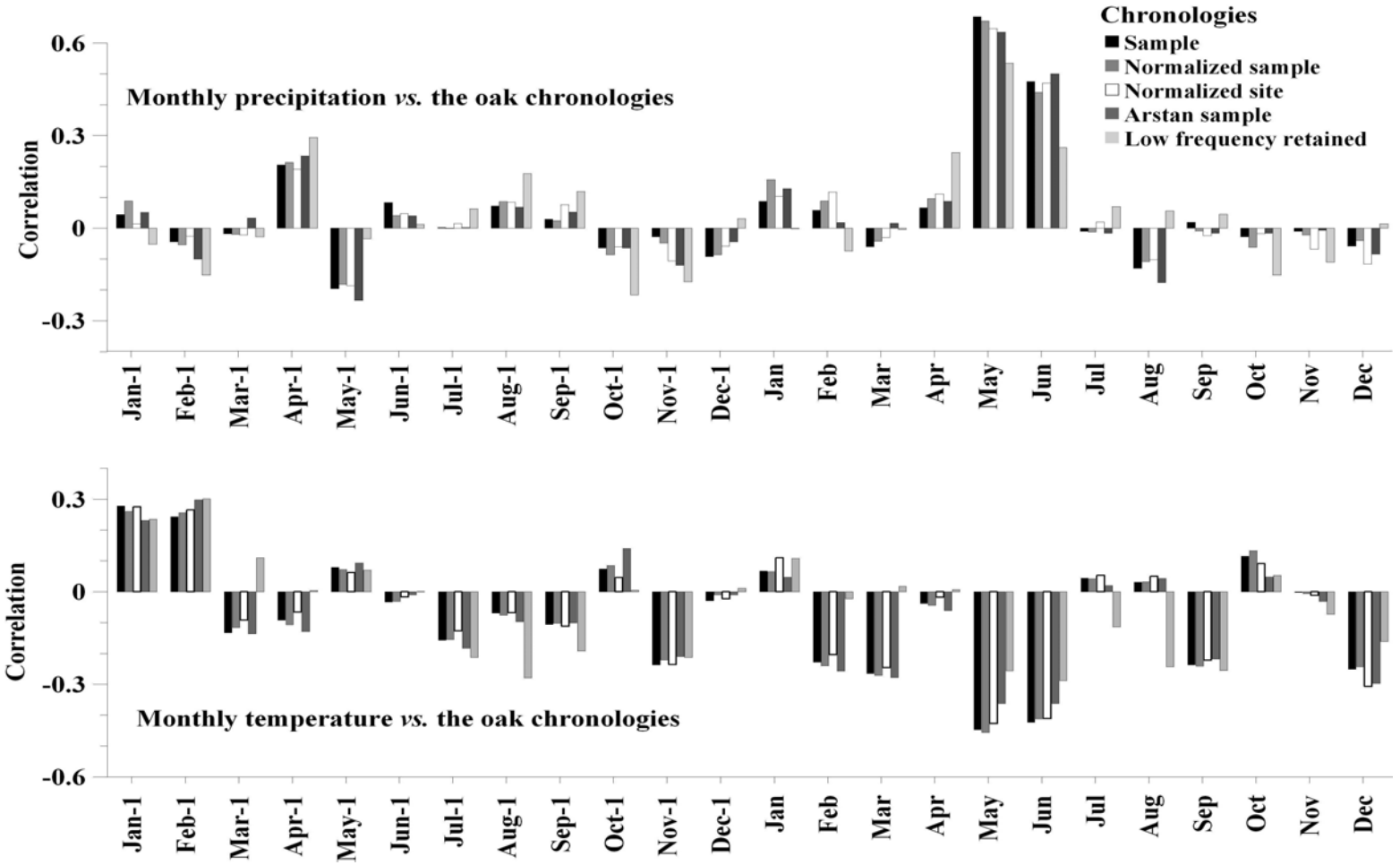

Figure 1.5. Correlation coefficients between the five method chronologies and the monthly precipitation and temperature anomalies for 1931-1985 indicate that the May and June precipitation is the primary growth limiting factor. Included months are those of the year before growth (followed by "-1") and the year of growth.

reconstruction of the majority of the data set. Correlation coefficients and sign tests were used to corroborate the fit with the MJ δP and the first-year differences (positive or negative) between the data sets[37] **(**Table 1.7**,** Figure 1.6). The May-June precipitation anomalies were then reconstructed from the complete chronology and converted into precipitation values for the region from 1089 to 1989.

Table 1.7. The correlation coefficients for the three periods of regression analysis, calibration, and verification between the five chronologies and the gridded May-June precipitation anomalies. All values are at the $p < 0.05$ probability level.

	1941-1970		1931-1940, 1971-1985		1900-1930
	CRU MJ δP	ADP MJ δP	CRU MJ δP	ADP MJ δP	CRU MJ δP
Methodology					
Detrended with cubic spline curve:					
CSP Sample	0.762	0.591	0.821	0.724	0.528
CSP Norm samp	0.762	0.594	0.819	0.724	0.492
CSP Norm site	0.788	0.613	0.786	0.673	0.547
ARS Sample	0.735	0.558	0.818	0.715	0.451
Low variance retained	0.749	0.550	0.515	0.414	0.509

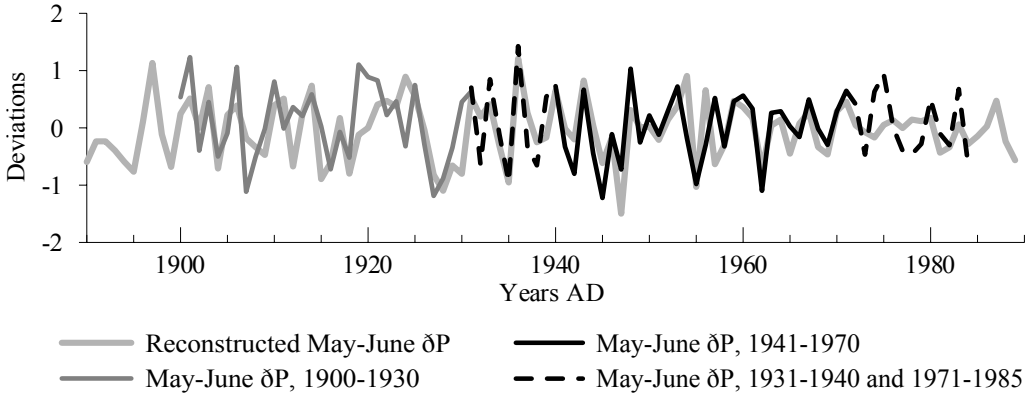

Figure 1.6. The May-June precipitation anomalies and the normalized site chronology, showing the division of the data sets used in calibration and verification.

[37] Cook and Kairiukstis 1989; Gordon 1988.

RESULTS AND DISCUSSION

The May-June regional precipitation reconstruction

The values of the reconstructed regional May-June precipitation, AD 1089-1989, are shown in Figure 1.7 and listed in Appendix A. They correlate significantly ($p < 0.05$) with the MJ δP from 11 of the 13 stations within the study area (Table 1.8). The correlations' highest values are with the station data of Thessaloniki, Greece, and Edirne and Samsun, Turkey, one station in each grid (Figure 1.2), indicating that the reconstruction accurately represents the regional May-June precipitation. The two insignificant correlations are with the MJ δP of the two stations at the minimum and maximum elevations of the oak species' ranges: three meters elevation on the east Aegean Sea coast (Çanakkale), and 1285 meters elevation on the eastern boundary of the study region (Sivas) on the Anatolian Plateau.

Table 1.8. Correlations between the reconstructed May-June precipitation and the meteorological stations' May-June δP for 1931 to 1985. Probability is at the levels of $p < 0.01$ with no superscript; "1" is $p < 0.05$, and "2" is $p > 0.05$.

Stations	Alt (m)	*r*-scores with CRU 20-40ºE May-June δP	*r*-scores with reconstructed May-June δP
Thessaloniki	30	0.545	0.513
Çanakkale	3	0.559	0.257[2]
Edirne	48	0.676	0.547
Istanbul	40	0.565	0.313[1]
Bursa	100	0.639	0.434
Eskisehir	783	0.543	0.378
Bolu	742	0.583	0.384
Ankara	894	0.451	0.306[1]
Kastamonu	799	0.621	0.499
Kirsehir	985	0.369	0.270[1]
Çorum	837	0.452	0.349
Samsun	44	0.587	0.567
Sivas	1285	0.241[1]	0.219[2]

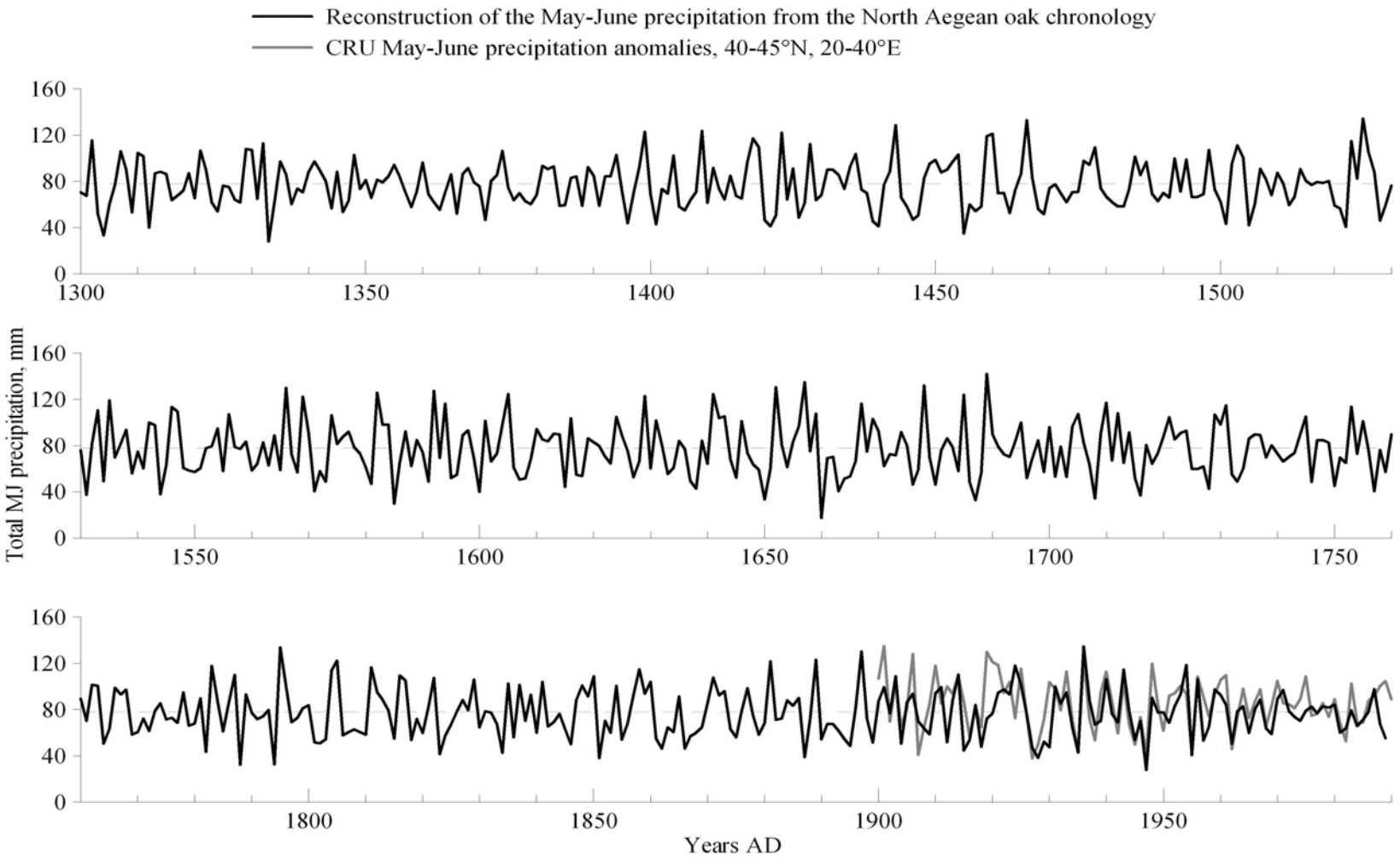

Figure 1.7. The AD 1089-1989 May-June precipitation reconstructed from the North Aegean oak tree-ring chronology and the May-June precipitation data from the four grids at 40-45ºN, 20-40ºE.

Growth response to May-June temperature

Any growth response of the oaks to May-June temperature is due to the close relationship between precipitation and temperature in this warm subhumid climate regime, and is a negative response. An increase in precipitation means more clouds, less direct heat, lower temperature, and less evaporation,[38] with more water available to the trees[39] and *vice versa*. The variance explained in the cubic spline chronology by the gridded MJ δT is less than 30%. However, the May-June temperature anomalies of two interior stations in the outer grids, Larisa (Greece) and Ankara (Turkey) correlate significantly with the regional May-June δP at -0.508 and -0.634, respectively. In a regression equation, the two explain 44.8% of the variance in the tree-ring chronology. The response of the oaks to temperature may not be sufficient to reconstruct the regional May-June δT accurately, but the reconstruction of the May-June precipitation anomalies may be regarded as an inverse of the approximate values of the May-June temperature anomalies in Ankara and Larisa over time (Figure 1.8).

The precipitation record and history

The significance of the years of high and low values in the reconstructed May-June precipitation were examined by comparing the cubic spline chronology and the low frequency-retained chronology to assess their similarities and differences due to the detrending processes (Figure 1.9). The difference between the cubic-spline chronology and the low frequency-retained chronology is mainly in the amplitude of certain years. The low frequency signal may either enhance or ameliorate the severity of each extreme (Figure 1.9). Enhancement can be seen in the years 1479 to 1485 when there was a severe drought, and amelioration in 1545-1547. Sustained periods

[38] Griffiths and Driscoll 1982.
[39] Kramer and Kozlowski 1979.

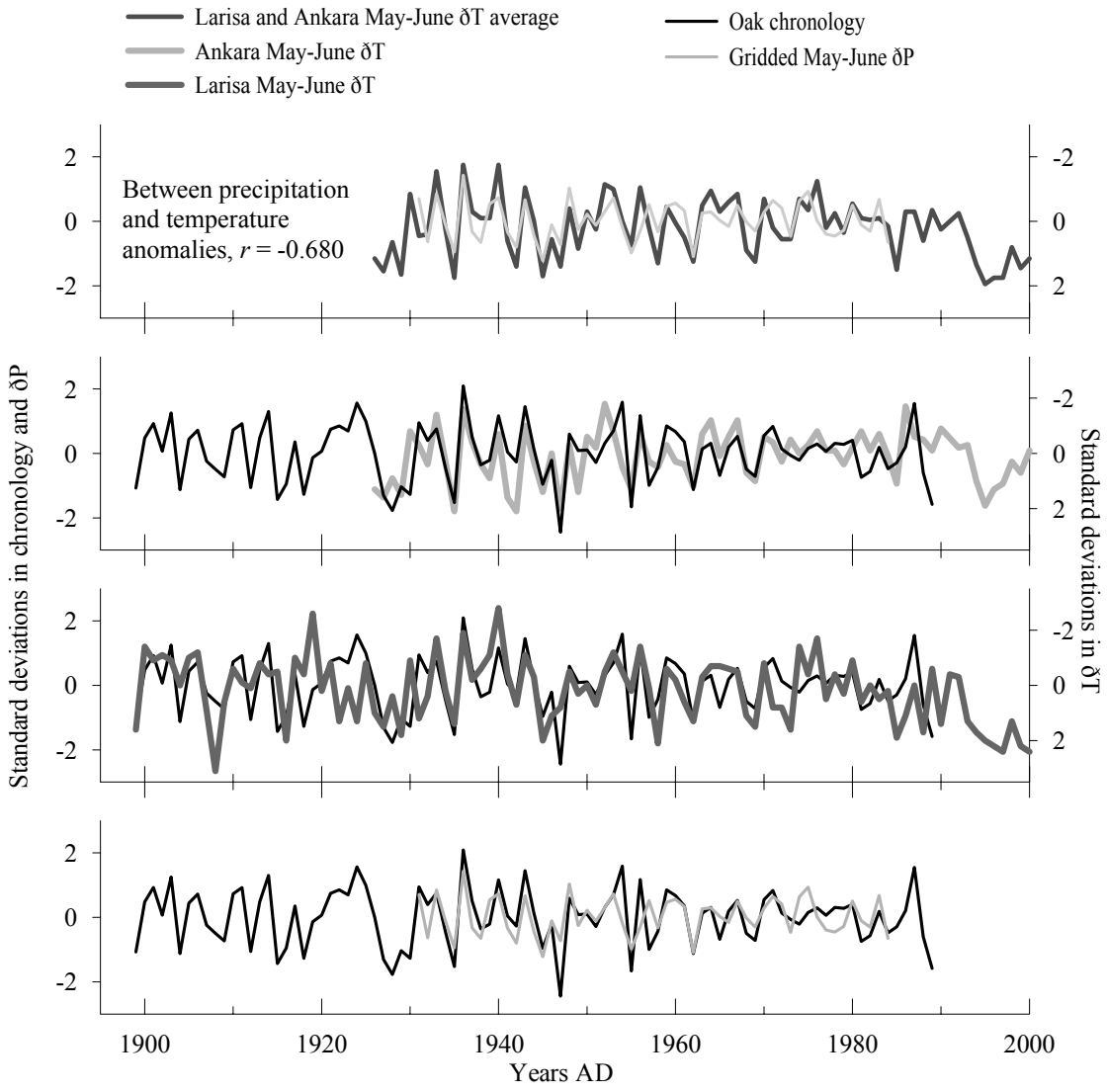

Figure 1.8. The Larisa (Greece) and Ankara (Turkey) May-June temperature anomalies compared together with the regional May-June precipitation anomalies (top) and each separately with the oak chronology (middle two graphs). For comparison, the bottom graph shows the regional May-June precipitation anomalies and the oak chronology. Note that the scales on the y-axes to the right are reversed.

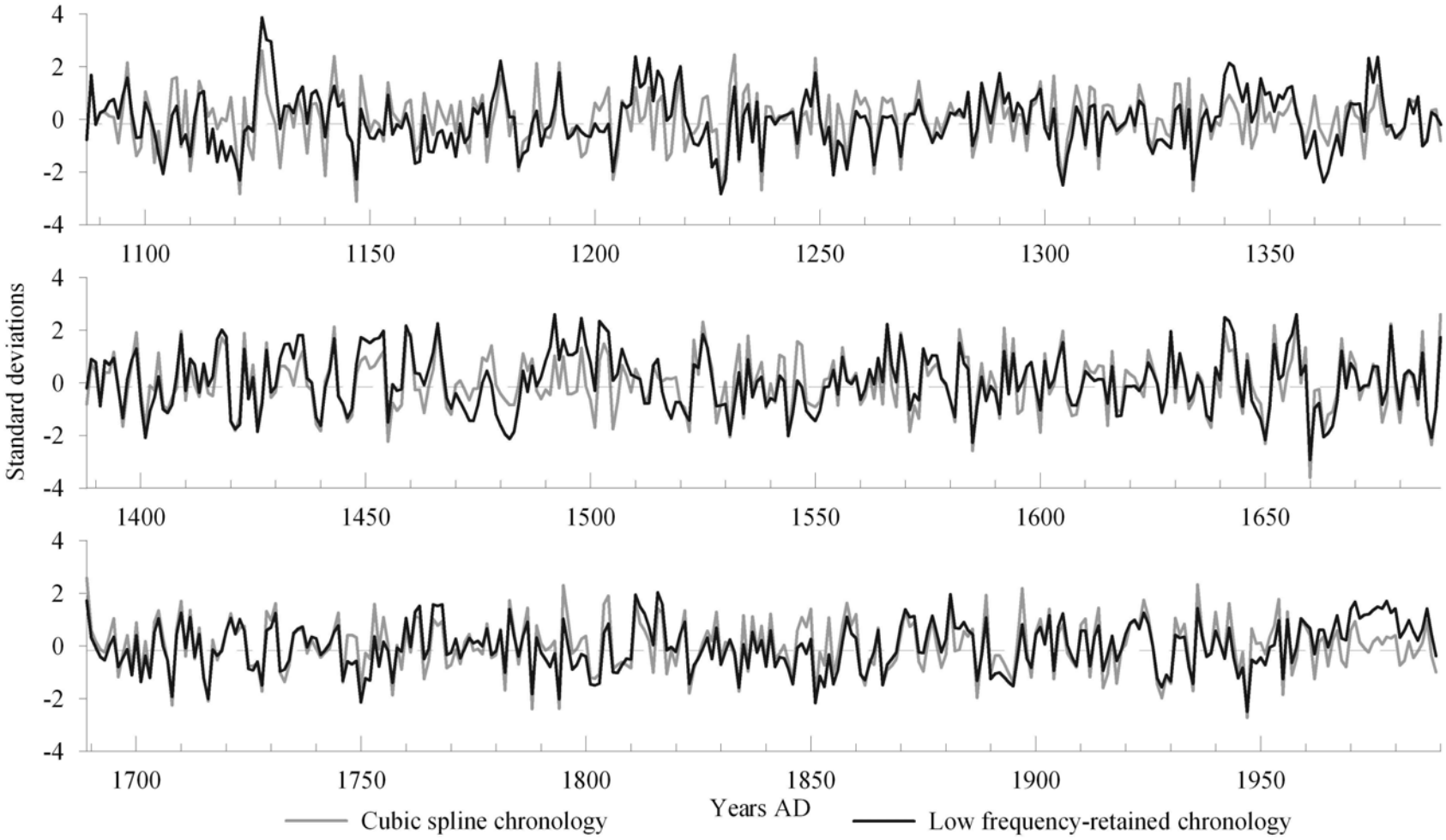

Figure 1.9. A comparison of the cubic spline (normalized site) chronology and the low frequency-retained chronology.

Table 1.9. The years where values of the two chronologies were either above or below the mean by two standard deviations. There is more difference between the two in the wet than in the dry years: only four of the 33 years are in common with the wet years, 12 out of 27 drought years. The CSP also reduced the number of consecutive years in the data sets from 5 to none.

Extreme drought years		Extremely wet years	
LFR	CSP	LFR	CSP
1104		1126	1126
1121	1121	1127	
1147	1147	1128	
	1204		1142
1228	1228	1179	
1229		1209	
	1237	1212	
1253		1219	
1304	1304		1231
1333	1333		1249
1362		1341	
1401		1342	
	1455	1372	
1482		1374	
1544		1418	
1585	1585		1443
1650	1650	1459	
1660	1660	1466	1466
1663		1492	
1687	1687	1498	
	1708	1502	
1716	1716	1503	
1750			1525
	1788	1566	
1794	1794	1641	
1851		1642	
1947	1947		1652
		1657	1657
		1678	1678
			1689
			1795
		1816	
			1936

of extremely low or high May-June precipitation (more than 2 standard deviations above or below) for two or more years only occur in the LFR chronology (Table 1.9), but there are many extended periods of the tendency in either direction (values above 1, below -1), and again they are more apparent in the LFR chronology (Figures 1.9 and 10A,10B). The frequency of extremes is greatest in the first half of the chronology through the 17th century and that may be an indicator of the onset of the

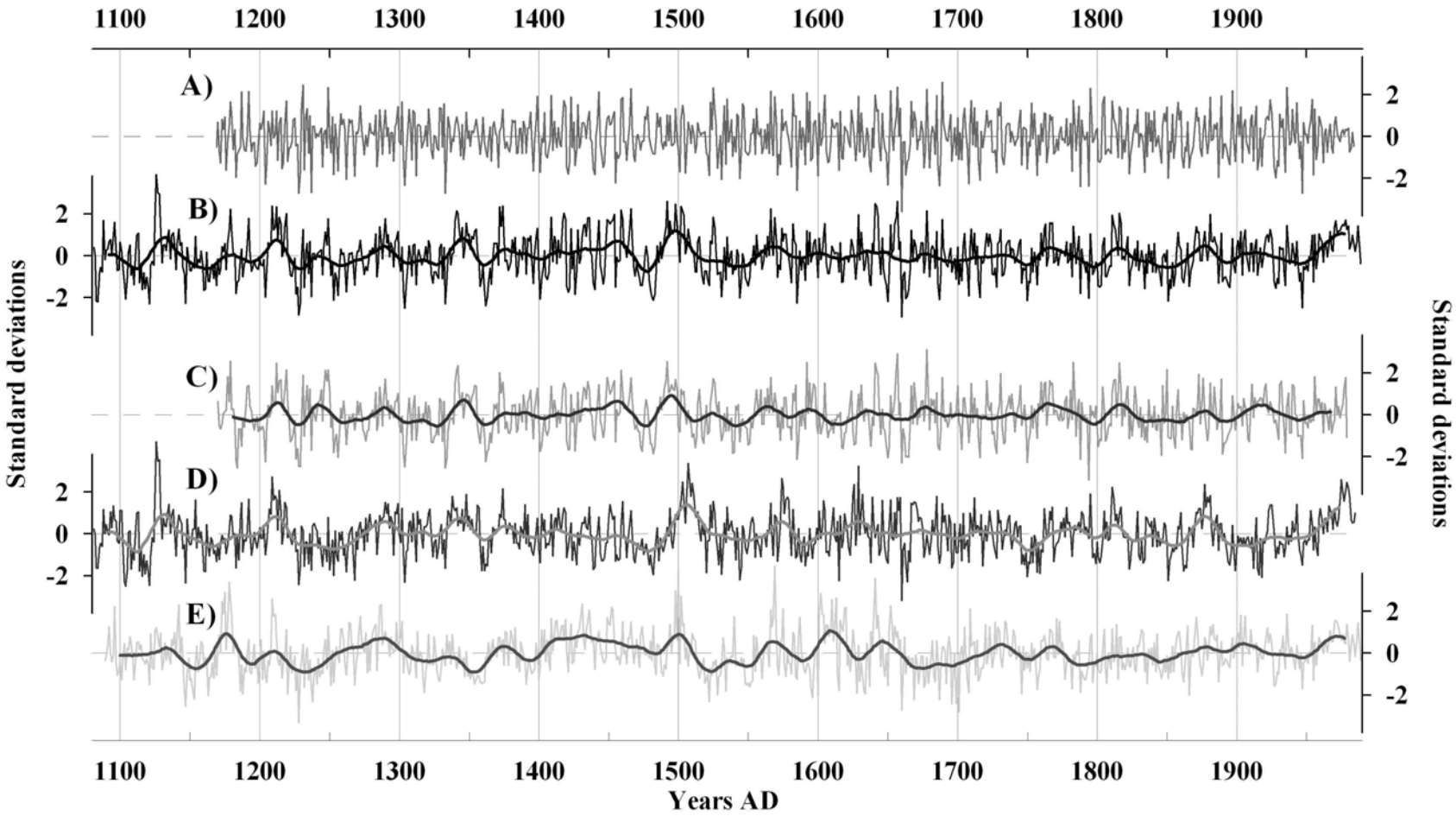

Figure 1.10. A) The cubic spline chronology, B) the low frequency-retained chronology, and C, D,and E) the three grid chronologies from grids 1, 2, and 3, respectively. It is clear from A) and B) that low-frequency is lacking in our reconstruction. However, the higher correlation with the regional precipitation indicates that the cubic spline chronology contains an accurate record of the regional variability of the May-June precipitation.

influence of the Little Ice Age in this region.[40] A comparison between the years of the extremes in the reconstruction and the historical climate record was attempted, but the latter is very limited in this area.[41] A visual comparison of the regional and three grids' LFR chronologies with the cubic spline chronology suggests that the low frequency removed in detrending reflects local climate variability over time (Figure 1.10C, D, and E). Evaluation of these differences is the key to accurately interpreting the climate record in the chronologies.

Comparison with other precipitation reconstructions around the north Aegean

We compared our May-June regional precipitation reconstruction with the reconstructions of D'Arrigo and Cullen, Akkemik et al., and Touchan et al.[42] D'Arrigo and Cullen's reconstruction (D&C) is February to June precipitation centered on Sivas, Turkey, the easternmost station in our study region, and uses five tree-ring chronologies from across Turkey, including one of the forest chronologies used here from the eastern grid. The Akkemik et al. reconstruction (A&all) is a single site reconstruction of March-June precipitation from an oak tree-ring chronology, and the site location is close to two of our sites in the eastern grid, (one of them also used in the D'Arrigo reconstruction). The Touchan et al. reconstruction includes two May-June precipitation reconstructions for southwestern Turkey, one based on the ring widths of juniper alone (*Juniperus excelsa*) from 1339 to 1998 (T1), and the other on the tree-ring growth of cedar (*Cedrus libani*), pine (*Pinus brutia* and *P. nigra*), and juniper from 1776 to 1998 (T2). The reconstruction is based on the 25-30ºE, 35-40ºN CRU May-June grid directly to the south of the center of our region, and we used that for comparison with the Touchan et al. reconstructions.

[40] Grove 2004; Grove and Grove 1992; Fagan 2000.
[41] Grove 2004; Fagan 2000; Lamb 1997.
[42] D'Arrigo and Cullen 2001; Akkemik et al., 2004; Touchan et al., 2003.

All the precipitation reconstructions correlate significantly with ours (Table 1.10A). The highest correlation is with the Akkemik et al reconstruction, which was expected since it is an oak chronology and from part of our region, yet despite the included months extending to March through June. The D'Arrigo and Cullen reconstruction of 1628-1980, composed of chronologies from around Turkey, also correlates well and includes one of our oak forest data sets, but their reconstruction includes the precipitation of February through April as well as May and June.

Table 1.10B indicates that the correlations between the oaks and the various precipitation anomalies are significantly higher than any correlation of the other reconstructions with the gridded precipitation data. The comparison with the other reconstructed precipitation parameters indicates that our reconstruction fits in well with the established data sets from this region. It appears that D'Arrigo and Cullen's reconstruction may tend more toward the southern Turkey region, possibly due to their inclusion of tree-ring data from that area. The species used have a much higher mean sensitivity and annual variance in their ring widths, which may indicate that the methodology used here for optimizing the oaks' response is key to a good reconstruction.

The southwestern Turkey May-June precipitation reconstruction, 1335-1998 correlates with our reconstruction at 0.183 ($p < 0.01$, n = 656), and the 1776-1998 reconstruction correlates at 0.238. ($p < 0.01$, n=213). A visual comparison between the longer of their reconstruction with ours (Figure 1.11) shows years of quite high correlation and years of opposite correlation with occasional 2-5 year sequences of opposite extreme growth patterns. A subtraction of their standardized reconstruction from ours clearly indicates periods of similarities, such as the second half of the 19th century when there appears to have been the same precipitation from north to south.[43]

[43] Griggs et al., 2006

Table 1.10. Correlation coefficients between reconstructed precipitation data sets and precipitation anomalies of various grids and monthly combinations from in and around our study region. Values below each correlation are the probability level, *p*.
A. Correlations between the reconstructions for the length shared by the two sets. B. Correlations between the indicated sets for 1900-1989. Bold numbers are the values for the correlation between the particular CRU grid or combined set of grids that are the closest to the origin of the included tree-ring chronologies.

A. Correlation for periods in common	Our May-Jun	Akk Mar-Jun	D&C Feb-Jun	T1 May-Jun
Precipitation reconstructions				
Akkemik et al. (2005)	0.546			
March-June, 1635-2001 [Akk]	0.000			
D'Arrigo and Cullen (2001)	0.398	0.391		
February-June, 1628-1980 [D&C]	0.000	0.000		
Touchan et al. (2003)	0.223	0.129	0.716	
May-June, 1339-1998 [T1]	0.034	0.224	0.000	
Touchan et al. (2003)	0.283	0.211	0.754	0.922
May-June, 1776-1998 [T2]	0.007	0.045	0.000	0.000

B. Correlations for 1900-1989	Reconstructions from tree-ring chronologies				
	Our May-Jun	Akk Mar-Jun	D&C Feb-Jun	T1 May-Jun	T2 May-Jun
Gridded δP instrumental data					
May-Jun δP 20-40E,40-45N	**0.631**	0.489	0.458	0.392	0.409
Used for our reconstruction	**0.000**	0.000	0.000	0.000	0.000
Mar-Jun δP 30-35E,40-45N	0.483	**0.561**	0.329	0.198	0.203
	0.000	**0.000**	0.003	0.061	0.055
Mar-Jun δP 20-40E,40-45N	0.491	**0.519**	0.317	0.180	0.189
	0.000	**0.000**	0.004	0.090	0.075
Feb-Jun δP 20-40E,40-45N	0.466	0.500	0.254	0.134	0.145
	0.000	0.000	0.022	0.209	0.173
May Jun δP 25-30E,35-40N	0.415	0.390	0.587	**0.574**	**0.577**
	0.000	0.000	0.000	**0.000**	**0.000**
May-Jun δP 20-40E,35-45N	0.556	0.497	**0.567**	0.515	0.539
	0.000	0.000	**0.000**	0.000	0.000

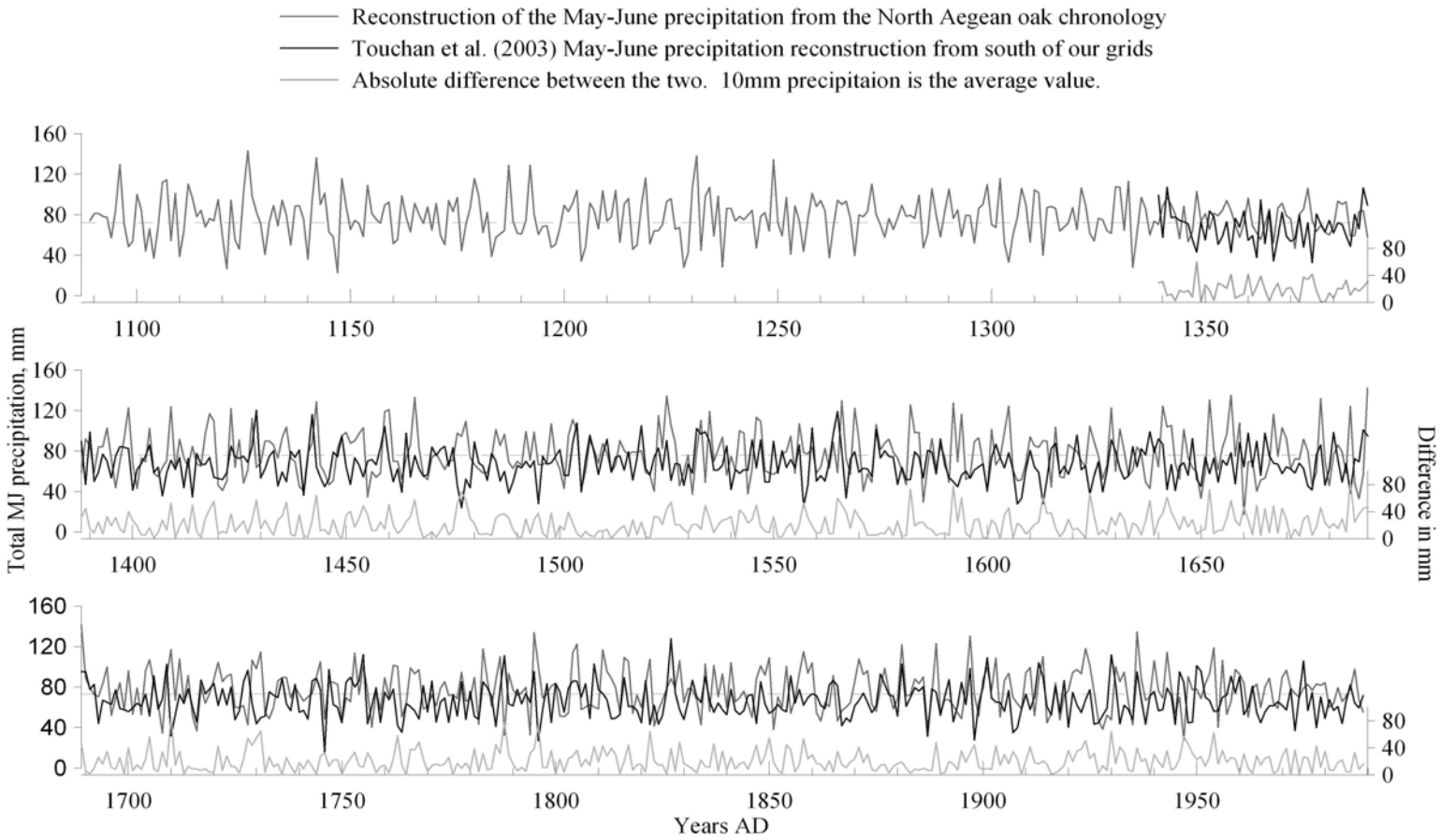

Figure 1.11. Our reconstructed May-June precipitation values compared to the 1338-1998 reconstruction of Touchan et al. (2003). [The mean value of the Touchan et al. reconstruction is about 10mm less than the mean of our reconstruction.] Of note are the years where there are considerable similarities (*e.g.* 1870-1900) and considerable differences (*e.g.* 1470-1480). These features are discussed in the text.

Periods of sustained opposite precipitation from north to south, indicated in the opposite values of the two reconstructions from 1476-1479, the longest severe drought period in SW Turkey in the last 600 years[44] are rare.

CONCLUSIONS

We have calculated May-June precipitation from the northern Aegean region for 1089-1989 AD, adding an extension of 234 years to the precipitation reconstruction for the area. We have also shown that the high frequency response in these oaks is primarily due to May-June precipitation, and that the data of samples collected for dendrochronological purposes are secure proxy data for the paleoclimate record of the region. Our tree-ring record also has the potential to be used as proxy data for site-specific May-June temperature changes due to the highly significant negative correlation between precipitation and temperature in the continental subregions where the oaks grow. In continuing research we have also explored decadal to multi-decadal variance in the tree-ring record for possible low-frequency forces and changes in the regional signal over time. Other limiting factors in the spatial and temporal variability of the ring widths are the May North Atlantic Oscillation (NAO),[45] plus a possible interrelationship between the winter NAO and the Atlantic Multidecadal Oscillation and their effects on this region.[46] Further studies of our tree-ring data plus other proxy data sets and tree-ring data from outside the region may provide a critical paleoclimate link between the Atlantic and Indian -Pacific Ocean arenas.

[44] Touchan et al., 2003
[45] Griggs et al., 2005.
[46] Touchan et al., 2005; Xoplaki 2002; Griggs et al., 2006.

The methodological tests conducted here indicate that the processes of detrending with cubic spline curves and the normalization of the oak ring widths optimize the high frequency record of the May-June precipitation.

The tree-ring record at the Malcolm and Carolyn Wiener Laboratory is a unique database with the potential for reconstructing climate parameters as far back as the seventh millennium BC. This will provide a better assessment of the region's climate, climate change, and its teleconnections to larger scale climate change over time. Future research also has great potential for clarifying answers to continuing questions about the impact of climate and climate change on human history, and *vice versa*, in one of the longest-civilized areas of the world.

APPENDIX 1.1

The reconstructed values of May-June precipitation for the North Aegean

Year	P(mm)	Year	P(mm)	Year	P(mm)	Year	P(mm)	Year	P(mm)
1089	74.2								
1090	81.1	1140	36.0	1190	61.1	1240	73.7	1290	105.3
1091	81.3	1141	94.0	1191	74.6	1241	78.4	1291	76.3
1092	78.3	1142	136.5	1192	129.2	1242	75.2	1292	84.9
1093	77.3	1143	90.0	1193	80.6	1243	79.4	1293	58.8
1094	57.0	1144	101.5	1194	60.6	1244	84.3	1294	79.5
1095	84.9	1145	63.0	1195	68.2	1245	47.1	1295	79.2
1096	129.4	1146	58.0	1196	69.2	1246	77.9	1296	51.9
1097	70.6	1147	22.8	1197	47.6	1247	82.0	1297	86.1
1098	48.2	1148	115.7	1198	50.5	1248	63.9	1298	90.3
1099	53.9	1149	88.5	1199	66.8	1249	134.6	1299	109.7
1100	100.1	1150	65.4	1200	89.5	1250	72.3	1300	70.6
1101	84.3	1151	74.5	1201	82.9	1251	59.2	1301	67.5
1102	44.0	1152	71.4	1202	91.3	1252	97.1	1302	115.6
1103	66.0	1153	58.4	1203	104.1	1253	41.1	1303	51.9
1104	36.9	1154	108.9	1204	33.9	1254	88.7	1304	33.1
1105	68.2	1155	81.1	1205	48.7	1255	73.9	1305	60.1
1106	112.2	1156	75.6	1206	91.7	1256	43.6	1306	77.0
1107	114.2	1157	71.9	1207	84.0	1257	75.7	1307	106.0
1108	54.3	1158	89.3	1208	66.2	1258	100.9	1308	90.1
1109	101.2	1159	92.2	1209	103.9	1259	88.2	1309	53.1
1110	38.8	1160	51.4	1210	73.6	1260	94.2	1310	104.6
1111	64.3	1161	55.5	1211	77.9	1261	83.7	1311	101.6
1112	110.3	1162	98.8	1212	104.1	1262	37.3	1312	39.9
1113	96.4	1163	77.7	1213	52.7	1263	67.2	1313	86.9
1114	78.0	1164	63.1	1214	90.3	1264	94.3	1314	88.1
1115	84.6	1165	91.3	1215	96.0	1265	90.0	1315	86.3
1116	67.8	1166	80.0	1216	45.6	1266	93.3	1316	63.7
1117	76.3	1167	71.5	1217	50.3	1267	76.3	1317	67.6
1118	74.1	1168	87.7	1218	88.5	1268	39.7	1318	72.0
1119	95.0	1169	64.7	1219	116.6	1269	79.7	1319	86.9
1120	58.7	1170	91.1	1220	51.5	1270	78.1	1320	65.5
1121	26.5	1171	59.8	1221	64.1	1271	83.4	1321	106.4
1122	94.5	1172	50.4	1222	64.3	1272	110.4	1322	89.8
1123	55.4	1173	94.1	1223	70.0	1273	80.4	1323	61.6
1124	46.0	1174	83.1	1224	93.2	1274	70.2	1324	53.9
1125	101.6	1175	97.0	1225	95.8	1275	57.7	1325	76.3
1126	142.9	1176	44.4	1226	65.6	1276	76.5	1326	75.2
1127	98.4	1177	70.1	1227	67.4	1277	65.3	1327	64.1
1128	82.8	1178	86.9	1228	28.0	1278	76.3	1328	61.6
1129	71.1	1179	115.5	1229	42.3	1279	89.5	1329	107.8
1130	40.6	1180	98.2	1230	107.0	1280	78.6	1330	107.2
1131	72.7	1181	62.4	1231	138.0	1281	79.4	1331	64.7
1132	88.9	1182	82.4	1232	44.7	1282	76.6	1332	113.0
1133	68.9	1183	38.8	1233	98.1	1283	99.4	1333	28.0
1134	94.3	1184	57.8	1234	107.1	1284	47.2	1334	61.7
1135	79.4	1185	61.2	1235	59.0	1285	60.8	1335	97.0
1136	50.1	1186	64.5	1236	98.6	1286	105.7	1336	86.0
1137	88.3	1187	128.6	1237	28.4	1287	79.6	1337	60.2
1138	89.2	1188	73.6	1238	86.6	1288	58.0	1338	73.6
1139	75.7	1189	61.9	1239	86.0	1289	82.9	1339	70.4

Year	P(mm)	Year	P(mm)	Year	P(mm)	Year	P(mm)	Year	P(mm)
1340	88.4	1390	84.6	1440	41.0	1490	70.1	1540	75.0
1341	97.0	1391	58.9	1441	77.1	1491	65.9	1541	60.3
1342	89.5	1392	84.1	1442	88.5	1492	99.5	1542	100.2
1343	80.2	1393	84.1	1443	128.7	1493	71.0	1543	97.6
1344	56.5	1394	102.8	1444	66.1	1494	98.8	1544	37.9
1345	88.3	1395	72.2	1445	58.0	1495	66.2	1545	63.1
1346	53.2	1396	43.7	1446	46.7	1496	66.7	1546	113.3
1347	63.3	1397	69.5	1447	50.7	1497	68.8	1547	109.5
1348	102.9	1398	92.2	1448	82.8	1498	107.1	1548	60.7
1349	73.5	1399	122.7	1449	95.0	1499	72.7	1549	58.5
1350	81.2	1400	68.3	1450	98.4	1500	62.2	1550	57.0
1351	65.6	1401	42.9	1451	87.8	1501	43.0	1551	60.6
1352	81.3	1402	73.2	1452	90.0	1502	95.0	1552	77.8
1353	79.0	1403	69.5	1453	96.9	1503	111.0	1553	79.3
1354	84.3	1404	102.3	1454	103.2	1504	100.5	1554	94.8
1355	94.1	1405	58.1	1455	34.8	1505	42.1	1555	58.1
1356	84.0	1406	54.7	1456	59.9	1506	60.1	1556	107.2
1357	70.2	1407	63.7	1457	54.2	1507	90.8	1557	78.7
1358	57.7	1408	70.8	1458	58.2	1508	81.5	1558	77.1
1359	71.3	1409	123.8	1459	118.7	1509	68.0	1559	83.6
1360	96.3	1410	61.5	1460	121.0	1510	87.4	1560	58.5
1361	69.0	1411	91.7	1461	69.6	1511	78.2	1561	64.4
1362	62.0	1412	73.5	1462	70.1	1512	59.5	1562	82.8
1363	55.5	1413	64.3	1463	52.6	1513	66.4	1563	62.9
1364	70.6	1414	84.8	1464	72.4	1514	90.4	1564	88.8
1365	85.9	1415	67.4	1465	86.6	1515	80.6	1565	58.8
1366	51.9	1416	65.0	1466	132.9	1516	76.8	1566	129.9
1367	86.2	1417	97.0	1467	82.8	1517	79.4	1567	72.7
1368	91.4	1418	117.2	1468	56.3	1518	78.6	1568	56.8
1369	79.0	1419	109.4	1469	51.7	1519	80.3	1569	122.2
1370	75.8	1420	46.6	1470	73.8	1520	59.1	1570	90.7
1371	46.6	1421	41.1	1471	77.5	1521	56.4	1571	40.5
1372	80.4	1422	50.4	1472	69.6	1522	40.5	1572	57.9
1373	85.5	1423	122.0	1473	61.9	1523	114.9	1573	48.9
1374	106.2	1424	64.2	1474	70.6	1524	82.3	1574	106.2
1375	74.7	1425	90.9	1475	70.8	1525	134.2	1575	81.4
1376	63.5	1426	48.4	1476	97.7	1526	105.3	1576	87.7
1377	69.7	1427	61.4	1477	94.3	1527	88.1	1577	91.9
1378	62.8	1428	112.3	1478	109.4	1528	45.9	1578	78.6
1379	60.2	1429	63.8	1479	73.9	1529	59.4	1579	73.2
1380	68.2	1430	68.3	1480	66.7	1530	76.1	1580	61.0
1381	93.3	1431	89.9	1481	62.1	1531	37.4	1581	46.8
1382	90.5	1432	90.0	1482	58.3	1532	81.3	1582	125.8
1383	92.7	1433	85.7	1483	58.2	1533	110.5	1583	98.0
1384	58.8	1434	73.2	1484	73.3	1534	49.2	1584	98.4
1385	59.4	1435	93.0	1485	101.5	1535	119.1	1585	29.8
1386	82.9	1436	103.7	1486	85.5	1536	69.7	1586	65.0
1387	84.1	1437	72.9	1487	96.7	1537	81.8	1587	92.3
1388	58.8	1438	69.7	1488	69.1	1538	93.6	1588	62.4
1389	92.1	1439	45.3	1489	62.8	1539	56.0	1589	84.9

Year	P(mm)	Year	P(mm)	Year	P(mm)	Year	P(mm)	Year	P(mm)
1590	74.2	1640	64.2	1690	89.6	1740	73.2	1790	77.3
1591	48.9	1641	124.4	1691	79.5	1741	66.1	1791	71.8
1592	127.5	1642	103.6	1692	72.7	1742	70.4	1792	74.4
1593	69.3	1643	105.4	1693	70.3	1743	73.8	1793	79.8
1594	116.4	1644	68.4	1694	83.5	1744	90.0	1794	32.7
1595	52.1	1645	52.2	1695	99.9	1745	105.2	1795	133.8
1596	54.9	1646	101.3	1696	52.1	1746	48.5	1796	100.0
1597	89.1	1647	73.4	1697	68.9	1747	84.7	1797	69.4
1598	93.1	1648	63.8	1698	84.6	1748	84.9	1798	73.0
1599	68.6	1649	59.1	1699	57.1	1749	82.7	1799	81.2
1600	39.9	1650	33.5	1700	96.0	1750	45.3	1800	83.8
1601	101.4	1651	60.2	1701	53.2	1751	69.8	1801	51.8
1602	66.3	1652	130.5	1702	79.2	1752	65.3	1802	50.9
1603	73.3	1653	80.9	1703	52.8	1753	113.8	1803	54.5
1604	98.3	1654	61.4	1704	96.6	1754	72.8	1804	113.9
1605	124.4	1655	83.5	1705	107.4	1755	101.2	1805	122.5
1606	61.1	1656	96.6	1706	82.6	1756	76.5	1806	57.8
1607	50.6	1657	135.0	1707	63.7	1757	40.4	1807	60.6
1608	51.7	1658	75.2	1708	34.4	1758	76.3	1808	62.9
1609	68.4	1659	107.6	1709	90.2	1759	57.3	1809	60.6
1610	94.2	1660	17.5	1710	117.2	1760	89.4	1810	58.5
1611	85.4	1661	69.1	1711	67.2	1761	70.3	1811	116.8
1612	83.7	1662	70.3	1712	107.9	1762	101.6	1812	95.3
1613	90.3	1663	40.6	1713	65.0	1763	100.6	1813	88.7
1614	89.7	1664	51.4	1714	91.3	1764	50.7	1814	79.6
1615	44.2	1665	53.5	1715	52.1	1765	63.6	1815	55.1
1616	103.7	1666	66.9	1716	36.8	1766	99.1	1816	109.6
1617	54.8	1667	116.4	1717	80.6	1767	93.2	1817	105.3
1618	53.7	1668	74.8	1718	64.3	1768	97.2	1818	54.0
1619	86.2	1669	103.2	1719	73.8	1769	58.4	1819	72.2
1620	82.8	1670	92.2	1720	87.7	1770	60.7	1820	59.9
1621	79.8	1671	62.2	1721	104.6	1771	72.4	1821	82.5
1622	70.5	1672	72.6	1722	85.3	1772	61.5	1822	107.5
1623	64.5	1673	71.8	1723	90.9	1773	78.8	1823	41.5
1624	104.9	1674	91.8	1724	92.8	1774	85.5	1824	57.5
1625	89.3	1675	79.9	1725	60.1	1775	71.7	1825	67.2
1626	75.4	1676	46.3	1726	59.7	1776	72.9	1826	78.6
1627	52.5	1677	59.1	1727	61.9	1777	68.8	1827	88.5
1628	66.6	1678	131.9	1728	42.7	1778	95.0	1828	79.6
1629	122.8	1679	70.1	1729	106.9	1779	66.1	1829	106.2
1630	60.2	1680	46.1	1730	98.3	1780	68.3	1830	64.7
1631	101.9	1681	76.1	1731	114.8	1781	89.8	1831	78.7
1632	80.6	1682	86.2	1732	55.2	1782	43.4	1832	77.5
1633	55.5	1683	78.9	1733	48.8	1783	117.8	1833	67.7
1634	60.9	1684	58.0	1734	60.2	1784	87.4	1834	42.7
1635	84.0	1685	124.0	1735	86.0	1785	61.2	1835	102.7
1636	77.0	1686	48.2	1736	89.6	1786	86.4	1836	56.0
1637	49.5	1687	32.9	1737	89.3	1787	110.1	1837	101.6
1638	43.0	1688	56.6	1738	69.6	1788	32.4	1838	70.5
1639	84.4	1689	142.0	1739	80.3	1789	93.4	1839	93.1

Year	P(mm)	Year	P(mm)	Year	P(mm)
1840	60.2	1890	54.5	1940	106.2
1841	104.1	1891	67.6	1941	76.5
1842	65.5	1892	67.7	1942	69.0
1843	69.4	1893	61.8	1943	114.6
1844	76.3	1894	54.7	1944	78.6
1845	63.4	1895	48.8	1945	53.9
1846	50.1	1896	81.5	1946	70.3
1847	88.3	1897	130.5	1947	27.8
1848	101.0	1898	72.4	1948	90.5
1849	91.7	1899	51.6	1949	77.5
1850	109.1	1900	87.4	1950	77.9
1851	38.2	1901	99.5	1951	68.7
1852	70.5	1902	77.0	1952	83.1
1853	60.2	1903	108.9	1953	93.4
1854	100.5	1904	50.6	1954	118.8
1855	54.2	1905	86.5	1955	40.5
1856	68.5	1906	93.8	1956	106.5
1857	93.1	1907	69.7	1957	53.3
1858	115.0	1908	63.9	1958	65.3
1859	93.7	1909	58.8	1959	97.6
1860	104.0	1910	94.0	1960	92.7
1861	55.1	1911	99.4	1961	84.4
1862	46.5	1912	51.9	1962	50.6
1863	64.7	1913	87.5	1963	78.6
1864	60.7	1914	110.3	1964	83.1
1865	91.4	1915	44.7	1965	59.7
1866	46.4	1916	54.1	1966	80.1
1867	56.9	1917	84.2	1967	88.7
1868	60.1	1918	47.8	1968	63.9
1869	65.0	1919	72.2	1969	59.1
1870	85.2	1920	77.0	1970	89.4
1871	107.8	1921	94.6	1971	97.0
1872	92.4	1922	97.6	1972	78.7
1873	96.1	1923	93.1	1973	73.9
1874	63.2	1924	118.1	1974	70.3
1875	56.1	1925	101.5	1975	79.1
1876	78.9	1926	75.5	1976	82.6
1877	98.7	1927	47.1	1977	76.9
1878	75.4	1928	38.6	1978	83.1
1879	58.6	1929	52.4	1979	81.9
1880	68.5	1930	47.7	1980	84.3
1881	122.0	1931	100.1	1981	60.2
1882	71.4	1932	85.3	1982	63.8
1883	72.4	1933	94.8	1983	79.5
1884	88.2	1934	64.7	1984	65.9
1885	83.5	1935	42.9	1985	71.2
1886	90.1	1936	134.6	1986	78.2
1887	38.9	1937	88.2	1987	97.7
1888	72.0	1938	67.0	1988	67.5
1889	123.2	1939	70.3	1989	55.6

REFERENCES CITED

Akkemik, Ü, N. Dağdeviren, and A. Aras. 2005. A preliminary reconstruction (A.D. 1635-2000) of spring precipitation using oak tree rings in the western Black Sea region of Turkey. DOI: 10.1007/s00484-004-0249-8. *International Journal of Biometeorology* 49:297-302.

Atalay, İ. 2002. *Türkiye'nin Ekolojik Bölgeleri (Ecoregions of Turkey).* T. C. Orman Bakanlığı Yayınları No: 163. Izmir: Meta Basımevi.

Baillie, M. G. L. 1982. *Tree-Ring Dating and Archaeology*. Chicago: University of Chicago Press.

Baillie, M. G. L. 1995. *A Slice Through Time.* London: B.T. Batsford, Ltd.

Baillie, M. G. L., and J. R. Pilcher. 1973. A simple cross-dating program for tree-ring research. *Tree-Ring Bulletin* 33:7-14.

Briffa, K. R. 1999. Interpreting high-resolution proxy climate data–the example of dendroclimatology. In *Analysis of Climate Variability,* eds. H. von Storch and A. Navarra, 2nd edition, 77-94. Berlin: Springer Verlag.

Cook, E. R., and R. L. Holmes. 1999. Users Manual for Program ARSTAN, February 1999 edition. Tucson: Laboratory of Tree-Ring Research, University of Arizona.

Cook, E. R., and L. A. Kairiukstis, eds. 1989. *Methods of Dendrochronology*. Dordrecht: Kluwer Academic Publishers.

Cook, E. R., and K. Peters. 1997. Calculating unbiased tree-ring indices for the study of climatic and environmental change. *The Holocene* 7:361-370.

D'Arrigo, R., and H. M. Cullen. 2001. A 350-year (AD 1628-1980) reconstruction of Turkish precipitation. *Dendrochronologia* 19(2):169-177.

Davis, P. H. 1982. *Flora of Turkey and the East Aegean islands,* Vol 7. Edinburgh: Edinburgh University Press.

Fagan, B. 2000. *The Little Ice Age.* New York: Basic Books.

Fritts, H. C. 1976. *Tree Rings and Climate.* London: Academic Press.

García-Suárez, A. M. 2005. The Influence of Climate Variables on Tree Ring Widths of Different Species. PhD dissertation, The Queen's University of Belfast, Northern Ireland.

Gassner, G., and F. Christiansen-Weniger. 1942. Dendroclimatologische Untersuchungen über die Jahresringentwicklung der Kiefern in Anatolien. *Nova Acta Leopoldina: Abhandlungen der Kaiserlich Leopoldinisch-Carolinisch deutschen Akademie der Naturforscher N.F.,* Band 12, Nr 80.

Gordon, G. A. 1983. Verification of dendroclimatic response. In *Climate from tree rings,* eds. M. K. Hughes, P. M. Kelly, J. R. Pilcher, and V. C. LaMarche, Jr., 58-61. Cambridge: Cambridge University Press.

Griffiths, J. F., and D. M. Driscoll. 1982. *Survey of Climatology.* Columbus: Charles E. Merrill.

Griggs, C. B. 2006. A Tale of Two: Reconstructing Climate from Tree-Rings of the North Aegean, AD 1089-1989, and Late Pleistocene to Present: Dendrochronology in Upstate New York, Ch. 3 (with A. T. DeGaetano, P. I. Kuniholm, and M. W. Newton) PhD Dissertation, Cornell University.

Griggs, C. B., A. T. DeGaetano, P. I. Kuniholm, and M. W. Newton. 2005. Phase changes of the winter North Atlantic Oscillation recorded in spatial changes in tree-ring patterns of North Aegean Oaks, AD 1190-1967. *EOS Transactions AGU* 86(52), Fall Meeting Supplement, Abstract PP41C-02.

Grove, J. M. 2004. *The Little Ice Ages*, 2nd edition, vol 1 (Routledge Studies in Physical Geography and Environment #5). London: Routledge.

Grove, J. M., and A. T. Grove. 1992. Little Ice Age climates in the eastern Mediterranean. In *European climate reconstructed from documentary data: methods and results,* ed. B. Frenzel. Palaeoclimate Research, Vol 7, Special issue: ESF Project "European Palaeoclimate and Man" 2, 45-50. Mainz: Akademie der Wissenschaften und der Literatur.

Hammond, N. 2005. Church has Frankish origin. *The London Times*, 4 January 2005.

Huber, B., and W. von Jazewitsch. 1956. Tree-ring studies of the forestry-botany Institutes of Tharandt and Munich. *Tree-Ring Bulletin* 21: 28-30.

Hughes, M. K., P. I. Kuniholm, J. K. Eischeid, G. Garfin, C. B. Griggs, and C. Latini. 2001. Aegean tree-rings signature years explained. *Tree-Ring Research* 57(1):67-73.

Hulme, M. 1992. A 1951-80 global land precipitation climatology for the evaluation of General Circulation models. *Climate Dynamics* 7: 57-72.

Hulme, M. 1994. Validation of large-scale precipitation fields in General Circulation models. In *Global precipitations and climate change,* eds. M. Desbois and F. Desalmand, 387-406. NATO ASI Series, Berlin: Springer-Verlag.

Hulme, M., T. J. Osborn, and T. C. Johns. 1998. Precipitation sensitivity to global warming: comparison of observations with HadCM2 simulations. *Geophysical Research Letters* 25:3379-3382.

Jones, P. D. 1988. Large-scale precipitation fluctuations: a comparison of grid-based and areal precipitation estimates. In *Recent Climatic Change, a regional approach,* ed. S. Gregory, 30-40. London: Belhaven Press.

Jones, P. D., and Hulme, M. 1996. Calculating regional climatic time series for temperature and precipitation: methods and illustrations. *International Journal of Climatology* 16: 361-377.

Kelly, P. M., H. H. Leuschner, K. R. Briffa, and I. C. Harris. 2002. The climatic interpretation of pan-European signature years in oak ring-width series. *The Holocene* 12(6):689-694.

Kelly, P. M., M. A. R. Munro, M. K. Hughes, and C. M. Goodess. 1989. Climate and signature in West European oaks. *Nature,* 340: 57-70.

Kramer, P. J., and T. T. Kozlowski. 1979. *Physiology of Woody Plants.* New York: Academic Press.

Kuniholm, P. I. 2000. Dendrochronologically dated Ottoman monuments. In *A Historical Archaeology of the Ottoman Empire: Breaking New Ground,* eds. U. Baram and L. Carroll, 93-136. New York: Kluwer Academic/Plenum.

Kuniholm, P. I. 1994a. Long tree-ring chronologies for the eastern Mediterranean. In *Archaeometry 94,* eds. Ş. Demirci, A. M. Özer, and G. D. Summers, 401-409. (Proceedings of the 29th International Symposium on Archaeometry, 9-14 May 1994, Ankara, Turkey). Ankara: TÜBITAK.

Kuniholm, P. I. 1994b. 1994 Aegean Dendrochronology Project Newsletter. On the website http://www.arts.cornell.edu/dendro/.

Kuniholm, P. I., and C. L. Striker. 1983. Dendrochronological investigations in the Aegean and neighboring regions, 1977-1982. *Journal of Field Archaeology* 10: 411-420.

Kuniholm, P. I., and C. L. Striker. 1987. Dendrochronological investigations in the Aegean and neighboring regions, 1983-1986. *Journal of Field Archaeology* 14:385-398.

Lamb, H. H. 1995. *Climate, History and the Modern World,* 2nd edition. London: Routledge Press.

Osborn, T. J., K. R. Briffa, and P. D. Jones. 1997. Adjusting variance for sample-size in tree-ring chronologies and other regional mean timeseries. *Dendrochronologia* 15:89-99.

Pilcher, J. R. 1995. Biological consideration in the interpretation of stable isotope ratios in oak tree-rings. In *Problems of stable isotopes in tree-rings, lake sediments and peat-bogs as climatic evidence for the Holocene,* ed. B. Frenzel, 157-161. Paleoclimate Research, vol 15. Mainz: Akademie der Wissenschaften und der Literatur.

Pilcher, J. R., and B. Gray. 1982. The relationship between oak tree ring growth and climate in Britain. *Journal of Ecology* 70: 297-304.

Pohl, R. 1997. Eine wissensbasierte Erweiterung des Programmsystems Corina zur Dendrochronologie (Unpublished version in English, *CORINA: The Cornell Ring Analysis Program,* available at the ADP laboratory). MS Thesis, Technische Universitaet, Berlin.

Schweingruber, F. H. 1990. *Anatomie europäischer Hölzer - Anatomy of European woods.* Berne and Stuttgart: Paul Haupt.

Touchan, R., E. Xoplaki, G. Funkhouser, J. Luterbacher, M. K. Hughes, N. Erkan, Ü. Akkemik, and J. Stephan. 2005. Reconstructions of spring/summer precipitation for the Eastern Mediterranean from tree-ring widths and its connection to large-scale atmospheric circulation. *Climate Dynamics* 25: 75-98.

Touchan, R., G. M. Garfin, D. M. Meko, G. Funkhouser, N. Erkan, M. K. Hughes, and B. S. Wallin. 2003. Preliminary reconstructions of spring precipitation in southwestern Turkey from tree-ring width. *International Journal of Climatology*, 23:(2)157-171. Data available at website: IGBP PAGES/World Data Center for Paleoclimatology.

Wilson, R., and W. Elling. 2004. Temporal instability in tree-growth/climate response in the Lower Bavarian Forest region: implications for dendroclimatic reconstruction, *Trees: Structure and Function* 18(1):19-28.

Wilson, R. J. S., J. Esper, and B. H. Luckman. 2004. Utilising historical tree-ring data for dendroclimatology: A case study from the Bavarian Forest, Germany, *Dendrochronologia* 21(2):53-68.

Yaltırık, Faik. 1984. Türkiye Meşleri. Istanbul: Yenilik Basımevi.

Xoplaki, E. 2002. Climate variability over the Mediterranean. Ph.D. Diss., Universität Bern, Switzerland.

Zohary, M. 1973. *Geobotanical Foundations of the Middle East,* Vols. 1 and 2 (Geobotanica selecta Band III). Stuttgart: Gustav Fischer.

CHAPTER TWO
A LOW-FREQUENCY RECONSTRUCTION OF THE NORTH ATLANTIC OSCILLATION FROM OAK TREE-RING CHRONOLOGIES IN THE NORTH AEGEAN, AD 1181-1967

by Carol B. Griggs, A.T. DeGaetano, P.I. Kuniholm, and M. W. Newton

SUMMARY

The low-frequency variance in the Gaussian-filtered North Atlantic Oscillation (NAO) May index explains 91.6% of the variance in a filtered oak tree-ring chronology from northeastern Greece and northwestern Turkey (39-42ºN lat 22-37ºE long) in the years 1915-1967. Before that period, the effect of the May NAO appears to weaken. Analyses of the tree-ring data, divided west to east into three grids of 3º latitude by 5º longitude, indicated that the response to the May NAO varies with the longitude over the region and is possibly moderated by both the winter (December-March) NAO and the annual Atlantic Multidecadal Oscillation (AMO). The May NAO is clearly recorded in the western grid chronology from 1833-1967 with the exception of 1877-1887 when its response was negative. This may be due to an extremely negative phase of the May NAO bringing little precipitation in May plus the natural response of oak ring growth to other factors that can override the limiting growth factor in such periods. Using the relationship between the three grids' filtered oak chronologies over time we here reconstruct the May NAO with periods of varying confidence levels from AD 1181 to 1967. Our 2005 collection of wood from this region will extend this analysis through 2004.

Correlations in 24-year moving windows between the grid chronologies highlight periods of similarities and periods of differences in their low-frequency tree-ring patterns over the region. The relationship changes in the same years in which there are changes in the phase of the May NAO, and also when there are similar changes in the AMO and winter NAO. The years of change indicated by this method

are used here to indicate periods of the same and periods of different response to the May NAO over the region, with an exploratory analysis of the moderation by the winter NAO and AMO. Future research will examine the effects of the AMO and winter NAO on this region and their paleoclimate record in this and our other archived tree-ring data sets extending farther back in time.

INTRODUCTION

Long-term change in climate and its effect on human history has always been an intriguing puzzle. There are many variations between the theoretical extremes that climate change has an immediate effect on human history and that climate change does not have any effect on civilization over time, but most agree that the truth is somewhere in between.[1] The focus questions are then: what kinds of climate change really affect our history; where, when, and how often do they occur; and how large is the affected region. Part of the problem with answering these questions and solving the puzzle is the human perspective of time: any climate change that persists in periods of a few months up to about two decades may be well-documented, but longer-term changes are much more difficult to interpret clearly from history.[2] Here we reconstruct the May North Atlantic Oscillation (NAO) and note its interplay with the Atlantic Multidecadal Oscillation (AMO) and the winter (December – March) NAO as is apparent in the ring growth of oak trees in the northern Aegean Sea region.

Northeastern Greece and northwestern Turkey, the region of study, is the southern boundary of the included oak species' ranges due to the limited amount of May-June precipitation. That climate parameter, the primary growth limiting factor of these oaks, explains 52.3% of the high-frequency ring-width variance for 1931-1985,

[1] Lamb 1995; Kuniholm 1990; Grove and Rackham 2001; deMenocal 2001.
[2] deMenocal 2001.

and has been reconstructed for the years AD 1089 to 1989.[3] The low frequency patterns, removed for that reconstruction, were retained in the chronologies examined here for correlations with low-frequency trends and phases in the NAO and AMO.

The NAO is a recurrent pattern of atmospheric variability, the result of pressure instabilities over the extratropical North Atlantic Ocean affecting the direction and strength of atmospheric flow.[4] This flow is affected by the placement of pressure centers on the ocean and the continents around the ocean all year long, with the greatest effect in the winter months.[5] The NAO index is the normalized difference in barometric pressure between one of two stations near the mouth of the Mediterranean Sea (~35° N latitude) and one of two stations in Iceland (~66° N latitude). The effects of the NAO on terrestrial climate over time have been examined in meteorological data plus tree-rings and other climate proxies from the continents on either side of the Atlantic Ocean.[6] The NAO's quasi-cyclic lengths of about 2.2, 8.8, and 24 years[7] have been found in tree-rings in Turkey;[8] the winter NAO accounts for 27% of the variance in streamflow in the Tigris and Euphrates river systems in eastern Turkey, Syria, and Iraq;[9] the Aegean Sea has been cited as having a bimodal effect on the winter NAO;[10] and sea-level variability in the Mediterranean has been linked to changes in the NAO in the last half of the 20th century.[11]

The AMO is a low-frequency cycle that is influenced by the strength of the NAO, which affects the temperature of the surface ocean layer and thus the thermohaline circulation.[12] The AMO index is a measure of the differences in sea

[3] Griggs et al., 2006.
[4] Walker and Bliss 1932; Sutton and Hodson 2003; Hurrell et al., 2003.
[5] Barnston and Livezey 1979.
[6] Hurrell et al., 2003; Cook et al., 1998; 2002, D'Arrigo et al., 1993, 2001; Appenzeller 1998.
[7] Jones et al., 1997, 2003; Hurrell 1995.
[8] D'Arrigo and Cullen 2002.
[9] Cullen and deMenocal 2000.
[10] Zervakis et al., 2004.
[11] Tsimplis and Josey 2001.
[12] Kerr 2000; Gray et al., 2004.

surface temperatures (SST) over the North Atlantic, and its cycle length is 40-60 years. The SST is closely interrelated to sea-level pressure (SLP), and the complex relationship between the AMO and the NAO makes causality difficult to determine.[13]

In our reconstruction of the annual May-June precipitation,[14] we found that the May NAO index explains 14.9% of the high-frequency variance in the tree-ring growth during the last century. The May NAO affects the location of persistent pressure centers around the Atlantic Ocean, thus the precipitation and temperature of the growing season in any particular locale, yet annual variation in the May NAO is not consistently recorded in the regional tree ring chronology. This indicates that the NAO often has different effects over the region due to the 15 degrees of longitude in the study area as well as its phase and strength over time. This obscures the annual variation on the regional scale. A division of the master chronology into three 5º longitude filtered grid chronologies focused on the low-frequency (multi-decadal) variance component unique to each grid. The correlation between the western grid chronology and the filtered May NAO index is significantly positive (Figure 2.1).[15] Between the eastern grid chronology and the May NAO the correlation is significant but positive in certain periods and negative in other periods. The central grid chronology's relationship to the NAO is more complex, but supplies a third dimension to our reconstruction by adding a small amount to the variance explained, especially during periods of different trends between the chronologies. We here reconstruct the low-frequency patterns of the May NAO back to AD 1181, with differing levels of confidence contingent upon the periods of reconstruction, and compare it with Luterbacher's May NAO reconstruction of AD 1670 to 2001.[16]

---

[13] Sutton and Hodson 2005.
[14] Griggs et al., 2006.
[15] A resampled Monte Carlo test was used to determine the significance levels of correlations between all filtered data sets. The significance level is $p < 0.05$.
[16] Luterbacher et al., 1999.

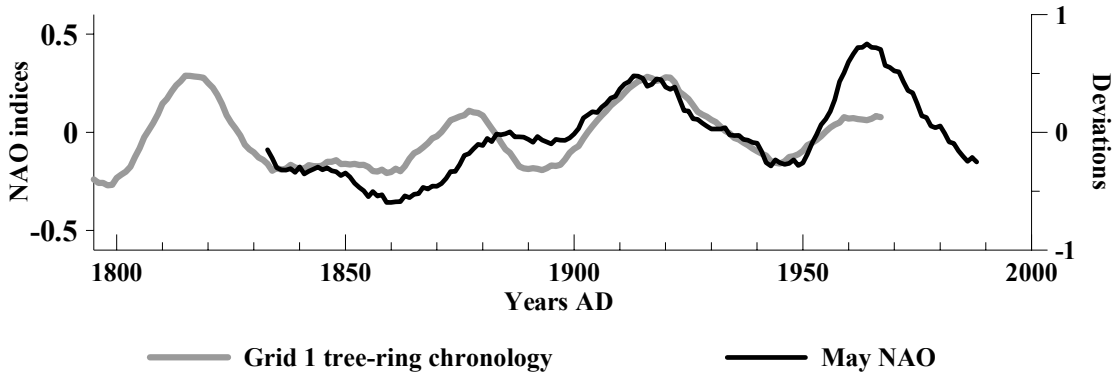

Figure 2.1. The Gaussian-filtered May NAO and western grid tree-ring chronology. Their correlation coefficient is 0.735, with $p < 0.05$, tested in a Monte Carlo simulation.

THE DATA

The region

The wood samples were collected from forest and building sites in northeastern Greece and northwestern Turkey, 39 to 42º N latitude, 22 to 37º E longitude (Figure 2.2). The 3° latitude by 15º longitude study region was divided into three grids, described below. The character of each grid's ecosystem(s) is influenced by its continentality and relationship to the Aegean, Marmara, and Black seas.[17]

The western grid (G1) is composed of sites around Thessaloniki, Greece, from 22-26˚ E. This grid includes the northwest corner of the Aegean Sea, with the Pindus and Rhodope Mountains to the west and north, respectively. The prevailing westerly atmospheric flow results in a relatively continental climate.

The middle grid (G2), centered on Istanbul, Turkey, contains wood from northeastern Greece and northwestern Turkey at 26-32˚E longitude. There is much more coastal influence on this grid's climate. The included oak forests are inland, one at ~70m, lower than all others, and the other at ~750m altitude.

[17] Atalay 2002.

The eastern grid (G3) contains wood from sites located within 32 to 37˚ E longitude, in northern central Turkey along the north side of the Anatolian Plateau and south of the Black Sea (Figures 2.2 and 2.3). It is a continental region with the eastern boundary at approximately the western boundary of the headwaters of the Tigris-Euphrates watershed in Turkey[18] where the higher precipitation is brought in by the prevailing westerly atmospheric flow across the Black Sea.

Monthly station temperature and precipitation data of the entire study region indicate a similar amount of May-June precipitation over the region, with a minimum precipitation of approximately 60mm and a slight increase from west to east. The climate is a mesothermic subhumid regime, bordering on the hotter Mediterranean regime to the south.[19]

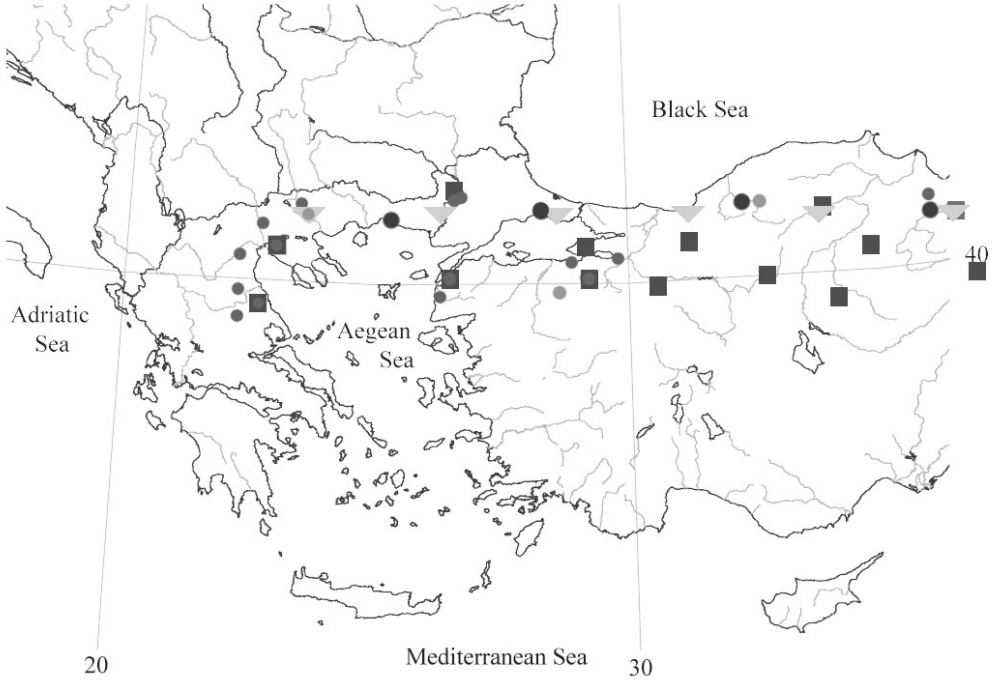

Figure 2.2. A map of the location of the forest and historic sites (round), meteorological stations (square) and centers of the CRU climate data grids (triangles) are shown here.

[18] Zohary 1973; Cullen et al., 2000, 2002.
[19] Griggs et al., (2006) in review.

The tree-ring data

The 511 tree-ring sections and cores come from 7 modern forest chronologies and 49 historic chronologies from 38 buildings[20] (Figures 2.2 and 2.3, Table 1.1). The ring count of the historic building samples ranges from 39 to 357 and the forest samples from 61 to 362. The 56 historic site and forest chronologies range from 59 to 787 years in length (Figure 2.3). The average sample length is 110 years, an indicator that low-frequency cycles of up to 55 years in length are preserved in the combined master chronology.[21]

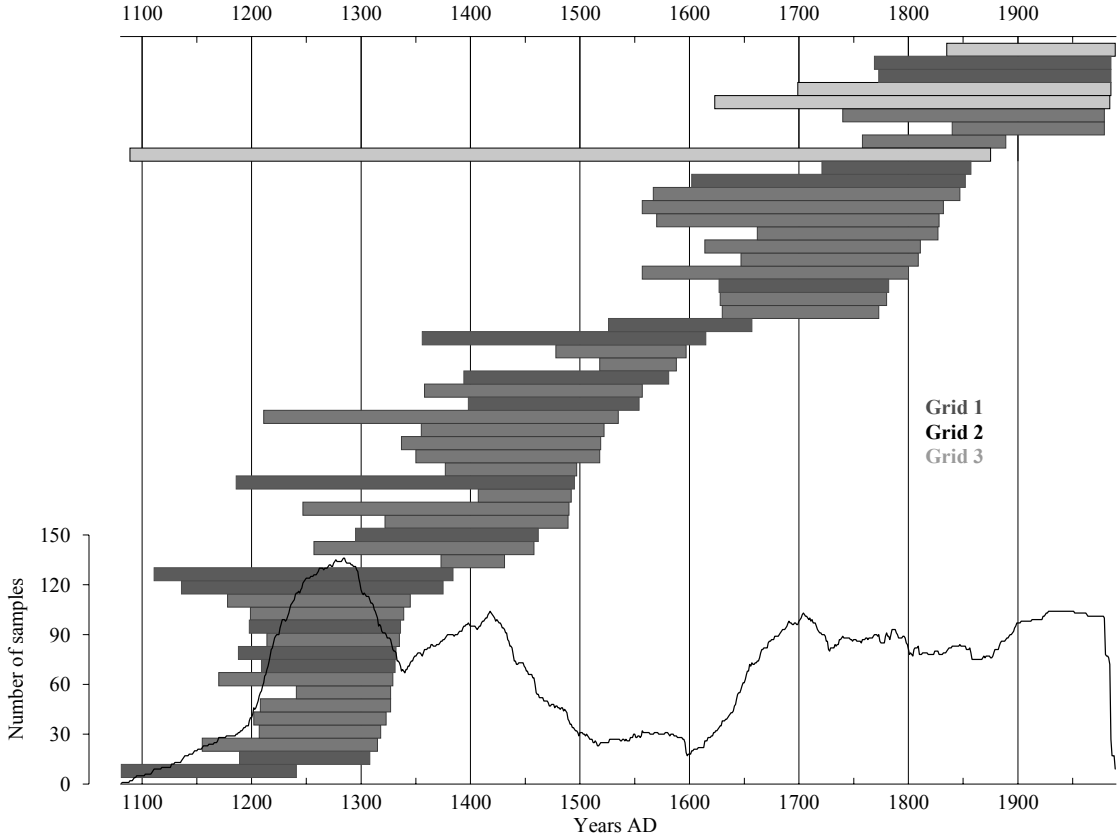

Figure 2.3. The historic and forest chronologies' dates and the number of samples over time. The grid represented by medium gray is the western grid (G1); black is the center grid (G2); and light gray is the eastern grid (G3). See Figure 2.2 and Table 1.1 for site locations

[20] Kuniholm and Striker 1983, 1987; Kuniholm, 1994, 2000; list is available on website http://www.arts.cornell.edu/dendro/
[21] Cook et al., 1995.

Table 2.1. The oak species represented by the forest samples.

***Quercus* species:**
Q. frainetto (= Q. conferta)
Q. hartwissiana
Q. petraea
Q. petraea iberica (= *Q. dschoruchensis*)
Q. petraea petraea (= *Q. sessiliflora*)
Q. robur

The included forest oak species are listed in Table 2.1. From the climatology of the region, the forest species' ranges, and the secure crossdating between the forest and historic chronologies, it was concluded that at least the majority and possibly all of the samples are of the same mesothermic species. The southern borders of the included oak species' ranges are dictated by the minimum May-June precipitation. Xeric oak species are common in the hotter Mediterranean climate zones directly to the south.[22]

The source of the wood in each historic building was considered in dividing the tree-ring data into their respective grids for an accurate spatial interpretation of variations in climate response over the 15º longitudinal range. The Grid 3 historic wood is certainly all from that grid due to the one historic site's close proximity to modern oak forests, but each historic site in grids 1 and 2 could contain data from logs transported to the site from within its own, or from any other, grid. However, each site chronology crossdates the best with the other chronologies from sites in the same grid, and less securely with chronologies from sites outside of its grid (Table 2.2). We are therefore confident with the assumption that the wood in each building was felled from a source within the building's grid rather than within another grid.

[22] Zohary 1973; Davis 1982. A detailed discussion about the species involved is in Griggs et al., 2005.

Table 2.2. Average correlations between sites within the same grid and from the other grids.

	Average correlation	N
Within:		
G1	0.291	211
G2	0.247	64
G3	0.328	5
Between:		
G1 and G2	0.192	252
G1 and G3	0.130	48
G2 and G3	0.220	24

Climate data

Monthly NAO data were downloaded from the website of the Climatic Research Unit (CRU) at the University of East Anglia.[23] The CRU data were calculated from differences between the instrumental air pressure records from stations in Iceland and stations in Gibraltar and the Azores and is the data set discussed throughout this paper. Reconstructed NAO monthly and seasonal indices were downloaded from the National Oceanic and Atmospheric Administration (NOAA) Paleoclimate website.[24] Luterbacher's monthly NAO reconstruction goes back to 1675, based mainly on historical records of pressure, temperature, and precipitation primarily over central Europe back to 1780, then proxy data from tree rings, ice cores, etc., plus a few historical records prior to 1780.[25] This reconstruction is hereafter labeled "L NAO."

The Atlantic Multidecadal Oscillation (AMO) index and a reconstruction of that index from tree-rings by Gray et al.,[26] were also downloaded and explored for

[23] Jones et al., 1997; data available at http://www.cru.uea.ac.uk/, Climatic Research Unit, Univ. of East Anglia, UK.
[24] Luterbacher et al., 1999; Cook et al., 2002, available at http://www.ncdc.noaa.gov/paleo/
[25] Luterbacher et al., 1999; Jones et al., 1999, proxy data from the European ADVICE project (Annual to Decadal Variability in Climate in Europe).
[26] Gray et al., 2003, available at http://www.ncdc.noaa.gov/paleo/paleo.html

their record in the oak ring growth (referred to as "G AMO"). The reconstruction of the AMO back to 1657 based on tree-ring chronologies from "hot spots" of North Atlantic sea-surface temperature variability included three chronologies of conifers from the eastern Mediterranean.[27] Two are chronologies of samples from southwestern Turkey, measured and processed at our lab, and the other is of Jordanian samples.

The monthly NAO indices plus the averaged December-March NAO indices were used for this analysis. The AMO annual values were used due to the monthly values' similarity throughout the year.[28] The reconstructed NAO and AMO indices were used in a comparison of the timing of their reversals to the timing of the reversals in the relationships between the two outer grid chronologies over time.

METHODS AND RESULTS

Tree-rings

Of the 511 samples, 372 samples' measurements were detrended by fitting a negative exponential curve to remove the normal decrease in ring widths over each tree's lifespan. For the other 139 samples, the negative curve did not fit well and each sample was conservatively detrended with an appropriate linear, polynomial, or cubic spline curve.[29] The detrended sample data were combined into site chronologies; the site chronologies were normalized to enhance the variance contained in their common signal[30] and then averaged together into the master chronology (Figure 2.4). Variance was adjusted over the chronology's 910-year length according to the average r-values between the included site chronologies in each year.[31] For each of the three grids,

[27] Gray et al., 2004.
[28] Kaplan et al., 1998.
[29] Cook and Kairiukstis 1989.
[30] Griggs et al., 2006.
[31] Cook 1985; Osborn et al., 1997, ARSTAN program available at http://www.ldeo.columbia.edu/res/fac/trl/public/publicSoftware.html

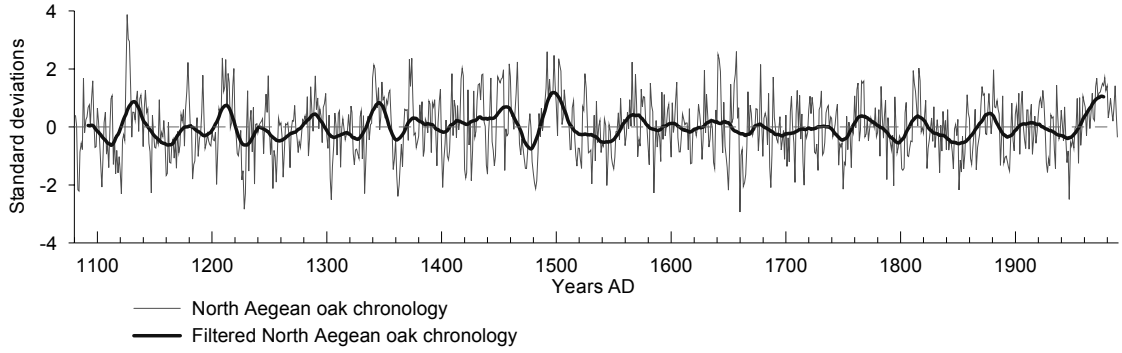

Figure 2.4. Master North Aegean oak tree-ring chronology and its 24-kernel Gaussian filter.

their site chronologies were similarly averaged together and variance was adjusted (Figures 2.5A, B, and C).[32] Figures 2.5D and E show the expressed population size (EPS)[33] of the chronologies and their standard error values over time. The master chronology has a high EPS except for the 1550-1650s, which is obviously exacerbated in the grid chronologies. In this analysis, the results of the period 1450-1650 are only tentative. The EPS below 0.80[34] of Grid 1 in the 20th century is due to either the locations of the two included forest sites at the east and west ends of the grid or to species difference, or both. The ring-width measurements of additional forest samples collected in 2005 will allow us to check those values and modify them if necessary.

Climate

The NAO and AMO data sets were standardized using the mean and standard deviations over their complete length. The filtering method is described below.

[32] The Grid 3 chronology contains only one site up to the 17th century. The between-sample correlations were used for adjustment up to 1700, then between-site correlations for the following years. This may need to be checked and adjusted, but it is not going to affect results to any significant extent.
[33] Briffa and Jones 1989, p.146. The EPS is calculated from (the mean correlation between samples times the number of samples) divided by (the same plus one minus the mean correlation), and is an indicator of the degree to which the chronology portrays the hypothetical perfect chronology.
[34] *Ibid.* Our break-off line at 0.80 is arbitrary, but reasonable for the use of deciduous trees and the mean correlation value of ~ 0.25 between samples.

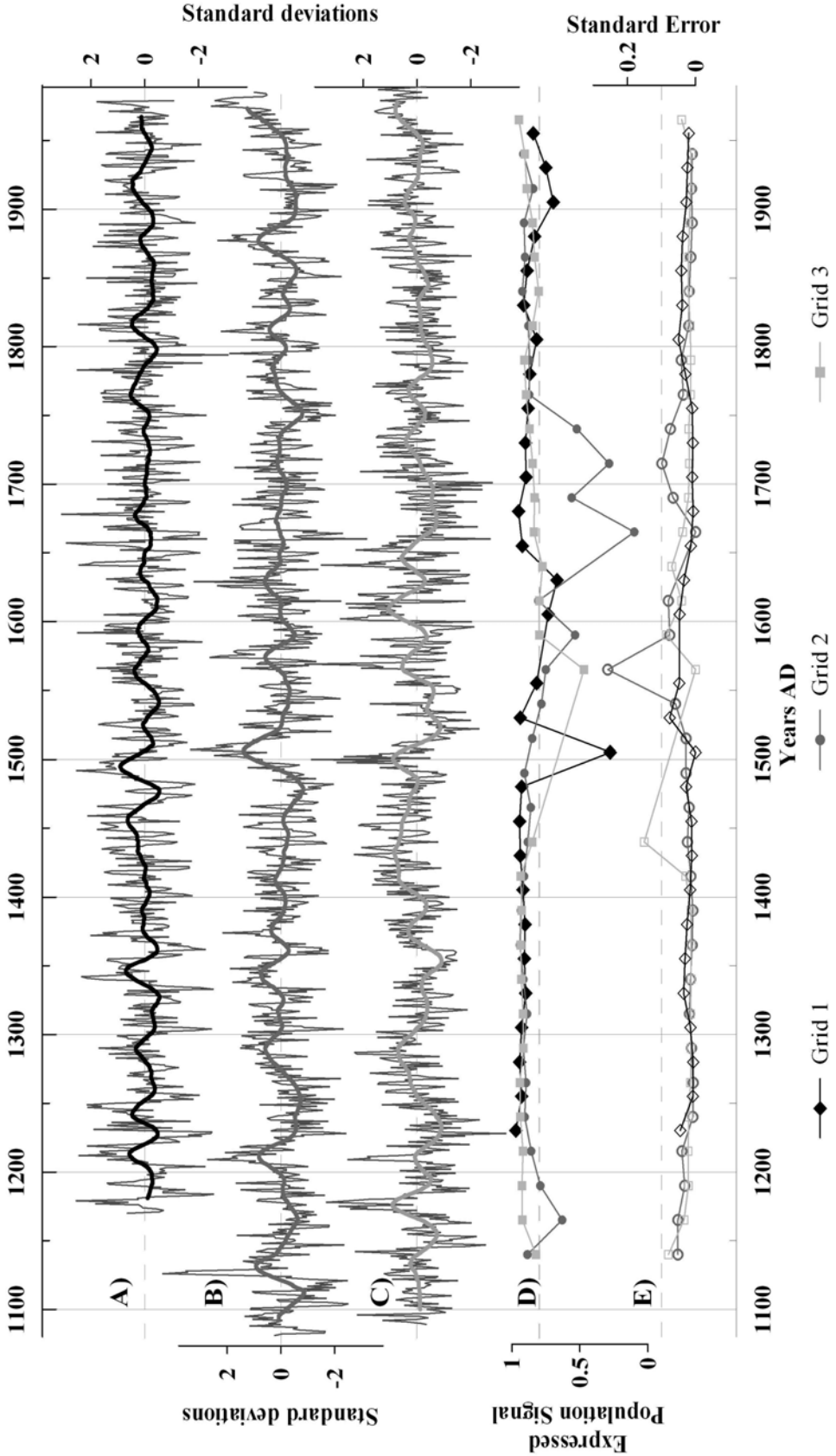

Figure 2.5. A, B, C. Grids 1, 2, and 3 chronologies from the west, center and east sections of the study region, respectively, and their 24-kernel Gaussian filtered chronologies. D and E. The EPS and standard error values of each grid chronology, discussed in the text.

Climate *vs.* tree-ring analysis

Correlations between the unfiltered (high-frequency) complete oak chronology and the NAO indices and the AMO index indicated April and May NAO as possible significant forces, their correlations at the 95% level in the 20th century (Table 2.3). With the full length of the period shared by the two data sets, 1821-1985, the correlation of the chronology with the May NAO decreases slightly, but that value is at the 99% level due to the longer segment length. The response to the April NAO decreased to just above the 90% level (Table 2.3). The winter and June NAO *vs.* the tree-ring chronology correlations are not significant in either case; and the AMO index *vs.* tree-rings only in the 20th century. The May NAO was examined as the most likely, continual limiting factor in the low-frequency variance, but the April, summer, and winter months' NAO and the AMO were all examined as possible effective forces over time.

Table 2.3. Correlations with probability values of the unfiltered master chronology and the indicated NAO and AMO indices for 1915-1985, and over the complete instrumental period. The winter NAO includes the months of December through March. The April NAO correlation is the highest in the 20th century, but its impact is not consistent over time. The May NAO correlation is borderline at the 95% level in the 20th century, but is significant in the complete set. The AMO correlation is significant at the 90% level in the 20th, but also has less direct effect in the 19th century.

	NAO Index				**AMO Index**
1915-1985	Winter	April	May	June	Annual
r	-0.073	-0.272	0.225	0.126	-0.196
p	0.532	0.018	0.052	0.282	0.092
1821-1985					
r	-0.042	-0.138	0.207	-0.004	-0.071
p	0.600	0.085	0.009	0.964	0.443

Table 2.4. The kernels and weights used in the 24-year Gaussian filter.

Kernels	Weights
±1	0.0156
±2	0.0198
±3	0.0245
±4	0.0297
±5	0.0353
±6	0.0409
±7	0.0463
±8	0.0513
±9	0.0556
±10	0.0588
±11	0.0608
±12	0.0615

All the data sets were filtered with a twenty-four kernel Gaussian filter (24GF), the approximate length of one NAO quasi-cycle,[35] to emphasize and preserve low-frequency patterns.[36] The kernels and weights are listed in Table 2.4. This process reduced the period in common between the tree-rings and the NAO indices to 135 years, AD 1833-1967. The Monte Carlo test was done with the full 135-year data sets (Table 2.5C).

Running correlations of windows 24 years in length were calculated between the three filtered and unfiltered grid chronologies along their total lengths (G1 *vs.* G2, G2 *vs.* G3, and G1 *vs.* G3, see Figure 2.6A or 2.9). The autocorrelation of the unfiltered data sets was tested, and the G1 chronology has none, the G3 chronology has a marginal amount, and the G2 chronology is highly autocorrelated. The significance levels of the correlations between serially-correlated data sets,[37] with or without autocorrelation, were determined by Monte Carlo random resampling of the paired G1, G2, and G3 unfiltered grid chronologies individually and in blocks[38] 10,000 times each. The data sets were paired to retain their spatial relationships. The randomized

[35] D'Arrigo and Cullen 2001.
[36] Jones et al., 2003; Gray et al., 2004. The indicated year is the 12th year of the included data.
[37] Enfield et al., 2001; Jones et al., 2003; Jones personal comm. 2005.
[38] Wilks 1997; the number of four is here arbitrarily chosen.

data sets were filtered, then running correlations calculated between each filtered set with the real filtered chronology of the other two grids. For the individually randomized sets, length of 24, the 90% significance levels indicate that the individual values in the running correlation sets are not often highly significant (Table 2.5B), an

Table 2.5. Results of tests for the significance levels of the filtered tree-ring data sets using our data with Monte Carlo resampling techniques. A**.** Significance levels for correlations between the paired filtered sets of G1 *vs.* G3 for the complete 135-year length. B**.** The Monte Carlo tests for the significance of the maximum and minimum plus differences between those values in the running correlations (N=24) between the filtered grids, 1833-1967. C**.** The number of crossings *r*-values of 0.2 and 0.4 in each correlation. See text about the nature of the random data sets.

A.

		r cutoff values	
Percentile	Count	Positive	Negative
0.05	500	0.537	-0.535
0.025	250	0.612	-0.612
0.005	50	0.735	-0.725
0.0005	5	0.837	-0.817

B.	Maximum running correlations		Minimum running correlations		Max-min differences	
	Observed	90%-ile	Observed	90%-ile	Observed	90%-ile
G1 *vs*. G2	*0.995	0.991	-0.625	-0.976	1.620	1.942
G1 *vs*. G3	0.960	0.993	-0.816	-0.967	1.775	1.936
G2 *vs*. G3	*0.998	0.994	*-0.997	-0.961	*1.995	1.932

C.	Number of r = 0.2 crossings		Number of r = 0.4 crossings	
	Observed	90%-ile	Observed	90%-ile
G1 *vs*. G3	4	4	4	4
G1 *vs*. G2	2	4	2	4
G2 *vs*. G3	3	4	2	4

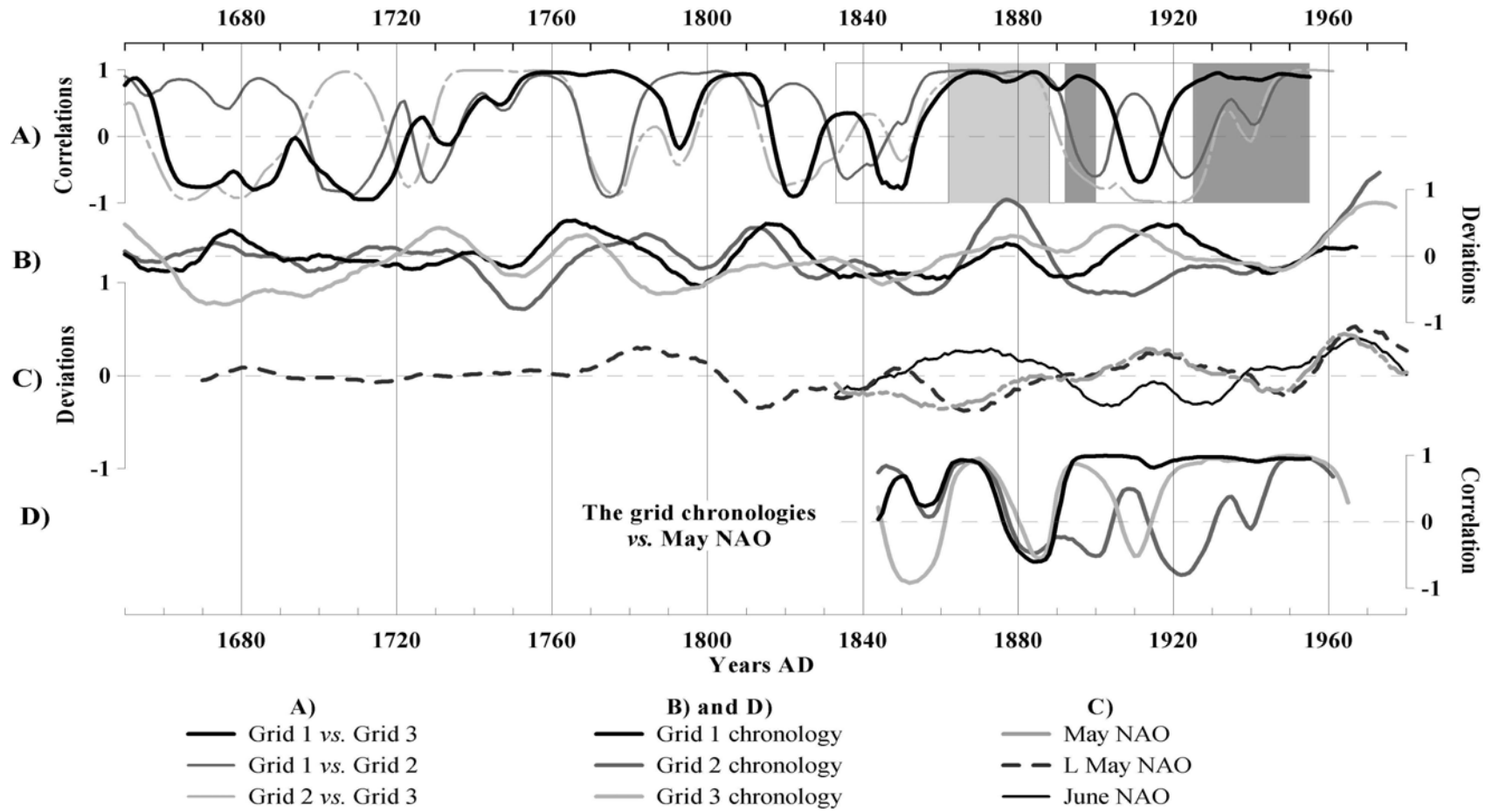

Figure 2.6. A. The 24-year window correlations between grid chronologies. B. The filtered grid chronologies. C. The May and June NAO indices and the reconstructed May NAO indices. D. The 24-year window correlations between the three grids and the May NAO. The colors of the lines match the colors of their respective grid chronologies in B. Note the similarities in the correlations of G1 *vs.* G2 and G3 and between May and those two grids except for in the 1870-1890 segment.

expected result with the high serial correlation of filtered data. We tested for the significance of two other characteristics of these correlation sets: the number of times the correlations cross over the values of 0.2 and 0.4. The results are marginally significant, at the 90% level, for correlations between G1 and G3 sets (Table 2.5C). Running correlations were also calculated between each of the grid chronologies and the May NAO index (Figure 2.6D). These correlations were also tested in a Monte Carlo random test, using the same filtered random sets of the grid chronologies and calculating their running correlations with the filtered May NAO data set to test for significance levels. The results are also similar to those calculated between the serially correlated grid chronologies discussed above. Here we tested whether the number of times the running correlations are above 0.90 for 1844-1955 was random. Both of the running correlations G1 *vs.* May NAO and G3 *vs.* May NAO contain a large number of years with *r*-values greater than 0.90. Both of those numbers are greater than its count in the 90th percentile of running correlations between the randomized grid chronologies and the May NAO (Table 2.6). That number in the G2 *vs.* May NAO was smaller than the random count.

All the following correlation values are significant at the $p < 0.05$ level unless otherwise noted.

Table 2.6. The Monte Carlo random test showing that the value of greater than the median value of 0.90 for running correlation coefficients between two sets of random values is statistically significant for both G1 and G3 *vs.* the May NAO.

May NAO *vs.*	Number of running correlations > 0.90 Observed	90th percentile
G1	68	39
G2	17	39
G3	47	39

The reconstruction of the May NAO from the tree rings

The correlation of 0.73 between the G1 chronology and the May NAO along with a visual inspection of the two (Table 2.5, Figure 2.1) indicate that the NAO is well-recorded in that grid's tree-ring chronology, but that the varying strength of the NAO results in varying degrees of amplitude of the response in the tree-rings over time. An adjustment of the data according to the strength of the NAO at any given time is needed. From the running correlations between the grids and the May NAO (Figure 2.6E) it appears that the longitudinal variation in the grids' chronologies does reflect the variation in the strength of the NAO over time, with more variation in the positive phases, and less in the negative phases. A regression analysis, using the three grids as predictors of the May NAO for 1833-1967, does explain 63.6% of the variance, an addition of ~ 10% to using the G1 chronology alone, and the fitted sequence is adequate but with no visual improvement of the fit of the G1 chronology to the May NAO (Figure 2.1).

It was possible that a more accurate reconstruction of the May NAO may result from the tree-ring data split into periods based on the correlations between the grids from this region. Characteristics unique to each period were established from the relative ring widths and running correlation values between the three grid chronologies since 1833.

The similarities of the G1 *vs.* G3 and the G1 *vs.* May NAO running correlations (Figure 2.6A and D) suggested splitting up the data by using some level(s) of the G1 *vs.* G3 running correlations as cutoff point(s). Several cutoff levels for the G1 *vs.* G3 correlations (0, 0.5, 0.7, 0.8, and 0.9) were tested with correlations and regression analyses using the grid chronologies as predictors and the May NAO index as the predictand for the period 1833-1955. The first set includes the years with

running correlation values above the cutoff level, and the second set is composed of the years when the value was less.

For the sets of data whose values were greater than any of the tested cutoff levels, a large percentage of the included years were of the 1860s through 1880s where the negative correlation between the G1 and the May NAO occurs. In the correlations between grids in the instrumental phase, this period is unique due to the sustained positive correlations between all grids (Figure 2.6A). It is also the only time in the last 150 years that the May NAO has been in an extremely negative phase with the June NAO in a highly positive phase (Figure 2.6C). These characteristics are used to separate the data of years 1863-1887 (set 1B) from the other data sets, thus isolating the negative correlation set. For the rest of the first data set, the regression analyses showed that above 81% of the variance is explained by the G1 and G3 chronologies in all the test cases. For the second data set of the years that G1 *vs.* G3 correlations are below the cutoff values, the three grid chronologies consistently explain over 90% of the variance in the May NAO, with a slight but insignificant decrease at the higher cutoff values. The final cutoff value of 0.82, the median value of the G1 *vs.* G3 running correlations, was chosen for the split. Set 1A is composed of the years in which the G1 *vs.* G3 running correlations are greater than or equal to 0.82 except for the period 1863-1887, with n = 37; set 1B of the years of sustained positive correlations between all grids, 1863-1887, and set 2 of the years in which the G1 *vs.* G3 correlations are less than 0.82, n = 61 (Table 2.7).

For set 1A, the predicting factors of G1 and G3 explain 84.2% of the May NAO variance at approximately equal weights (Table 2.8). The addition of the G2 chronology as another predictor adds little to the variance explained.

Table 2.7. Periods of the running correlation values divided by $r = 0.82$ to split the data set. The bars in Figure 2.6A indicate the segments included in each set.

G1 *vs*. G3 *r* values	
≥ 0.82	< 0.82
Set 1A	Set 2
1893-1899	1833-1862
1926-1955	1888-1892
	1900-1925
Set 1B	
1863-1887	

For set 1B (1863-1887) a separate regression analysis was calculated, with variance explained at 92.5% (Table 2.8). The equation gives weights to the predictors that are not easily interpretable as is the case in the other sets' equations.

The regression equation for set 2 uses all three grid chronologies as the predictors for the May NAO index, and explains 92.8% of the variance (Table 2.8). The equation coefficients are highest for G1 and approximately equal for G2 and G3. Its confidence limits are the smallest of the three.

Table 2.8. Regression equations for the discussed data sets, their dates indicated by the bars in Figure 2.6A and listed in Table 2.7.

Set	Division	Regression equation	N	r^2	*F* values
1A	G1 vs G3 > 0.82	May NAO = 0.0143 + 0.402 G1 + 0.326 G3	37	84.2	96
1B	All correlations high 1863-1887	May NAO = - 0.644 - 1.73 G1 + 0.505 G2 + 1.43 G3	25	92.5	100
2	G1 v G3 < 0.82	May NAO = 0.0738 + 0.512 G1 + 0.244 G2 + 0.287 G3	61	92.8	258
1A & 2	All except 1863-1887	May NAO = 0.0619 + 0.455 G1 + 0.199 G2+ 0.331 G3	98	93.9	564

Our three sets of reconstructed May NAO indices are shown in Figure 2.7A. The similarity of the equations and reconstructions from sets 1A and 2 indicated that there is little difference between the two despite the absence of Grid 2 in the set 1A equation, and slight differences in the weights. For verification and to test this similarity, the two regression equations calculated for the reconstruction of data sets 1A and 2 were used with the other data set (2 and 1A, respectively) to reconstruct the May NAO: the variance explained was 94.2% and 86.2%, respectively.[39] Those two data sets were then combined, and an equation was calculated for a reconstruction of the May NAO for the total chronology length (variance explained 93.7%), excluding the two periods of sustained positive correlations between all the grids, 1863-1887 and 1263-1307. Those two segments were reconstructed by the third equation and were added in for the total May NAO reconstruction (Figure 2.7B).

DISCUSSION

The reconstructed May NAO

The low-frequency May NAO index values for AD 1181-1967 (Figure 2.7C) have been reconstructed from the three filtered grid chronologies. The low-frequency spatial variance over time in the oaks' ring widths appears to reflect the phases of the May NAO and perhaps its trends. Changes between phases in the May NAO are evident from significant changes in the relationships between the three grids (e.g. 1890 when the completely positive correlations change to both positive and negative relationships). In the calibration period, strongly positive May NAO phases are indicated by the presence of both highly positive and highly negative running correlations (light gray blocks in Figure 2.8), indicating that at least in the 19th century the positive May NAO brought the same weather pattern to two of the three grids

[39] Both significant at the 0.05% level.

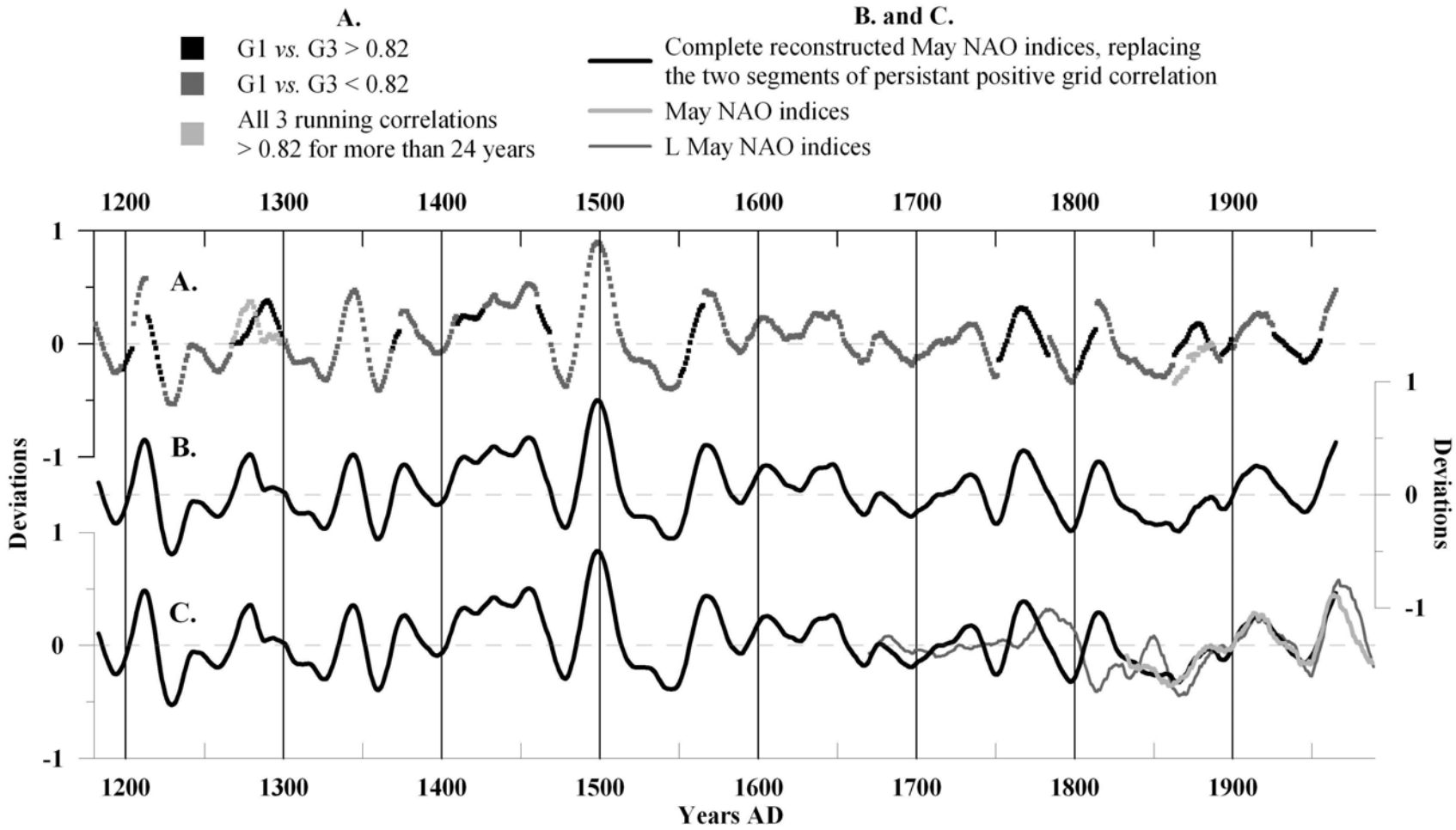

Figure 2.7. A. The results of the three regression equations. B. The final combination of the three sets (see text). C. The reconstructed May NAO compared to the instrumental May NAO and the L May NAO reconstruction.

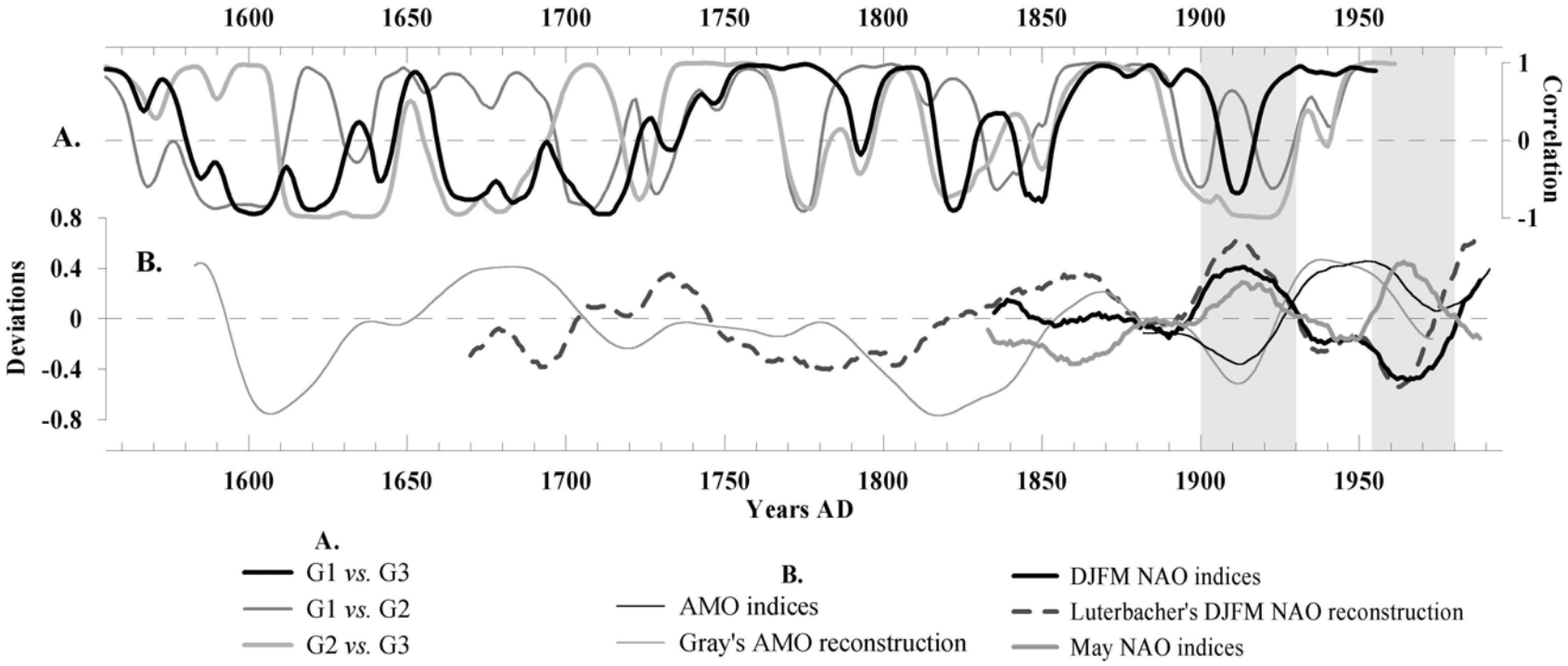

Figure 2.8. A. The correlations between the three grids. B. The comparison of the May NAO with the winter NAO and AMO. In the gray sections, the May NAO is positive and the winter NAO is either very positive or negative. When the May NAO is weak or negative, the winter NAO is also weak. Of note is also that the AMO changes phases at approximately the same time, and that the period when there was little or no response to the May NAO (1877-1887, see text) is marked by all the oscillations' filtered values at about zero.

during that period. Whether that holds true for 1950 to the present in the tree-ring patterns will be assessed by samples collected in 2005 that are currently being measured. When all the correlations are predominantly negative (more local than regional patterns, prior to 1860) or positive (same patterns over the whole region, 1860-1900 and 1930-1953) the May NAO is in a negative phase. This relationship is based on patterns in both the tree-ring widths and the pressure data from the 1820s on: similar patterns occur from 1720 to 1830 (Figures 2.8 and 2.9). Around 1720 there was a possible reversal in the effect of the phases of the May NAO in this region, and possibly 2 or more reversals before that, back to 1400 (Table 2.9), and these may reflect the influence of the Little Ice Age (LIA). In the Medieval Warm Period the reconstructed positive phases occur in periods with persistently high correlations between the grid chronologies (Figure 2.8), opposite to what has occurred in the last two centuries. These observations have to be tested further to determine whether any of them are valid.

Table 2.9. Approximate years that all the correlations were changing in the manner listed below. Whether these indicate actual reversals in the response to the May NAO still needs to be tested. The abbreviations ▲ = increase and ▼ = decrease.

G1 *vs.* G2	G2 *vs.* G3	G1 *vs.* G3	Years occurred	
▲ to ▼	positive to ▼	▲ to positive	1370	1760
▲ to positive	▲ to ▼	positive to ▼	1410	1785
▼ to negative	negative to ▲	▲ to ▼	1438	
▲	▼	▲ to ▼	1610	1720s
▼	▲	▲ to ▼	1695	

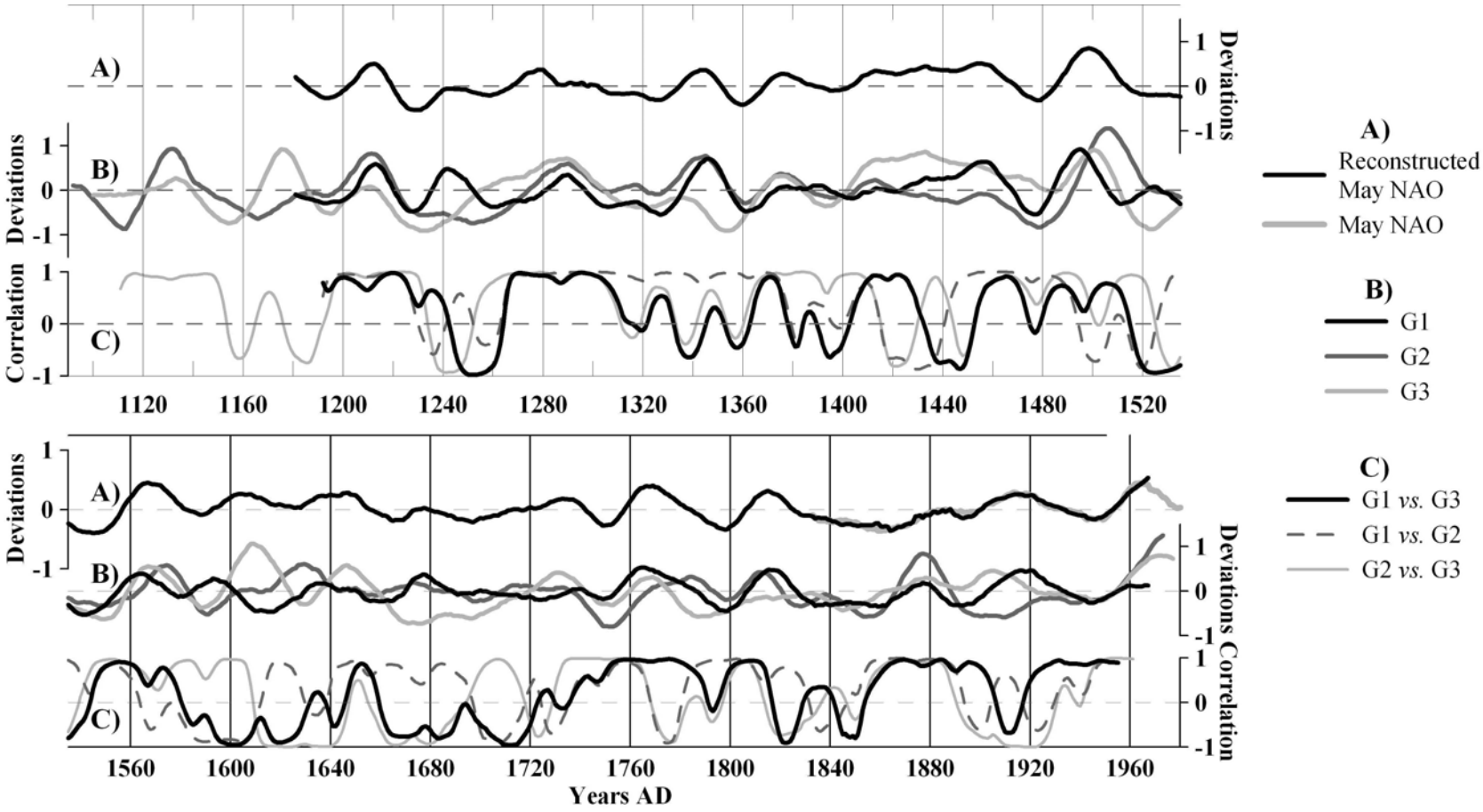

Figure 2.9. A. The May NAO indices, reconstructed and instrumental. B. The three grids' filtered values. C. The running correlations between the three grids over time.

Changes over time

The pattern of running correlations, the grid chronologies, and the reconstructed May NAO indices over time show several intriguing periods (Figure 2.9). One is the persistence of high positive correlations between all grids for more than 20 years, periods of the same relationship between their average ring-widths, thus under the same influence of the May NAO. It happens only in 1863-1887 and in the 13th to early 14th centuries, the Medieval Warm Period (MWP)[40] (Figure 2.9).

The periods of 1181 to at least 1400 (perhaps up to 1580), and 1720 to present are similar in three ways. The periods of highly positive persistent correlation between all grids is one similarity; a second one is the overall dominantly positive correlation, thus lack of persistent negative correlations; and finally there are periods of differences between the chronologies lasting for about the same length of around 30 years. This similarity needs to be further tested to determine if we can link the current climate regime to that of the Medieval Warm Period.

The most different relationship over the region, with no analog in the instrumental record, is the strength and persistence of the negative correlations between the G1 and G3 chronologies from 1580 to 1720. The positive correlations in that period are only between adjacent grids, G1 *vs.* G2 or G2 *vs.* G3. This relationship occurs during the Little Ice Age (LIA),[41] and may indicate a different climate regime where the two outer grids are constantly influenced by opposite pressure systems. A number of possible reversals appear in the response of the tree-ring growth to the May NAO from 1400 to 1740 (Table 2.9). From 1450-1650, however, the relatively low sample count must also be taken into consideration.

[40] Hughes and Diaz 1994.
[41] "…past climate of the eastern Mediterranean…, one of the regions within Europe which has been neglected by climate historians." Grove 2004, p. 376.

The running correlations

The 24-year running correlations between the three grid chronologies appear to illustrate the effect of the NAO on the weather patterns over the region. They indicate periods of similarities and differences over time and space. Further testing will show if these periods and the possible reversals indicated by times of change in all the correlations are good indicators of change in the effect of the low-frequency May NAO over time.

Comparisons with the instrumental and reconstructed May NAO indices

The correlation of our reconstruction with the May NAO indices is 0.97, and with Luterbacher's May NAO indices is 0.83 from 1833-1967. In comparing our pre-instrumental reconstruction with the L May NAO (Figure 2.7C) it is evident that one is an approximate mirror image of the other from 1725-1825. They are directly comparable in 1670-1725, when the data that the L May NAO reconstruction is based on is mainly proxy data. The mirror image may be due either to a substantial difference between the effects of the May NAO on the weather in central Europe and in the Mediterranean region, or to the availability of historical data.

There is little recognizable evidence in our tree-ring record for reversals such as that used by Luterbacher for 1830-1833. However, there is more evidence of a possible reversal in the 1720s (discussed above). We will leave our sequence "as is" for now and continue searching for more evidence of the reversals.

Tree rings *vs.* other oscillations

A visual inspection of the running correlations, the May and winter NAO, and the AMO in the last two centuries shows that changes in the sign of the correlations occur at the times of change in the phase of the May NAO. These sign changes also

occur at times of change in the winter NAO (Figure 2.8). Since 1833 the winter NAO has been in strong positive and negative phases (steep trends) during periods of positive May NAO, and has nearly horizontal trends when the May NAO was weak. The AMO likewise changes trends generally opposite to the winter NAO but offset by a few years. Exploratory regression analyses with the winter NAO as predictand indicated that the 3 grid chronologies plus their running correlations and the reconstructed May NAO explain 85% of the variance in the winter NAO. Correlations indicate that the reconstructed winter NAO index and the G3 chronology are potentially significant predictors but more research is necessary.

CONCLUSIONS

Our reconstruction of the low-frequency May NAO indices, calculated from the low-frequency tree-ring patterns in eastern Mediterranean oaks, provides a record of that month's long-term climate and climate change over the region for the last 825 years. More testing is needed for the possible reversals and no-analogue periods during the Little Ice Age. Little or no teleconnection may be the reason for the periods of high correlation across and outside the region, and that also needs to be tested. An answer to that question will help to determine if the response in the tree-rings to the NAO during the Medieval Warm Period is the same as the response today.

The record of the low-frequency May NAO in the oak ring widths of this region appears to be due to its influence on the May-June precipitation of the region, especially the Aegean area, since the oaks respond primarily to the May-June precipitation.[42] Whether this record is unique to this climate, this area, or the oaks, or whether it is a response that can be found in ring-growth everywhere around the North Atlantic remains to be seen.

[42] Griggs et al., 2006.

Our reconstruction from tree-rings extends our current understanding of the NAO, the region's climate, and changes in both over time. Future research with our archived tree-ring data and similar proxy data from other regions and other sources will allow a more complete NAO reconstruction and a better understanding of climate and climate change in the Near East.

REFERENCES CITED

Appenzeller, C., T. F. Stockton, and M. Anklin. 1998. North Atlantic oscillation dynamics recorded in Greenland ice cores. *Science* 282:446-450.

Atalay, İ. 2002. *Türkiye'nin Ekolojik Bölgeleri* (Ecoregions of Turkey). T. C. Orman Bakanlığı Yayınları No: 163. Izmir: Meta Basımevi.

Barnston, A. G., and R. E. Livezey. 1987. Classification, seasonality, and persistence of low-frequency atmospheric circulation patterns. *Monthly Weather Review* 115:1083-1126.

Briffa, K. R., and P. D. Jones. 1989. Basic chronology statistics and assessment. In *Methods of dendrochronology*, eds. E. R. Cook and L. A. Kairiukstis, 137-152. Dordrecht: Kluwer Press.

Broecker, W. S., and W. S. Hemming. 2001. Climate swings come into focus. *Science* 294:2308-2309.

Cook, E. R. 1985. A Time-Series Analysis approach to Tree-Ring Standardization. Ph.D. dissertation, University of Arizona.

Cook, E. R., K. R. Briffa, D. Meko, Graybill, and Funkhouser, G. 1995. The 'segment length curse' in long tree-ring chronology development for palaeoclimatic studies. *The Holocene* 5:229-237.

Cook, E. R., R. D'Arrigo, and K. R. Briffa. 1998. A reconstruction of the North Atlantic Oscillation using tree-ring chronologies from North America and Europe. *The Holocene* 8:9-17.

Cook, E. R., and L. A. Kairiukstis, eds. 1989. *Methods of Dendrochronology*. Dordrecht: Kluwer Academic Publishers.

Cook, E. R., and K. Peters. 1997. Calculating unbiased tree-ring indices for the study of climatic and environmental change. *The Holocene* 7:361-370.

Cullen, H. M., and P. B. deMenocal. 2000. North Atlantic influence on Tigris-Euphrates streamflow. *International Journal of Climatology* 20:853-863.

Cullen, H. M., A. Kaplan, P. A. Arkin, and P. B. deMenocal. 2002. Impact of the NAO on the Middle East climate and streamflow. *Climate Change* 55:315-338.

Davis, P. H. 1982. *Flora of Turkey and the East Aegean islands*, Vol 7. Edinburgh: Edinburgh University Press.

D'Arrigo, R., E. R. Cook, G. Jacoby, and K. R. Briffa. 1993. NAO and sea-surface temperature signature in tree-ring records from the North Atlantic sector, *Quaternary Science Review* 12:431-440.

D'Arrigo, R., and H. M. Cullen. 2001. A 350-year (AD 1628-1980) reconstruction of Turkish precipitation. *Dendrochronologia* 19(2):169-177.

DeMenocal, P. B. 2001. Cultural response to climate change during the Late Holocene, *Science* 292:667-673.

Enfield, D. B., A. M. Mestas-Nuñez, and P. J. Trimble. 2001. The Atlantic multidecadal oscillation and its relation to rainfall and river flows in the continental U.S. *Geophysical Research Letters* 28(10):2077-2080.

Gray, S. T., L. J. Graumlich, J. L. Betancourt, and G. T. Pederson. 2004. A tree-based reconstruction of the Atlantic Multidecadal Oscillation since 1567 A.D. *Geophysical Research Letters* 31:19932-19935, L12205, doi:10.1029/2004GL019932.

Griffiths, J. F., and D. M. Driscoll. 1982. *Survey of Climatology*. Columbus: Charles E. Merrill.

Griggs, C. B., A. T. DeGaetano, P. I. Kuniholm, and M. W. Newton. 2006. A regional reconstruction of May-June precipitation in the north Aegean from oak tree rings, AD 1089-1989. In review.

Grove, J. M. 2004. *Little Ice Ages: Ancient and Modern*, 2nd Ed., Vol 1. London:

Routledge.

Grove, A. T., and O. Rackham. 2001. *The Nature of Mediterranean Europe, An Ecological History*. New Haven: Yale University Press.

Hughes, M. K., and H. F. Diaz. 1994. Was there a "Medieval Warm Period," and if so, where and when? In *The Medieval Warm Period,* eds. M. K. Hughes and H. F. Diaz, 109-142. Dordrecht: Kluwer Academic Publishers.

Hughes, M. K., P. I. Kuniholm, J. K. Eischeid, G. Garfin, C. B. Griggs, and C. Latini. 2001. Aegean tree-rings signature years explained. *Tree-Ring Research* 57(1):67-73.

Hurrell, J. W. 1995. Decadal trends in North Atlantic Oscillation: regional temperature and precipitation. *Science* 269:676-679.

Hurrell, J. W. 1996. Influence of variation in extratropical wintertime connections on northern hemisphere temperature. *Geophysical Research Letters* 23:665-668.

Hurrell, J. W., Y. Kushnir, G. Ottersen, and M. Visbeck, eds. 2003. *The North Atlantic Oscillation: Climatic significance and Environmental Impact*, Geophysical Monograph No. 134. Washington, DC: American Geophysical Union.

Hurrell, J. W., and H. van Loon. 1997. Decadal variations in climate associated with the North Atlantic Oscillation. *Climate Change* 36:301-326.

Jones, P. D. 1988. Large-scale precipitation fluctuations: a comparison of grid-based and areal precipitation estimates. In *Recent Climatic Change, a regional approach*, ed. S. Gregory, 30-40. London: Belhaven Press.

Jones, P. D., and M. Hulme. 1996. Calculating regional climatic time series for temperature and precipitation: methods and illustrations. *International Journal of Climatology* 16:361-377.

Jones, P. D., T. Jónsson, and D. Wheeler. 1997. Extension to the North Atlantic Oscillation using early instrumental pressure observations from Gibraltar and

South-west Iceland. *International Journal of Climatology* 17:1433-1450.

Jones, P.D., T.D. Davies, D.H. Lister, V. Slonosky, T. Jónsson, L. Bärring, and 16 others. 1999. Monthly mean pressure reconstruction for Europe for the 1780-1995 period. *International Journal of Climatology* 19:347-364.

Jones, P. D., T. J. Osborn, and K. R. Briffa. 2003. Pressure-based measure of the North Atlantic Oscillation (NAO): a comparison and an assessment of changes in the strength of the NAO and in its influence on surface climate parameters. In *The North Altantic Oscillation: Climatic Significance and Environmental Impact,* eds. W. Hurrell, Y. Kushnir, G. Ottersen, and M. Visbeck, Geophysical Monograph No. 134, 51-62. Washington, DC: American Geophysical Union.

Kaplan, A., M. A. Cane, Y. Kushnir, and A. C. Clement.1998. Analysis of global sea surface temperatures 1856-1991. *Journal of Geophysical Research* 103(C9): 18567-18590, 10.1029/98JC01736.

Kerr, R.A. 2000. A North Atlantic climate pacemaker for the centuries. *Science* 288(5473): 1984-1986.

Kuniholm, P. I. 1990. Archaeological evidence and non-evidence for climatic change. In *The Earth's Climate and Variability of the Sun Over Recent Millennia*, eds. S. J. Runcorn and J.-C. Pecker, 645-655. *Philosophical Transactions of the Royal Society of London A*.

Kuniholm, P. I. 1994. Long tree-ring chronologies for the eastern Mediterranean. In *Archaeometry 94*, eds. Ş. Demirci, A. M. Özer, and G. D. Summers, 401-409. Proceedings of the 29th International Symposium on Archaeometry, 9-14 May 1994, Ankara, Turkey). Ankara: TÜBITAK.

Kuniholm, P. I. 2000. Dendrochronologically dated Ottoman monuments. In *A Historical Archaeology of the Ottoman Empire: Breaking New Ground*, eds. U. Baram and L. Carroll, 93-136. New York: Plenum Publishers.

Kuniholm, P. I., and C. L. Striker. 1983. Dendrochronological investigations in the Aegean and neighboring regions, 1977-1982. *Journal of Field Archaeology* 10: 411-420.

Kuniholm, P. I., and C. L. Striker. 1987. Dendrochronological investigations in the Aegean and neighboring regions, 1983-1986, *Journal of Field Archaeology* 14: 385-398.

Lamb, H. H. 1995. *Climate, History and the Modern World*. 2nd ed. London: Routledge.

Luterbacher, J., E. Xoplaki, D. Dietrich, P. D. Jones, T. D. Davies, D. Portis, J. F. Gonzalez-Rouco, H. von Storch, D. Gyalistras, C. Casty, and H. Wanner. 2002. Extending North Atlantic Oscillation reconstructions back to 1500. *Atmospheric Science Letters* 2:114-124 (doi:10.1006/asle.2001.0044).

Luterbacher, J., C. Schmutz, D. Gyalistras, E. Xoplaki, and H. Wanner. 1999. Reconstruction of monthly NAO and EU indices back to AD 1675. *Geophysical Research Letters* 26:2745-2748.

Osborn, T. J., K. R. Briffa, and P. D. Jones. 1997. Adjusting variance for sample-size in tree-ring chronologies and other regional mean timeseries. *Dendrochronologia* 15:89-99.

Sutton, R. T., and D. L. R. Hodson. 2003. Influence of the ocean on North Atlantic climate variability 1871-1999. *Journal of Climate* 16:3296-3313.

Touchan, R., E. Xoplaki, G. Funkhouser, J. Luterbacher, M. H. Hughes, N. Erkan, U. Akkemik, and J. Stephan. 2005. Reconstructions of spring/summer precipitation for the Eastern Mediterranean from tree-ring widths and its connection to large-scale atmospheric circulation. *Climate Dynamics* 25:75-98.

Touchan, R., G. M. Garfin, D. M. Meko, G. Funkhouser, N. Erkan, M. K. Hughes, and B. S. Wallin. 2003. Preliminary reconstructions of spring precipitation in

southwestern Turkey from tree-ring width. *International Journal of Climatology*, 23(2):157-171. Data available at website: IGBP PAGES/World Data Center for Paleoclimatology.

Tsimplis, M. N., and S. A. Josey. 2001. Forcing of the Mediterranean Sea by atmospheric oscillations over the North Atlantic. *Geophysical Research Letters* 28(5):803-806.

Walker, G. T. and E. W. Bliss.1932. World Weather V. *Memoirs of the Royal Meteorological Society* 4(36): 53-84.

Wilks, D. S. 1998. Resampling hypothesis tests for autocorrelated fields. *Journal of Climate* 10(1): 65-82.

Wilson, R., and W. Elling. 2004. Temporal instability in tree-growth/climate response in the Lower Bavarian Forest region: implications for dendroclimatic reconstruction, *Trees: Structure and Function* 18(1): 19-28.

Xoplaki, E. 2002. Climate variability over the Mediterranean. Ph.D. diss., Universität Bern, Switzerland.

Zervakis, V., D. Georgopoulus, A. P. Karageorgis, and A. Theocharis. 2004. On the response of the Aegean Sea to climatic variability: a review. *International Journal of Climatology* 24:1845-1858.

Zohary, M. 1973. *Geobotanical Foundations of the Middle East*, Vols. 1 and 2 (Geobotanica selecta Band III). Stuttgart: Gustav Fischer.

CHAPTER THREE

WOOD MACROFOSSILS AND DENDROCHRONOLOGY OF THREE MASTODON SITES IN UPSTATE NEW YORK

by Carol B. Griggs and Bernd Kromer[1]

SUMMARY

Arboreal macrofossils including wood, bark, twigs, and cones were found in three mastodon excavations located in Hyde Park, Watkins Glen, and in North Java, NY. Identification of the genus, and species if possible, plus the stratification of the sites to a limited extent, agree with environmental changes over time inferred from pollen and other paleoecological studies from around the region. Radiocarbon dates of select samples indicate possible periods of deposition and non-deposition at all the sites.

The oldest wood macrofossils include two boreal species: spruce (*Picea* A. Dietr. sp.) and tamarack (*Larix laricina* (Du Roi) K. Koch). The oldest radiocarbon dates at each site (12,548±38 ^{14}C BP at Hyde Park, 12,365±75 ^{14}C BP at Watkins Glen/Chemung, and 12,254±44 ^{14}C BP at North Java, all spruce wood samples) reflect the southeast to northwest retreat of the ice sheet and subsequent migration of spruce into and across New York State. The oldest tree-ring dates are from 500 to 1500 years older than the dates of the mastodon bones at all three sites. Two single samples plus two floating tree-ring chronologies cover over seven centuries of the Bølling-Allerød chronozone of 12,500-11,000 ^{14}C BP. The changes in radiocarbon production that mark the Older Dryas, a brief 25-50 year interval between the Bølling and Allerød

---

[1] Heidelberger Akademie der Wissenschaften, Institut für Umweltphysik, D-69120 Heidelberg, Germany.

Interstadials, are evident in a ~150 year shift in the radiocarbon ages of tree rings that grew within three decades of each other.

INTRODUCTION

This paper is a report of arboreal macrofossils found during the excavations of three mastodon sites in New York State. These macrofossils represent the arboreal taxa present at those sites in the late Pleistocene through Holocene epochs. Twigs, branches, boles, and roots were found in addition to cones, needles, leaves, and bark. All sizes of material were collected from all levels and used to identify the taxa present at each site, for dendrochronological analysis, and, in selected cases, for radiocarbon dates. The results were analyzed to interpret the environment and climate represented by the assemblages of taxa and the tree ring record of different time intervals. This paper concentrates on the macrofossils from the late Pleistocene Epoch with a brief description of the Holocene macrofossils. The dendrochronology of the Holocene wood is reported in Chapter 4 of this dissertation.[2]

The calibration of any late Pleistocene radiocarbon date is dependent on the ongoing research that has improved the accuracy of the radiocarbon calibration for dates prior to 10,400 ^{14}C BP.[3] For the Chemung mastodon excavation in 1999, the calibration of radiocarbon dates of greater than 12,000 ^{14}C BP resulted in a calibrated date with a 1-sigma error that was 10 times greater than the ^{14}C error. This was due to the lack of terrestrial-based values for any age above 10,400 BP in the IntCal98 calibration curve. In 2000, the Cariaco calibration curve, based on marine foraminifera found in varves in the Cariaco Basin, provided more accurate calibrated dates older than 10,400 ^{14}C BP, adjusting for the differences between terrestrial and

---

[2] Griggs 2006.
[3] Friedrich et al., 2001; Hughen et al., 2000; Kromer et al., 2004; Reimer et al., 2004.

marine ^{14}C with the 400-year reservoir value established for the Holocene.[4] Since then it has been suggested that there was significantly more variation, with a reservoir value of 500 to 650 years, in the marine ^{14}C sequestration prior to the Younger Dryas due to large fluctuations in the upwelling of ^{14}C-depleted bottom water.[5] The large fluctuations in the upwelling were probably caused by variations in the water mass structure of the North Atlantic.[6] Our radiocarbon dates are reported here in radiocarbon age because the research is still in progress, but their current calibrated values are indicated in the figures. Holocene dates are given in both radiocarbon and calibrated years. The chronozones equivalent to the study period of the late Pleistocene Epoch are the Bøllling Interstadial, Older Dryas, Allerød Interstadial, and Younger Dryas.

THE THREE SITES AND THEIR MACROFOSSILS

The locations of the three mastodon sites are shown in Figure 3.1. The Pleistocene bones were found as the owners each excavated their ponds for expansion and a deeper basin. The Chemung mastodon bones were found in John and Elaine Gilbert's pond in Chemung County, near Watkins Glen; originally it was a kettle pond, the result of a very large chunk of glacial ice left buried in the ground as the glacier retreated. The Hyde Park mastodon was found in Larry and Cheryl Lozier's pond in Hyde Park, Dutchess County; the pond originated as an oxbow of a paleo-meander of nearby Fall Kill. The North Java mastodon was found in Bob Moffett's pond in North Java, Wyoming County; this pond was most likely also a kettle pond formed in a kame. Each of the sites was excavated with a different strategy

[4] Hughen et al., 2000.
[5] Friedrich et al., 2001; Kromer 2004.
[6] Broecker 1998; Bjorck et al., 1996, 1998; Hughen et al., 2004; Reimer et al., 2004.

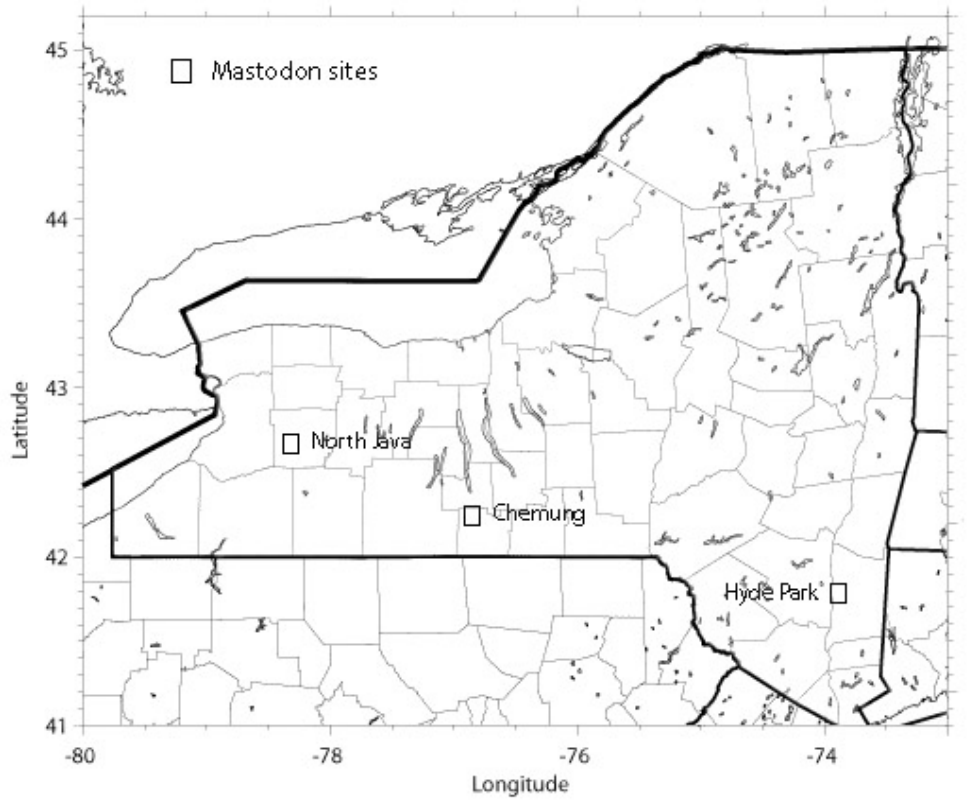

Figure 3.1. The locations of the three mastodon site across New York State. One degree of latitude equals ~111km distance.

The Chemung site (CHE)

This site was a shallow anoxic pond surrounded by an acidic bog. Once the first mastodon bone was found, and the pond drained, the stratigraphic layers were visible and excavated separately. There was a top layer of anoxic pond sediments, including peat, organic detritus, gravel, and silt; then a 1-2m layer of "mastodon matrix" - unusually well-preserved green organic detritus of mastodon dung plus bone and gravel, similar in texture to a wallow. Below that, there was an irregular and thin layer of glacial cobbles, and under that, glacial clay.

The amount of well-preserved arboreal macrofossils was immediately notable. Seven logs up to approximately 0.5m in diameter and at least 3 meters in length were

found in the anoxic layer with some immediately above the mastodon-matrix level and thus from contemporaneous to post-mastodon dates. Sections of each log were cut by chain saw for dendrochronological analysis and for radiocarbon dates of the stratigraphic layer. These were the largest logs recovered at this site. Within the mastodon-matrix level the wood segments were less then 0.25m in diameter and always less than a meter in length: most were of branches less than 0.1m in diameter. A total of 42 samples were specifically collected for dendrochronology and hundreds more for species identification. Of the 42 tree-ring samples, 8 were selected for radiocarbon dates, their selection depending on species, stratigraphic level, and relationship to the mastodon bones at the site. The dated samples include: an oak log (*Quercus* spp., CHE-1) found in the anoxic level on top of the matrix; one each of oak (CHE-18) and elm (*Ulmus* spp., CHE-19) segments plus three hemlock (*Tsuga canadensis*) segments found within the matrix (CHE-20, 21, and 24); one pine (*Pinus* spp.) segment found directly with mastodon bones (CHE-3A); and finally one spruce (*Picea* spp.) root segment found in the top of the glacial clay layer (CHE-17). Two pieces of bone were also sent for dating, one mastodon, and the other mammoth, discussed elsewhere in this volume.[7] Results are listed in Table 3.1 and shown in Figure 3.2.

The radiocarbon-dated spruce sample (CHE-17) is one of two samples of spruce recovered from this site that contain over 50 rings. The dated sample has two radiocarbon dates of 12,269 ±66 and 12,365±75 ^{14}C BP (Hd-20780 and 20795, Table 3.1) from two segments that were used for wiggle matching (described below). The spruce cones found in the matrix are all of *Picea glauca* (Moench) Voss., which implies that the two samples are also *P. glauca*.

---

[7] Shoshani 2006; Hodgson et al., 2006

Table 3.1. The radiocarbon dates for wood samples from the three mastodon sites. HDP = Hyde Park, CHE =Chemung, and NJV = North Java. The laboratories are Hd = Heidelberg Laboratory and Beta = Beta Analytic, Inc

Ref No.	Lab and Analysis No	Site-Sample No.	Genus	Material Dated	Begins	Ends	^{14}C Age	Δ^{13}C
Chemung (CHE)								
C1	Hd-20780	NY-CHE-17	*Picea*	Root	1011	1020	12269±66	-27.10
C2	Hd-20795	NY-CHE-17	*Picea*	Root	1041	1060	12365±75	-27.60
	Beta-176929	NY-CHE	*Mammuthus*	Bone			10890±50	NA
	Beta-176930	NY-CHE	*Mammut*	Bone			10840±60	NA
	Hd-21416	NY-CHE-3A	*Pinus*	Bole	1084	1103	8028±60	-24.23
	Hd-21418	NY-CHE-21	*Tsuga*	Branch	1025	1044	7388±51	-25.38
	Hd-21413	NY-CHE-19	*Ulmus*	Bole	1001	1020	6729±40	-25.96
	Hd-21420	NY-CHE-18	*Quercus*	Bole	1068	1077	5993±56	-26.78
	Hd-20752	NY-CHE-1	*Quercus*	Bole	1081	1090	1929±30	-26.34
	Hd-20754	NY-CHE-1	*Quercus*	Bole	1268	1277	1726±24	-24.83
	Hd-21396	NY-CHE-24	*Tsuga*	Branch	1021	1040	1059±24	-25.02
	Hd-21414	NY-CHE-20	*Tsuga*	Branch	1061	1095	635±28	-26.07
Hyde Park (HDP)								
H1	Hd-22687	NY-HDP-1	*Picea*	Bole	1001	1020	12416±33	-24.91
H2	Beta-168585	NY-HDP-1	*Picea*	Bole	1036	1045	12230±80	-24.60
H3	Hd-22395	NY-HDP-1	*Picea*	Bole	1071	1105	12548±38	-24.98
H4	Hd-22583	NY-HDP-1	*Picea*	Bole	1076	1085	12416±31	-25.15
H5	Hd-22595	NY-HDP-1	*Picea*	Bole	1086	1110	12396±53	-24.92
	Beta-141061	NY-HDP	*Mammut*	Bone			11480±50	NA
North Java (NJV)								
NI1	Hd-22780	NY-NJV-39	*Picea*	Bole	1100	1138	12254±60	-25.94
NI2	Hd-22596	NY-NJV-G24	*Larix*	Bole	1052	1061	12064±44	-24.23
NI3	Hd-22585	NY-NJV-19	*Picea*	Bole	1041	1050	12092±32	-25.09
NI4	Hd-24121	NY-NJV-19	*Picea*	Bole	1051	1060	12049±27	-25.15
NI5	Hd-24123	NY-NJV-G24	*Larix*	Bole	1082	1106	11966±25	-23.87
NI6	Hd-24122	NY-NJV-19	*Picea*	Bole	1061	1070	12056±29	-25.33
	Beta-168586	NY-NJV-G21	*Picea*	Bole	1011	1040	11970±80	-25.40
NI7	Hd-23065	NY-NJV-G21	*Picea*	Bole	1021	1030	11902±51	-25.81
NI8	Hd-24119	NY-NJV-G21	*Picea*	Bole	1041	1060	11969±19	-25.75
NI9	Hd-22597	NY-NJV-G21	*Picea*	Bole	1071	1115	12046±74	-25.38
NI10	Hd-22782	NY-NJV-F17	*Picea*	Bole	1002	1030	12030±45	-24.15
	Beta-176928	NY-NJV	*Mammut*	Bone			11630±60	NA
NII1	Hd-22598	NY-NJV-F15	*Picea*	Bole	1051	1060	11328±61	-25.49
NII2	Hd-22586	NY-NJV-F15	*Picea*	Bole	1071	1080	11296±44	-24.87
	Hd-22775	NY-NJV-F36	*Pinus*	Bole	1000	1009	9509±29	-26.73
	Hd-22772	NY-NJV-F36	*Pinus*	Bole	1110	1119	9367±23	-24.15

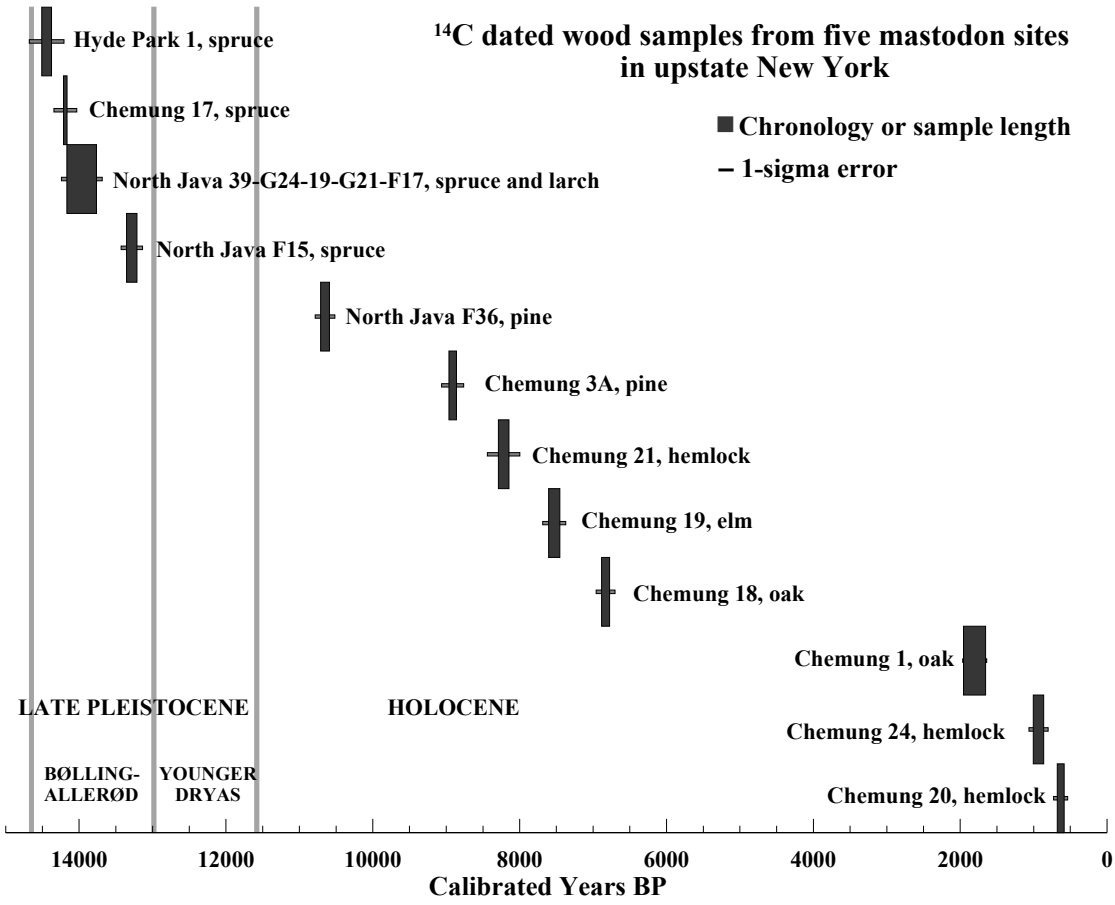

Figure 3.2. The calibrated radiocarbon dates and ranges of the radiocarbon-dated wood samples and chronologies from the three mastodon sites. All radiocarbon dates are beta-decay dates. The dates for the Bølling-Allerød and Younger Dryas periods are from Hughen et al., 2000.

All of the radiocarbon dates of other wood samples, except for the pine sample (CHE-3A), as well as the small size of the segments in the mastodon matrix, indicate intrusion of later-deposited materials into the mastodon matrix level throughout the Holocene. Such samples include hemlock branch segments (CHE-20, 21, and 24), the oak (CHE-18), and the bole of elm (CHE-19) that was found in the matrix but extended down into the glacial clay with its branch collar upside-down. They were not expected to date contemporaneously with the mastodon due to the established migration patterns of each taxon from pollen studies around the region. Their location

in the matrix and glacial clay made their radiocarbon-dating important to establish possible periods of deposition as well as intrusion and non-intrusion of the upper-level sediments into the matrix and clay during the Holocene, long after the mastodons disappeared.

Table 3.2. Tree taxa found at each mastodon site from east to west. An 'X' indicates the presence of the taxa and a number indicates how many dendrochronological samples of the taxa were collected. They are split into periods according to their ^{14}C dates and the pollen analyses of sites in New York and Pennsylvania (Davis 1993, Miller 1973, 1988).

Arboreal Taxa	Common names	Hyde Park	Chemung	North Java
Late Pleistocene Epoch, Bolling-Allerod-Younger Dryas, ca. 14,500-11,000 Cal BP				
Picea A. Dietr spp.	Spruce spp.	1	4	28
P. glauca (Moench) Voss (cones)	White spruce	X	X	X
Betula L. spp.	Birch spp.	X	X	
Betula papyrifera Marsh. (bark)	Paper birch		X	
Abies balsamea Mill.	Balsam fir	X	2	1
Populus L. spp.	Poplar spp.	X	X	X
Salix L. spp.	Willow spp.	X	X	X
Larix laricina (Du Roi) K.Koch	Tamarack / Larch		2	5
Alnus spp.	Alder spp.	X	X	
Mainly from the early Holocene, following the Younger Dryas up to ca. 8,500 Cal BP				
Pinus L. sp.	Pine spp.	X	4	
Pinus banksiana Lamb.	Jack pine		1	1
Pinus resinosa Ait.	Red pine		1	
Holocene and Recent, from ca. 8,500 Cal BP to present				
Tsuga canadensis (L.) Carr.	Eastern hemlock	X	14	44
Fraxinus spp.				27
Fraxinus nigra Marsh.	Black ash		1	
Ulmus americana L.	American elm	X	6	32
Quercus L. sp.	Oak spp.	1	4	1
Thuja occidentalis L.	Northern white cedar		2	3
Prunus L. sp.	Cherry spp.		1	
Acer rubrum L.	Red maple		X	
Juglans nigra L.	Black walnut		X	
Fagus grandifolia Ehrh.	Beech			6
Castanea dentata (Marsh.) Borkh.	American chestnut		X	1

Hundreds of smaller samples were also collected for genus and species identifications (Table 3.2). The count of 19 taxa found at this site is remarkable and is probably due to both the lengths of the deposition intervals represented by the radiocarbon dates and location of the site within major migration routes for many taxa

(Webb et al., 1993). Most of these taxa still naturally occupy the region with the exception of the spruce, white birch, and jack pine (Harlow 1979).

Indirect evidence of fauna from the arboreal samples includes thousands of twigs digested by the mastodons; their taxa were identified and are discussed below. Beaver-tooth gnawing marks are evident on several branches, and muskrat bones were also found in the matrix. The tunneling of both may have added to the bioturbation of the layers at any time since deglaciation, but this activity may have been limited to periods of a wetter climate.

The colors of the organic matter in the mastodon matrix, including the wood, twigs, needles, and leaves, were extraordinarily vibrant and lifelike. Unfortunately most of the colors were lost within an hour after the material was exposed to the air. Five-pound bags of matrix were sent to anyone interested in searching for small fossils; the recipients were asked to search for small bone, plant, shell and other remains, then wash and screen for even smaller fragments. The returned material so far includes at least 5 liters of twigs that had been digested by mastodons, similar in size and character to those reported by Laub et al., (1994, Figure 2, p. 136). The identification of the taxa of nearly 1,000 digested twigs (Table 3.3) indicates that

Table 3.3. The taxa of digested twigs found in the mastodon matrix at the Chemung site. The distinction between spruce and tamarack and between poplar and willow in twigs is very difficult, therefore they are listed together.

Taxa	Number of twigs	Percentage
Picea or *Larix* sp.	758	77.9
Populus or *Salix* sp.	88	9.0
Pinus sp.	74	7.6
Abies balsamea	47	4.8
Unidentified	6	0.6
Totals	**973**	**100.0**

spruce and/or tamarack were the dominant food source for the mastodons. However, the inclusion of poplar and/or willow (*Populus/Salix*), pine, and fir (*Abies*) twigs indicate that the mastodons did not dine exclusively on spruce.

The Hyde Park Site (HDP)

This pond was an oxbow pond formed by a paleo-meander of the Fall Kill (stream), now to the east of the site. The stratigraphic layers, discussed in detail in Miller (2006), consisted of ~0.1 m of fine-grained peat at the top, then 0.6-0.8cm of peaty marl (the spruce zone), ~1.0m of clayey silt, and ~0.5m of silty clay with cobbles of increasing sizes down to the glacial clay at the base of the excavated section.

Many small macrofossils of arboreal species were collected from the spruce zone and above, but there are only two (HDP-1 and HDP-2) that contain enough rings for dendrochronology. One sample is a spruce log (HDP-1), found at the same level as the mastodon. This is the oldest spruce macrofossil from the three study sites (Table 3.1), with a diameter of *ca*. 0.5m (a radius of 0.187m plus an estimated 0.06m to the pith) and was about 8m in length. The wood has an average ring increment of over 1mm in width, the widest of ring widths in all the sites' spruce samples. The relatively wide ring widths and size of the log indicate an open tundra/woodland setting or riverbank environment with little or no competition, as well as favorable soil, drainage, and climate.[8] The smooth exterior of the log and branches worn down close to their branch collars but not entirely worn off are indicators of some transportation to the site and/or weathering by the paleo-Fall Kill, before the meander turned into the oxbow.[9] Three other collected samples of spruce, all with fewer than

[8] Schweingruber 1996.
[9] Miller 2006.

50 rings, are not branches of HDP-1 as they are too large in diameter. They do contain comparable tree-ring widths to HDP-1. Similar to the Chemung site, many spruce cones of only white spruce were found (Table 3.2) with some directly below the log, implying that this spruce log is also *Picea glauca.* A piece of mastodon bone was also dated from this site (Table 3.1 and Figure 3.2).

The other Hyde Park sample with a high ring count is oak (HDP-2), from a level above the mastodon and spruce. This sample has yet to be radiocarbon dated. Other tree macrofossils include numerous white spruce cones and small wood segments from various other species (Table 3.2). This site's arboreal species diversity is the least of the three sites, due to the open forest environment in the Late Pleistocene and the lack of deposition in the Holocene.[10]

The North Java Site (NJV)

This pond was excavated before researchers arrived at the site, so the wood collected was part of a recovery from excavated sediments deposited around the pond. The pond, a probable kettle pond, is located on a kame and is extremely alkalinic due to a limestone source for the deposit.[11] This site is unique due to the pond's location nearly at the top of the kame, with very little relief in the surrounding topography.

153 samples were collected for dendrochronology. They include 34 samples of boreal species,[12] mainly of spruce with a few tamarack (Table 3.2). Two floating chronologies have been constructed mainly of spruce, and both date to within the Bølling-Allerød Interstadial chronozone (Figures 3.2 and 3.3). The earliest

[10] Miller 2006.
[11] Chiment, pers comm.; Calkin and McAndrews 1980.
[12] Webb et al., 1993.

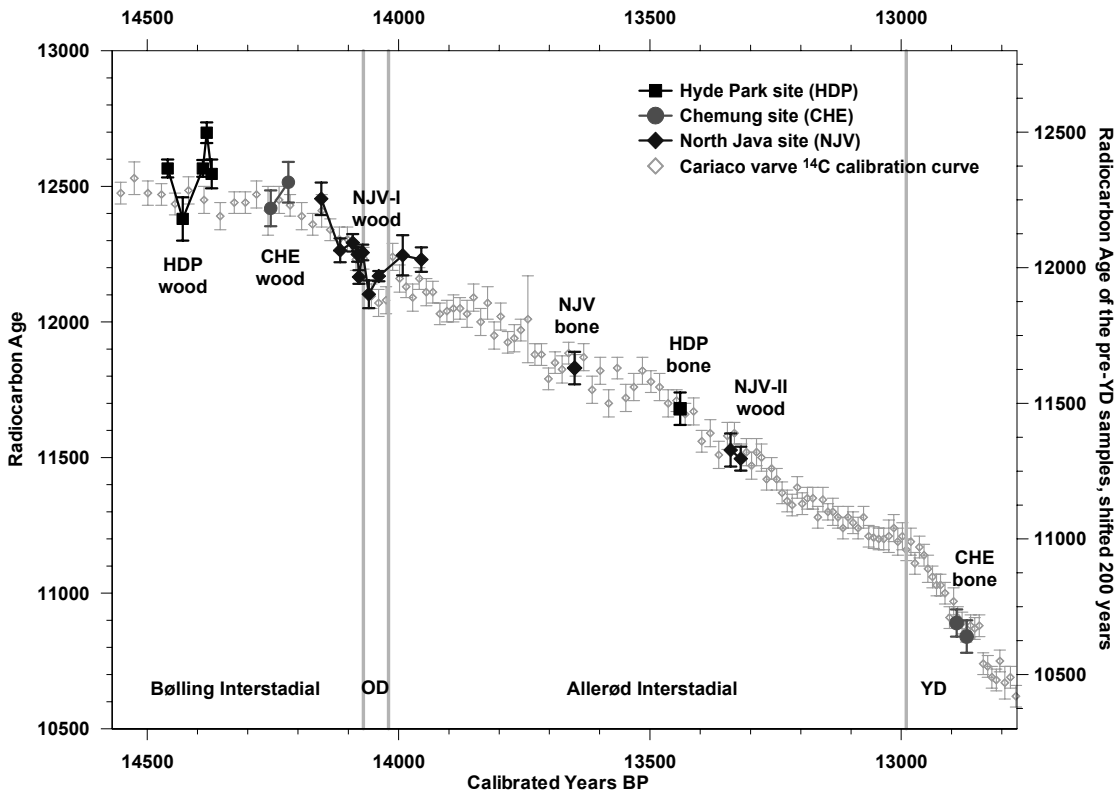

Figure 3.3. The radiocarbon dates of Late Pleistocene wood and mastodon bone samples placed on the Cariaco Basin calibration curve with the 200-year ^{14}C reservoir adjustment indicated by the vertical axis on the right. The Hyde Park and Chemung samples are single trees; the North Java I and II chronologies include several samples along with the dated segments (see text and Figures 3.4 and 3.5).

chronology is 405 years in length and includes the Older Dryas interval, its onset indicated by an abrupt change in the amount of radiocarbon contained in the atmosphere (Figure 3.3; Table 3.1). The second spruce chronology dates towards the end of the Allerød Interstadial (Figure 3.3; Table 3.1). One bone sample was dated.

For the other 119 wood samples, there are approximately equal quantities each of hemlock, elm, and ash (*Fraxinus* L. spp.), and small amounts of other taxa (Table 3.2). All migrated into this region during the Holocene.[13] Of the samples of the three

[13] Webb et al., 1993; Davis 1993.

predominant taxa, 17 chronologies of 114 to 325 years in length with a total of 2882 years have been constructed (see Chapter 4). More radiocarbon dates and dendrochronological research are needed for completing the analysis of the Holocene samples.

THE ARBOREAL SPECIES FOLLOWING DEGLACIATION

The arboreal species gradually migrated into New York following the path of the retreating ice sheet, but each taxa followed different routes.[14] Miller characterized the earliest vegetation at the Hyde Park site as grassland/tundra with the earliest radiocarbon date of non-arboreal macrofossils from that site at 12,880±50 ^{14}C BP (AMS, Beta-175557), 332 radiocarbon years earlier than our earliest spruce date of 12,548±38 ^{14}C BP (Hd-22395).[15] The values of the oldest radiocarbon date of arboreal samples at each site (12,548 Hyde Park to 12,365 Chemung to 12,254 North Java, all ^{14}C BP) nicely reflect the southeast to northwest retreat of the Wisconsin ice sheet.[16]

Stratigraphic association is good at the Chemung site for the spruce (CHE-17) found at the bottom of the matrix, the pine (CHE-3A) found in a shallow depression with the bones, and the large logs found above the matrix of pine, hemlock, and oak. The positions of the smaller Holocene samples in the mastodon matrix were due to settling and bioturbation of the pond sediments. The 2 tree-ring samples at Hyde Park both have good stratigraphic association. For the North Java site, only the pine (NJV-F36), which was excavated from the bottom of the pond at the time of collection, has stratigraphic definition. However, for all the sites, the taxa (Table 3.2) and associated

[14] Davis 1993; Webb et al., 1993; Overpeck et al., 1992.
[15] Miller 2006.
[16] Muller and Calkin 1993.

radiocarbon sample dates (Table 3.1) compare well with the established migration of each taxon into upstate New York following deglaciation as inferred from pollen analyses.[17] The presence and radiocarbon dates of the boreal taxa macrofossils in each pond indicate deposition and preservation at all sites at that time - an indicator of a cool, wet environment throughout the Bølling-Allerød Interstadials.

The relatively high numbers of certain Holocene taxa (hemlock and elm [CHE, NJV], ash [NJV]) and the low numbers of other taxa (pine, oak, maple, beech) are most likely due to their preferred habitats, and the limited Holocene deposition at Hyde Park. Hemlock and elm and at least one species of ash grow best in wetter conditions, and the latter four grow best on well-drained, dryer soils.[18]

From the samples of all three sites combined, there appears to have been less preservation of arboreal detritus from the Younger Dryas into early Holocene, and in the mid to late Holocene until the last two millennia (Figure 3.2). Biases in field collection and selection of samples for radiocarbon dating may have caused the gaps in our data, but these intervals of deposition and non-deposition are similar to those seen at the Hiscock site.[19] Radiocarbon dates of the North Java spruce and pine samples indicate that the late Pleistocene-early Holocene gap is most likely present; more dates are needed to determine whether there is also a mid-late Holocene gap. Also underway is a project that includes oxygen isotope analyses of modern trees that were recently cored at all three sites to compare with isotope analyses of the samples contained in the radiocarbon-dated chronologies to look for variations in precipitation over time in New York State. All of this research plus what has been found in other paleoecology studies around the region will help to prove whether the depositional

---

[17] Miller 1988, 2006; Davis 1993; Webb et al., 1993; Calkin and McAndrews, 1980; Robinson 2006.
[18] Harlow et al., 1979.
[19] Miller 1988.

gaps are real, if they are the result of regional or local climate change, and why they occurred.

THE DENDROCHRONOLOGY OF THE SAMPLES

Methods

Wood samples collected for dating purposes are prepared by cutting a cross-section, then surfacing with a razor blade. Ring widths are measured twice, ecompared, and for any differences of greater than 3%, the widths are measured yet again. Sample data are detrended by fitting an appropriate curve to the time series of measurements and dividing each measurement by the value of the curve at the corresponding year.[20] Samples of the same taxon are crossdated by visually and statistically matching the patterns in two or more detrended time series[21] (*e.g.* Figure 3.4C). The match is never perfect, but year-to-year changes in ring widths create recognizable patterns in the data sets over time that are the key to a statistically significant correlation and good visual fit between samples and/or chronologies.

For each site, when two samples' measurements crossdate securely, they are combined into a genus-specific site chronology. This process is repeated with all the samples from one site. Samples that do not securely crossdate with other samples or chronologies are left out. Similarly, each site chronology built from these results is crossdated with other site chronologies, and the securely crossdated chronologies are combined into regional chronologies, again genus or species-specific.

Samples are generally selected for radiocarbon dates from chronologies. More than one segment from each sample and/or chronology is dated by wiggle-matching (defined below), which generally gives a calibrated date with a lower error value. For

---

[20] Cook and Kairiukstis 1989; Griggs 2006.
[21] Fritts 1976; Cook and Kairiukstis 1989.

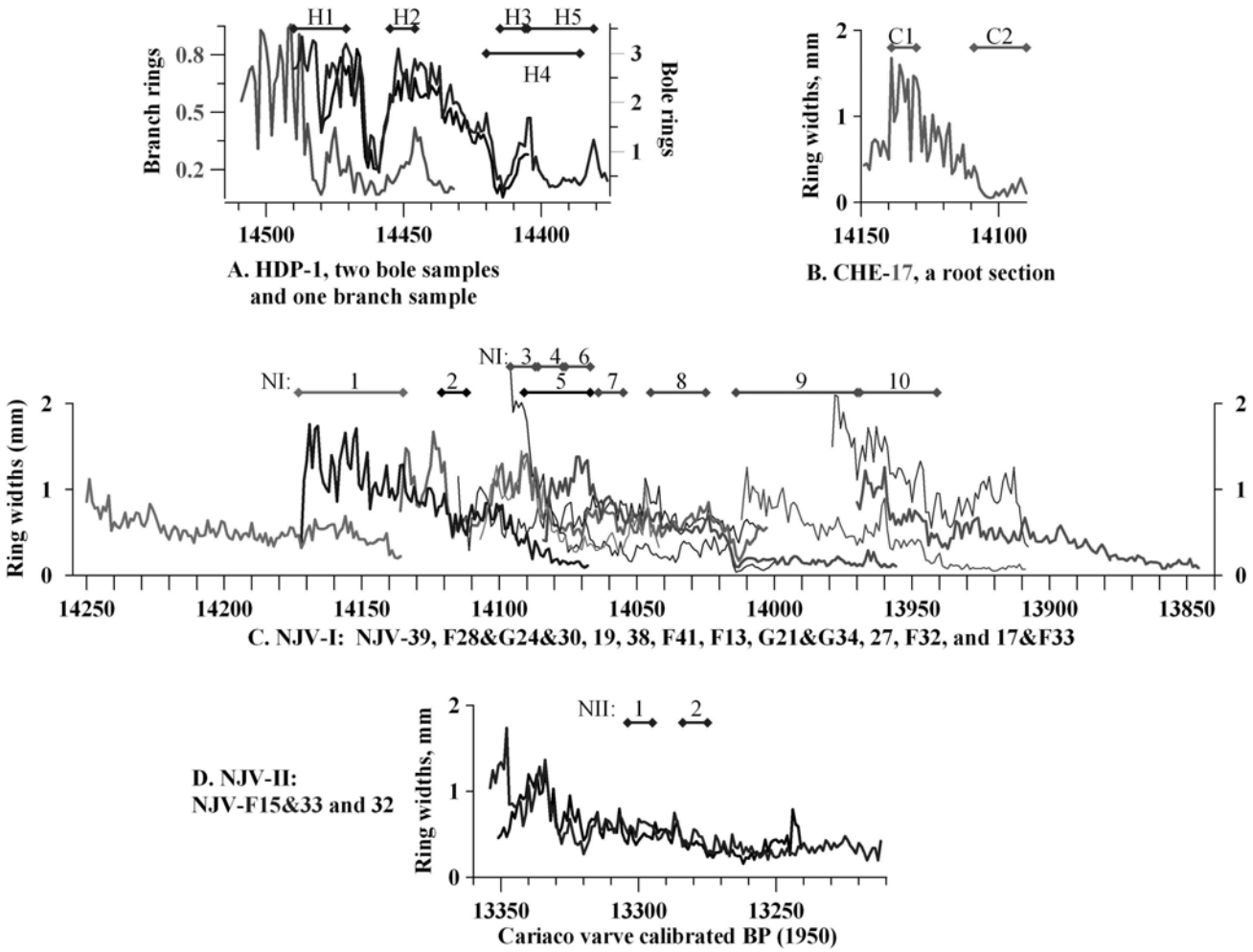

Figure 3.4. Samples and chronologies of the late Pleistocene. A. The Hyde Park spruce sample. B. The Chemung root sample. C. The 14-sample North Java chronology (NJV-I). D. The 3-sample North Java chronology (NJV-II). The horizontal lines represent the radiocarbon-dated segments listed in Table 3.1.

the chronologies, more than one sample is radiocarbon-dated for assurance that they are accurately placed in time. The dates were calibrated with the IntCal98 or IntCal04 radiocarbon calibration curves;[22] the older samples were also calibrated with the Cariaco Basin marine radiocarbon curve with adjustments as discussed below.[23]

Wiggle-matching uses both the radiocarbon dates from segments containing known numbers of annual rings plus the known number of rings between segments for a better fit to the calibration curve. For our samples, 25 to 50 grams of wood were needed per segment for beta-decay radiocarbon analysis due to the wetness of the samples. Each dated segment consisted of 10 to 45 rings, depending on the widths of the rings and the geometry of the sample.

The tree-ring chronologies

Of the 197 wood samples from the sites with sufficient ring count for dendrochronological analysis, 163 had been measured by June 2005, and 24 chronologies have been built with a few more in progress. The chronologies, composed of several samples, dampen the trees' individual responses to their micro-environments, and emphasize the response that the trees share in common to the site's geomorphologic (*e.g.* a small valley with limited drainage) and climate (*e.g.* precipitation) parameters. A site chronology is necessary for an accurate analysis of their common response to changes in the environment and climate parameters. The shared response allows a secure crossdate between the site chronology and other chronologies and sample data sets from the same time period.[24] The chronologies are generally genus or species-specific. The accuracy of crossdating between

[22] Stuiver et al., 1998a; Reimer et al., 2004.
[23] Hughen et al., 2000; Kromer et al., 2004.
[24] Fritts 1976; Cook and Kairiukstis 1989.

chronologies of different taxa ranges from very good to limited due to the level of similarity in each taxon's primary growth-limiting factor(s). One example is that for oaks, the factors are mainly growing season precipitation, and for hemlocks it is a combination of the precipitation plus temperature.[25]

The Late Pleistocene Epoch

The Chemung and Hyde Park sites each have only one spruce sample that was both measured and radiocarbon-dated (Figure 3.4A and B). Both date to the Bølling Interstadial chronozone. The North Java site has a remarkably large number of boreal taxa macrofossils dating from the very end of the Bølling Interstadial through the Older Dryas interval and into the Allerød Interstadial chronozone.

Of the 33 spruce and tamarack samples from the North Java site, one spruce chronology is constructed of 13 samples from 10 trees and is 405 years long (NJV-I, Figures 3.4C and 3.5). The samples in this chronology are all spruce with the exception of 3 tamarack samples, all from the same tree. The ring-width patterns of the individual trees indicate a fairly open environment with little suppression-release patterns, yet the small ring widths of the North Java samples indicate a cooler summer climate, assuming that temperature was the primary limiting growth factor for boreal species in that environment.[26] The data set of the averaged tamarack samples (NJV-G24&F28&30) was combined with the spruce data in the NJV-I chronology for two reasons. One is the good crossdating between the spruce chronology and the tamarack samples. The second reason is that one of the tamarack sample's radiocarbon dates shows the same ~150-year change in radiocarbon dates over a 40-year segment as do

[25] Fritts 1976.
[26] Briffa et al., 1994.

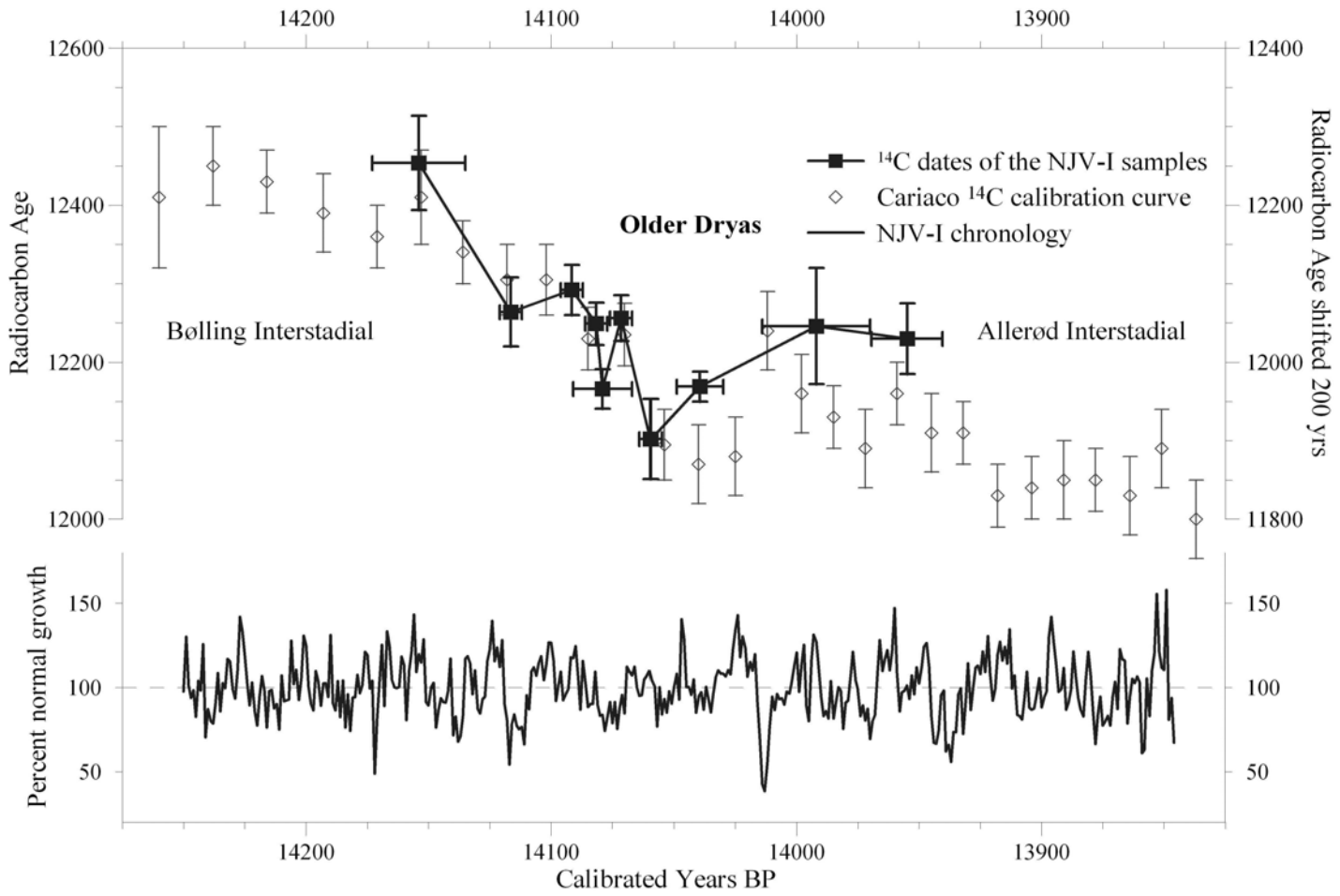

Figure 3.5. (Top) The dates from the NJV-I chronology fitted to the Cariaco radiocarbon calibration curve with a 200-year shift (right vertical axis) to correct for the marine-terrestrial difference in radiocarbon. (Bottom) The NJV-I chronology. From both, note the dip in the radiocarbon ages from 14,075-14,050 Cal BP, the onset of the Older Dryas interval, and the sharp decrease in ring widths at the end of that interval.

the radiocarbon dates of two spruce samples, and that matches the radiocarbon pattern of the calibration curve that marks the Older Dryas (Figures 3.3 and 3.5).

The Older Dryas chronozone is a prominent cooling event in the North European hemisphere.[27] The change in ^{14}C in the samples over the beginning of that event is very evident in the dates of sections from two samples in our chronology (Figures 3.4C and 3.5). With that change in ^{14}C as a time marker for the Older Dryas, our data show that the marine reservoir age was ca. 600 years going into the Older Dryas, but possibly reduced during and at the onset of the Allerød Interstadial (Figure 3.5). The end of the Older Dryas is possibly indicated by an extreme reduction in ring widths between 14,020-14,015 Cal BP (Figure 3.5). The marked decrease is seen in the ring-widths of all four samples that grew in that period.

A second North Java chronology was built of 3 spruce samples from 2 trees, of 145 years' length (NJV-II, Figure 3.4D). Radiocarbon dates for two segments of one sample place the chronology towards the end of the Allerød Interstadial, later than this site's mastodon bone date (Figure 3.3 and Table 3.1). Two shorter chronologies from that site, one of spruce and one of tamarack, have yet to be radiocarbon dated.

The Holocene

The Chemung site has five tree-ring chronologies for the Holocene. These include a 301-year oak chronology, a 171-year pine chronology, a 153-year elm chronology, and two hemlock chronologies, one of 240 years and one of 237 years in length. The oak, elm, and the 240-year hemlock chronology are radiocarbon-dated as shown by their placement in Figure 3.2, and dates for the samples from the other chronologies are in progress.

---

[27] Björck et al., 1998; Walker et al., 1999.

The Hyde Park site has the oak sample that has yet to be radiocarbon dated.

The 104 hemlock, elm, and ash samples from North Java have been measured. Forty-four samples are included in 14 chronologies with an average length of 169 years, and they cover a total of 2,357 years. Of the 15 samples still to be measured, maple (*Acer* L. spp.) and beech (*Fagus grandifolia* Ehrh.) are the major components. Radiocarbon dates are needed for samples included in the longer chronologies.

CONCLUSIONS

Upper New York State, after the recession of the last ice sheet and during the reign of the mastodon, was a boreal environment with a cool, humid climate regime. The tundra environment that immediately followed the recession of the ice sheet gradually changed into open spruce forests with poplar, paper birch, tamarack, fir, and pine which are indicated by the boreal taxa, their radiocarbon dates, and the relative ring widths of the dendrochronological samples. The radiocarbon dates of the first spruce wood at each site are up to 1500 years older than the radiocarbon dates of the mastodon bones at each site, the Chemung site having the largest gap, with the North Java mastodon bone dating in between the older and younger chronologies. The lack of large wood samples with the same dates as the mastodon bones (Figure 3.3), and the fact that the mastodons' diet consisted mainly of spruce twigs (Table 3.3), implies that the arboreal flora was cleared out from at least immediately around the pond by their eating habits. Future work will include radiocarbon dates of the digested twigs that may indicate that there were mastodons on the sites earlier than is indicated by the bone dates, and will give a better time frame for the length of their habitation over the region.

Despite the limited stratigraphic record of samples at the Chemung site, the radiocarbon dates of the spruce, pine, earliest hemlock, and elm samples are very similar to their temporal migration into this region as has been inferred from the regional pollen record.[28] The paucity of samples from the Younger Dryas through early Holocene, and mid- to late- Holocene may indicate drier periods. The ongoing oxygen isotope analysis, and radiocarbon dates of the Holocene samples from the North Java site will further indicate whether this pattern is real (not due to sample bias), and whether all sites were similarly affected. Holocene wood has also been collected from other sites around New York, and the results of their taxa, ring widths, and radiocarbon dates will add to the interpretation.[29] With more samples, more dendroclimatological analysis will be possible.

The current calibrated late-Pleistocene radiocarbon record is critical to placing any evidence of change in the correct time frame. In the past, reports on the geologic and environmental changes during and immediately after deglaciation in New York State and elsewhere have regularly included remarks that the time frame, especially for changes in the water drainage systems, seemed very short.[30] The current terrestrial calibration curve extends the Late Pleistocene time frame back by a few centuries, which is not a large extension, but may be more acceptable. This study's record of the Late Pleistocene macrofossils along with the current calibration curves adds to the growing body of revised data sets currently available for a clear interpretation of the Late Pleistocene record in New York State.

---

[28] Webb et al., 1993.
[29] Griggs 2006.
[30] *e.g.* Muller and Calkin 1993.

REFERENCES CITED

Björck, S., B. Kromer, S. Johnsen, O. Bennike, D. Hammarlund, G. Lemdahl, G. Possnert, T. L. Rasmussen, B. Wohlfarth, C. U. Hammer, M. Spurk. 1996. Synchronized terrestrial-atmosphere deglacial records around the North Atlantic. *Science* 274:1155-1160.

Björck, S., M. J. C. Walker, L. W. Cwynar, S. Johnsen, K. -L. Knudsen, J. Lowe, B. Wohlfarth. 1998. An event stratigraphy for the Last Termination in the North Atlantic region based on the Greenland ice-core record. *Journal of Quaternary Science* 13(4):283-292.

Briffa, K. R., P. D. Jones, and F. H. Schweingruber. 1994. Summer temperatures across northern North America: Regional reconstructions from 1760 using tree-ring densities. *Journal of Geophysical Research* 99 (D12): 25,835-25,844.

Broecker, W. S. 1998. Paleocean circulation during the last deglaciation: A bipolar seesaw? *Paleoceanography* 13: 119-121.

Calkin, P. E., and J. H. McAndrews. 1980. Geology and paleontology of two late Wisconsin sites in western New York State. *Geological Society of America Bulletin*, Part I, 91:295-306.

Cook, E. R. and L. A. Kairiukstis, eds. 1989. *Methods of Dendrochronology*. Dordrecht: Kluwer Academic Press.

Davis, M. B. 1993. Holocene vegetational history of the eastern United States. In *Late-Quaternary Environments of the United States*. Vol. 2: The Holocene, ed. H.E. Wright, 166-181. Minneapolis: University of Minnesota Press.

Friedrich, M., B. Kromer, K. F. Kaiser, M. Spurk, K. A. Hughen, and S. J. Johnsen. 2001. High-resolution climate signals in the Bølling-Allerød Interstadial (Greenland Interstadial 1) as reflected in European tree-ring chronologies

compared to marine varves and ice-core records. *Quaternary Science Reviews* 20:1223-1232.

Fritts, H. C. 1976. *Tree Rings and Climate*. London: Academic Press.

Griggs, C. B. 2006. Holocene dendrochronology in upstate New York: modern, historic, and subfossil tree-ring chronologies. Ch. 4, Ph.D. Dissertation, Cornell University.

Harlow, W. H., E. S. Harrar, and F. M. White. 1979. *Textbook of Dendrology*. 6th ed. New York: McGraw-Hill.

Hodgson, J.A., Allmon, W.D., Nester, P.L., Sherpa, J. and Chiment, J.J. 2006. Osteology of Late Pleistocene proboscidean remains at the Gilbert Site, Chemung County, New York. *Palaeontographica Americana* (under review).

Hughen, K. A., J. R. Southon, S. J. Lehman, and J. T. Overpeck. 2000. Synchronous radiocarbon and climate shifts during the last deglaciation. *Science* 290:1951-1954.

Hughen, K. A., M. G. L. Baillie, E. Bard, J. Warren Beck, C. J. H. Bertrand, P. G. Blackwell, et al. 2004. Marine04 Marine Radiocarbon Age Calibration, 0-26 Cal Kyr BP. *Radiocarbon* 46(3): 1059-1086.

Kromer, B., M. Friedrich, K. A. Hughen, F. Kaiser, S. Remmele, M. Schaub, and S. Talamo. 2004. Late Glacial 14C-ages from a floating, 1270-ring pine chronology. *Radiocarbon* 46(3): 1206-1209.

Laub, R. S., C. A. Dufort, and D. J. Christensen. 1994. Possible mastodon gastrointestinal and fecal contents from the late Pleistocene of the Hiscock Site, western New York State. In *Studies in Stratigraphy and Paleontology in Honor of Donald W. Fisher,* ed. E. Landing, 135-148. *New York State Museum Bulletin* 481.

Miller, N. 1973. Late glacial plants and plant communities in northwestern New York State. *Journal of the Arnold Arboretum* 54:123-159.

Miller, N. 1988. The Late Quaternary Hiscock Site, Genesee County, New York: Paleoecological studies based on pollen and plant macrofossils. In *Late Pleistocene and Early Holocene Paleoecology and Archaeology of the Eastern Great Lakes Region*, eds. R. S. Laub, N. G. Miller, and D. W. Steadman, 83-93. *Bulletin of the Buffalo Society of Natural Sciences*, Vol. 33.

Miller, N. Forthcoming 2006. Contemporary and prior environments of the Hyde Park, New York, mastodon on the basis of associated plant macrofossils. *Palaeontographica Americana* (under review).

Muller, E. H. and P. E. Calkin. 1993. Timing of Pleistocene glacial events in New York State. *Canadian Journal of Earth Sciences* 30:1829-1845.

Overpeck, J. T., R. S. Webb, and T. Webb, III. 1992. Mapping eastern North American vegetation change of the past 18 ka: no-analogs and the future. *Geology* 20: 1071-1074.

Reimer, P. J., M. G. L. Baillie, E. Bard, A. Bayliss, J. W. Beck, C. J. H. Bertrand, et al. 2004. IntCal04 Terrestrial radiocarbon age calibration, 0 – 26 Kyr BP. *Radiocarbon* 46(3): 1029-1058.

Robinson, G. 2006. The Hyde Park mastodon and palynological clues to megafaunal extinction. *Palaeontographica Americana* (under review).

Schweingruber, F. H. 1996. *Tree Rings and Environment Dendroecology.* Berne: Paul Haupt.

Shosahni, J. 2006. Form and function of hyoid elements from *Mammut* and *Mammuthus* from three mastodon sites, New York, USA. *Palaeontographica Americana* (under review).

Stuiver, M., P. J. Reimer, E. Bard, G. S. Burr, K. A. Hughen, B. Kromer, G. McCormac, J. Plicht, M. Spurk. 1998. INTCAL98 Radiocarbon Age Calibration. *Radiocarbon* 40(3):1041-1083.

Webb, T., III, P. J. Bartlein, S. P. Harrison, K. H. Anderson. 1993. Vegetation, lake levels, and climate in eastern North America for the past 18,000 years. In *Global Climates Since the Last Glacial Maximum*, eds. H. E. Wright, J. E. Kutzbach, T. Webb III, W. F. Ruddiman, F. A. Street-Perrott, and P. J. Bartlein, 415-467. Minneapolis: University of Minnesota Press.

CHAPTER FOUR

HOLOCENE DENDROCHRONOLOGY IN UPSTATE NEW YORK: MODERN, HISTORIC, AND SUBFOSSIL TREE-RING CHRONOLOGIES

by Carol B. Griggs

SUMMARY

Over 30 tree-ring chronologies that represent various windows of time from 11,000 Cal BP to the present[1] have been constructed of wood collected from six modern woodlands, seven historical structures and timbers, and eight river, stream, and pond sediments in upstate New York. The chronologies are composed of oak, hemlock, pine, elm, or ash. Regional chronologies date from AD 1625 to 2004 for the modern and historic oaks, AD 1593 to 2003 for the modern and historic hemlocks, and AD 1681 to 1848 for the historic pines. Dates of the subfossil[2] wood chronologies range from nearly 9,000 BC to the mid-14th century AD.

INTRODUCTION

The Pleistocene to Present Dendrochronology of Upstate New York project (PPD) began with the discovery and collection of a large quantity of well-preserved wood samples in a kettle pond at a mastodon excavation site. From there it progressed through the excavation of two more mastodon sites with a grand total of 210 samples of subfossil wood plus cores from 33 modern trees. Both the quantity and the quality of the subfossil wood samples illustrate a remarkable preservation in such niches

[1] Wood samples dating from the Late Pleistocene, 15,000 to 11,000 Cal BP, are discussed in Griggs and Kromer, in review 2006. "Cal BP" refers to Calibrated years Before Present: 0 Cal BP = AD 1950.
[2] "Subfossil" refers to anything buried but not yet totally mineralized.

despite the temperate climate regime in which most fallen trees decompose within a few years. The species of each sample and its measured rings represent the environment and climate in its lifespan and the whole ensemble represents various slices in time from the Late Pleistocene through modern.

The PPD shifted to its present historical collection phase in order to assess the climate and environmental record in the modern and historical wood for a clear interpretation of the changes recorded in the tree-ring patterns from this area throughout the Holocene. All the sites' locations are shown in Figure 4.1. This report marks the project's progress as of August 2005. There are still many samples to be measured and many buildings and collection sites to be visited.

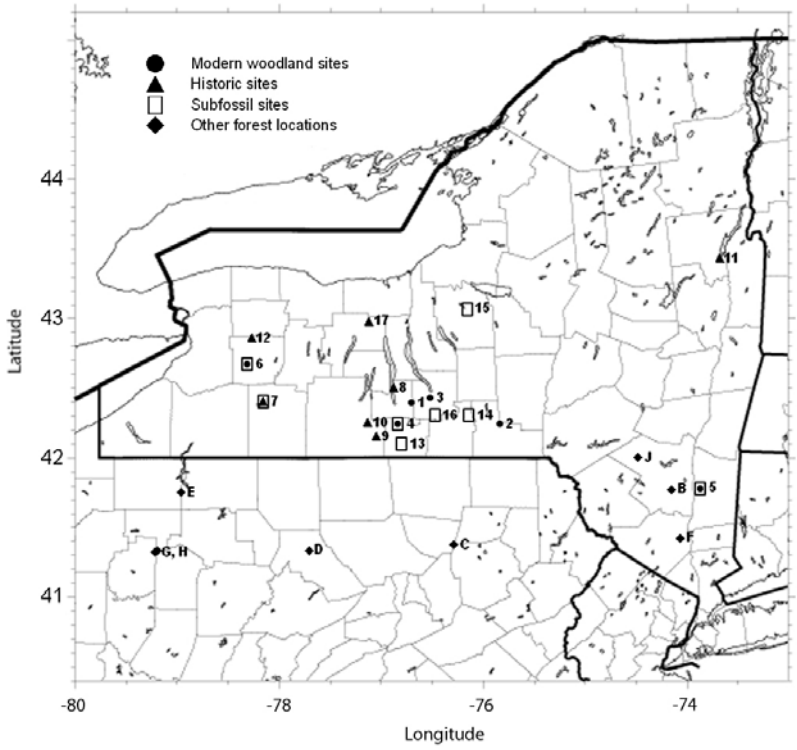

Figure 4.1. The locations of sites around New York. Site names are listed by the map numbers in Table 4.1. The lettered points are the sites of other chronologies: A. Pack Forest, B. Mohonk Lake, C. Rickett's Glen, D. East Branch, E. Tionesta, F. Dark Hollow, G. Fire Tower, H. Longfellow Trail, and I. Shawangunk Mountains (Cook, ITRDB). One degree latitude = ~111km.

Table 4.1. The locations of the sites, periods that they represent, and the genera collected. The genera included are oak, hemlock, pine, elm, and ash (represented by o, h, p, e, and a, respectively). Sites in more than one section include samples from both periods.

No. on Map	Lat N	Long W	County, Town, Site	No. of samples	Genera included
	Modern				
1	42.39	76.71	Schuyler, Hector, Judy's Hill	5	o
2	42.24	75.85	Broome, Chenango Forks, C.F. High School	1	o
3	42.43	76.53	Tompkins, Ithaca, Coy Glen	6	h
4	42.24	76.85	Chemung, Pine City, Gilbert Mastodon site	10	h
5	41.78	73.89	Dutchess, Hyde Park, Lozier Mastodon site	11	p
6	42.67	78.32	Wyoming, North Java, Moffett Mastodon site	12	p
	Historical				
7	42.40	78.17	Allegany, Houghton, railroad support posts & house board	6	p
8	42.50	76.89	Shuyler, Hector, Seneca Lake pier posts	3	o
9	42.15	77.06	Steuben, Corning, Patterson Inn built in 1796	4	o
10	42.25	77.14	Steuben, Campbell, Wixson Log Cabin	7	p,o
11	43.43	73.70	Washington, Lake George, logged hemlock with ID	1	h
12	42.86	78.28	Wyoming, Attica, Stevens's barn	2	p,h
17	42.98	77.13	Ontario, Phelps, Hiram Edson Home	10	p.h,o,e
	Ancient				
4	42.24	76.85	Chemung, Pine City, Gilbert Mastodon, acidic kettle pond	42	p,h,o,e,a
7	42.40	78.17	Allegany, Houghton, Genesee riverbed logs	14	h,o
13	42.17	76.81	Chemung, Bowman's Quarry, edge of pond in gravel pit	1	o
5	41.78	73.89	Dutchess, Hyde Park, Lozier Mastodon, acidic kettle pond	1	o
14	42.30	76.15	Tioga, Berkshire, Rabenstein's farm on Wilson Creek	9	h
15	43.07	76.17	Onandaga, Syracuse, S of Onondaga Lake, 10m in well	1	h
16	42.30	76.49	Tompkins, Danby, Michigan Hollow Rd. creekbed	6	h
6	42.67	78.32	Wyoming, North Java, Moffett Mastodon, alkalinic pond	153	p,h,e,a

Central and western upstate New York is a relatively new region of study in the science of dendrochronology. The climate is certainly similar to the surrounding regions, but there are substantial variations due to topography and proximity to lakes Erie and Ontario.[3] To the northeast, east, and south, Cook and others[4] have built many modern oak, hemlock, and pine chronologies from trees in the Adirondack and Catskill Mountains, the Hudson River valley, and in northern Pennsylvania. Their

[3] Burnett et al., 2003; Yarnal 1994.
[4] Cook and Jacoby 1977, 1979.

longest chronology dates back to AD 1425, but the majority begin sometime in the late 16th to 18th centuries. To the northwest, eastern white cedar trees with lifespans of up to 1600 years grow on the Niagara escarpment that runs from near Niagara Falls northwest up to Tobermary, Ontario, and chronologies of those trees, living and dead, date to back to AD 610 with floating chronologies back to about 6,500 years ago.[5] My collection complements those chronologies, expanding the time period back another 8,500 years, albeit sporadically. The Late Pleistocene samples, dating from ~15,000 to 11,000 Cal BP, are discussed in Griggs and Kromer.[6] Here the chronologies built from samples dating through the Holocene are presented. The species include oak, hemlock, pine, elm, and ash (*Quercus* spp., *Tsuga canadensis*, *Pinus* spp., *Ulmus* spp., and *Fraxinus* spp., respectively). My chronologies may not crossdate well with the Niagara escarpment cedar chronology due to species difference, but the modern and historic chronologies crossdate securely with the chronologies of the same species developed by Cook and others.[7]

Wood subfossils in upstate New York sediments have mostly been deposited since the last deglaciation and are exposed whenever wetlands, ponds, stream or riverbeds are excavated, catastrophically altered, or change their course. The wood preservation is due mainly to the pH level (alkaline or acidic) and anaerobic nature of their depositional environment. Wood samples from three mastodon sites were collected from all of the strata in the ponds plus cored from trees presently growing at each site. Wood samples from the other Holocene sites were collected from recently exposed logs noticed mainly by the landowners.[8]

---

[5] Buckley et al., 2004; Kelly and Larson 1997; Larson and Kelly 1991.
[6] Griggs and Kromer, in review, 2006.
[7] E.R. Cook, ITRDB website:http://oas.ngdc.noaa.gov/paleo/ftpsearch.treering.
[8] For all the sites, the landowners' recognition of buried wood as such, and their report of its existence was critical. I am very grateful for the help of everyone involved.

Each tree-ring chronology is composed of samples generally of the same species, but for the oak and pine chronologies each is composed of samples from their respective genera unless the wood is from standing timbers. The identification at species level is straightforward from leaves or needles, bark, twigs, seeds, etc., but not from wood alone. For the hemlocks, *Tsuga canadensis* is the only species that grows in northeastern North America.[9] Most elm and ash species have identifiable wood properties.[10] The oaks species that live in this area may have some differences in ring patterns in different species, but they still crossdate securely. Pine, however, does have different tree-ring patterns in the ring growth of certain species, which may hinder a secure crossdating between their chronologies. Species identification is critical in correctly interpreting each species' presence, ring growth patterns, and the surrounding environment from the wood (see below), but for secure crossdating, pattern replication is the important factor.

The idiosyncrasies in individual trees' growth patterns are removed by averaging the ring widths together. The resulting chronology is considered to only contain the "common signal," which are annual variations in the tree-ring widths that are common to all the samples and that are generally the result of variation in certain climate parameters in the region over time.

METHODS

Sample Collection

For living trees, an increment borer was used to collect at least two samples from each tree. Sections were sawn from stumps and felled timbers whenever

[9] Harlow et al., 1979.
[10] Panshin and de Zeeuw 1970.

possible. For the intact historic sites, a Henson hollow drill was used to take cores from beams and posts. Sections were sawn from abandoned railroad support beams, a drowned logged timber, barn beams and boards, and waterfront pier posts that were being replaced. For the subfossil wood, sections from very large logs were tied with string to preserve their structure, then sawn off. All wet samples are stored at cool temperatures in plastic wrap to preserve the wood and inhibit shrinkage.

It is ideal to collect two cores from each of at least 10 trees, logs, or timbers of the same species to build a chronology that contains an accurate common signal. In modern woodlands, that number of samples is not generally a problem. On historic and subfossil wood sites, the ideal number is outweighed by the availability of wood, and the number of samples collected at each site ranges from one to more than one hundred.

Measurements

Each sample is sanded with paper up to 200 grade for surfacing, up to 400 grade for polishing. Wet samples are surfaced with razor blades. The rings are measured under a microscope using a Henson measuring machine with the measurements recorded on a computer. Each radius is measured twice and the two measurements are reconciled to 0.01mm with a 3% error. The signs (positive or negative) of year-to-year change in ring widths are reconciled to 100% agreement.

The terms included in the samples' dates below are: ***p*** for the presence of the pith, or center ring, in a sample, just before the first measured ring; ***±p*** for the first measured ring being close to the pith; + for one partial ring after the last complete and measured ring; ++ for more than one unmeasurable ring after the last measured ring; ***vv*** for unknown number of rings cut off; ***v*** for a felling date close to the last ring

measured; ***W*** for waney edge, where the last ring is indeed the outer ring, but no bark is present; and ***B*** for bark present on the sample.

Analysis

Sample measurements are detrended by fitting a curve to the data, then dividing the measurements with the curve's corresponding values over time (Figure 4.2). This removes ring-width variance due to age, competition, and any other factors unique to each tree and enables a comparison and identification of similar ring patterns in trees with very different average ring widths.[11]

The detrended data from samples of known felling or coring date are then averaged into the modern site chronologies. For each historical and subfossil site, the detrended samples were crossdated[12] with each other to find any patterns that are shared in their ring growth. If the patterns match, the samples are assigned relative dates (RD), relative to each other's dates rather than to calendar years. Those dates are used to place the samples in the correct position, and then each site chronology is built by combining the relatively dated samples together. The same crossdating procedure is used to compare site chronologies and establish their relationship in time.

For accurate crossdating, the number of rings and the species of the samples are critical factors. There needs to be at least 70 rings on any sample for secure crossdating, unless two samples are from the same tree. Similar patterns of up to 50 years can occur randomly, and it is only with very similar patterns of length 70 years and more, that the similarity becomes unique.[13] Three statistical tests used in matching the patterns are Student's *t*-scores, trend coefficients, and Pearson

[11] Stokes and Smiley 1968; Cook and Kairiukstis 1989.
[12] A dendrochronological term for the visual and statistical analyses used to match similar ring-width patterns in two or more samples.
[13] Wilson et al., 2004.

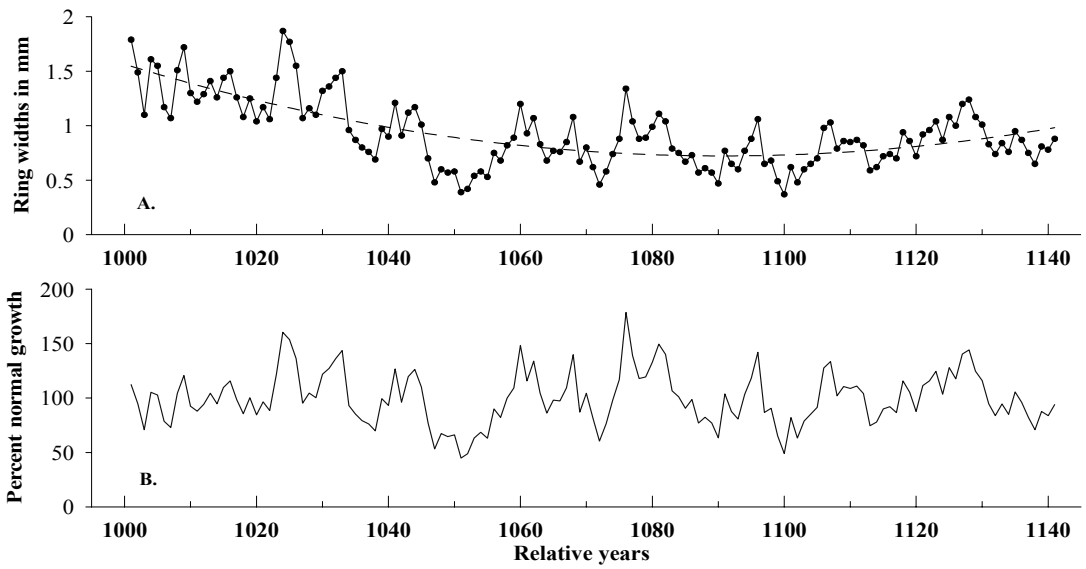

Figure 4.2. An example of detrending the ring width measurements. A. The dots indicate the original measurements assigned to their respective relative year dates and connected with the solid line. The dashed line is the curve that was fitted to them. B. The detrended data, calculated by dividing each measurement by the value of the fitted curve in the same year. This equalizes the data over time for easier visual comparison with data from the other samples.

correlation coefficients. The Student's *t*-score indicates the statistical probability of the amount of variance, both annual and long-term, that the samples have in common. The trend coefficient test counts the number of signs of the differences between year-to year ring-widths that two samples have in common relative to the shared number of rings. The correlation coefficients indicate the presence and significance of any linear relationship between two sets of ring widths.

Visual pattern recognition plus an awareness of the level of probability in the statistics are both of great importance in crossdating: statistics alone can be deceiving. Conversely, the statistics can indicate a correct date that the dendrochronologist did not consider due to a preconceived notion of when the building should date. An example of this might occur when a building has been repaired. The chronology's end

date would give the repair date, or at least a date "*terminus post quem*" (= the building date is after the end date of the sample). If this date was not expected and examined, the date given to the building could be incorrect or dating abandoned due to no good crossdating around the estimated building date.

Accurately dating a single sample will always be a problem. Many times there is a very good statistical and visual crossdate between a single sample and a chronology, but there is a much greater probability that it may be incorrect. The common signal that is contained in a chronology is generally the species' response to the same growth-limiting factor(s). Single sample measurements contain idiosyncrasies unique to the individual tree.

Crossdating between samples of the same species is valid; crossdating between different species is questionable unless it is established that two species generally have the same ring patterns due to a similar response to the same limiting growth factor by previous studies or experience. One major limiting growth factor in temperate climates is growing season precipitation, but species do respond differently, even within the growing season months, so caution must be taken. The measurements of species from different genera are never combined into one chronology for dating purposes; different species of the same genus may be combined with caution.

The end date of a chronology is not necessarily the felling date (bark date) of the trees or the building date. If there is no bark or waney edge (defined above), or sapwood in a few species, the ending date indicates only a *terminus post quem* date for both the felling and building dates. The presence of bark gives the felling date, but the building date could be the same year or a year or two later, depending on the amount of time given for the wood to dry. The presence of sapwood rings in samples of oak and a few other species allows a reasonable estimate of the felling date based on the average number of sapwood rings found in those species.

THE SITES AND THEIR CHRONOLOGIES

A. Modern Woodlands and Historical Sites

Figure 4.1 shows the sites' locations by the numbers indicated in Table 4.1. The length and placement in time of each of the modern and historical chronologies and samples are shown in Figure 4.3.

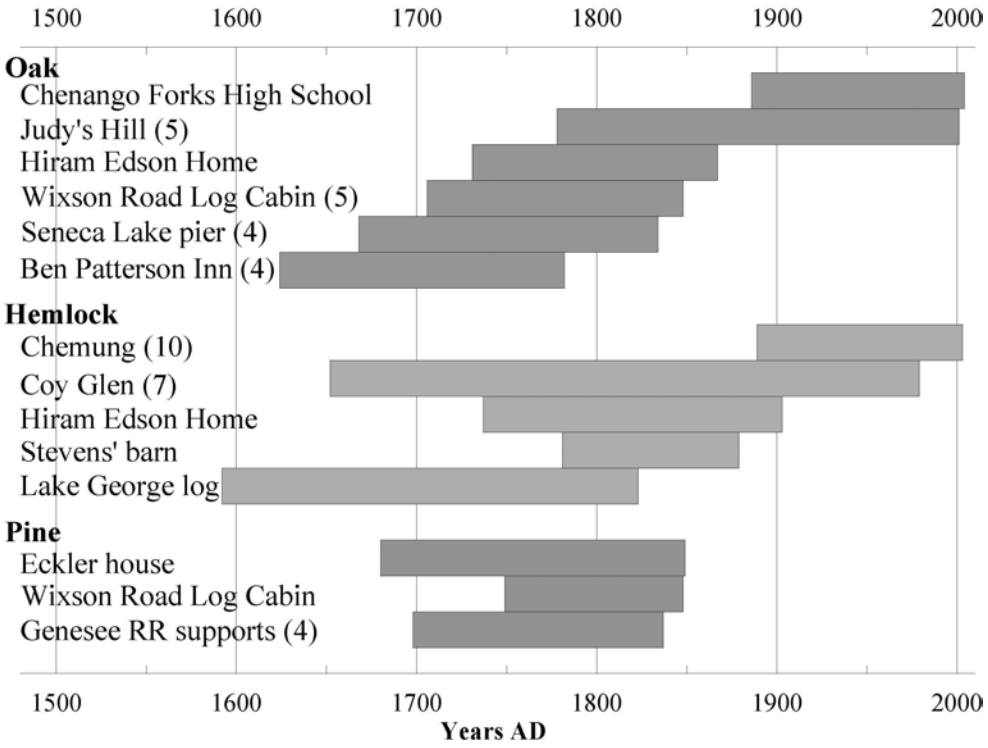

Figure 4.3. The modern and historic chronologies and samples in time. The numbers in parentheses are the numbers of samples (>1) included in the chronology indicated.

<u>Modern Woodlands</u>

Schuyler County, Hector, Judy's Hill

Oak, 5 samples *AD 1778p-2001B*

Five samples were sawn from five stumps of trees felled for commercial use. One is a white oak and the other 4 are red oak. The woodland is on the southeast face

of a glacial drumlin with a steep slope at ~ 450m elevation. The chronology contains precise historical documentation of the immediate area. A felling date of 1849-1850 for surrounding timbers is clearly marked by the large increase in ring growth in1851 due to the opening of the canopy (Figure 4A). In 1914-1915 more surrounding timbers were cut down and the 5 trees then became part of the dominant trees, with the rings on average growing 3 times wider than the earlier rings. The detrended ring widths also correlate very well with the precipitation record of June and July from Ithaca from 1888 to present.

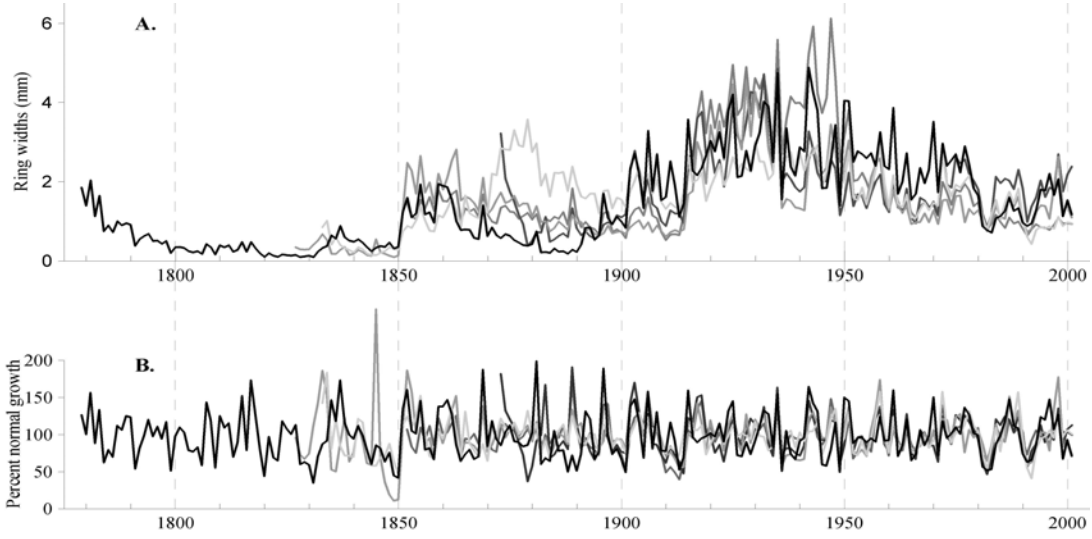

Figure 4.4. The five oak samples from Judy's Hill. **A.** The ring measurements, showing the suppression in ring growth prior to 1850 when the widths increased due to the felling of surrounding trees. In the next 60 years these trees were growing wider rings but were still sub-canopy. In 1913 surrounding trees were again cut down and these trees became the dominant canopy trees. **B.** The detrended samples.

Broome County, Chenango Forks, Chenango Forks High School

Oak, 1 sample *AD 1886p –2004+B*

Science teacher Tim Conner and his students noticed this oak's minimal leaf growth in 2003 and its death in 2004, wondered what was recorded in the ring widths,

and took this section off for an inspection. The ring widths indicate a full canopy environment with no periods of suppression or release, thus little competition, but in both 2003 and 2004 it grew very narrow rings. The wood contains no clear reason for the tree's demise. The ring measurements contain a remarkably accurate record of the June-July precipitation for Binghamton (Figure 4.5).

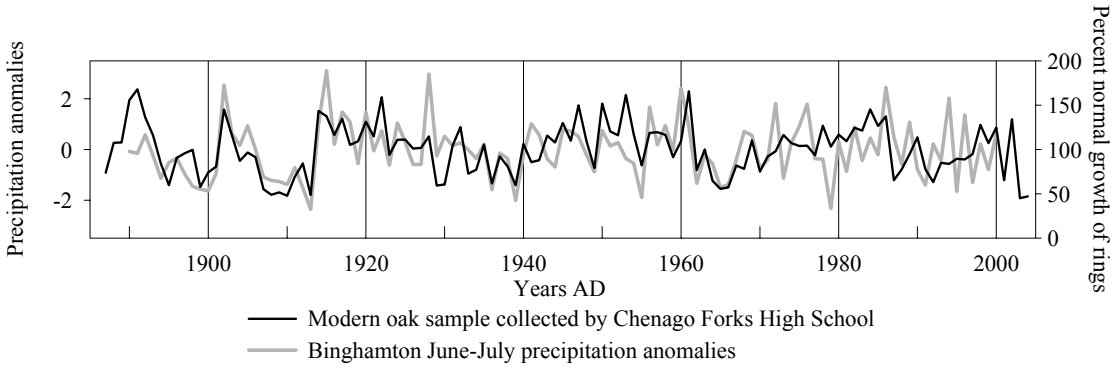

Figure 4.5. The oak sample collected from an oak on the grounds of the Chenango Forks High School, New York, that died in 2004. The ring patterns show a clear ring-growth response to the amount of precipitation in June and July from nearby Binghamton, NY. The response is clear from the late 1800s up to 1970, and then the response seems muted, similar to the climate response in other tree-ring growth patterns from around the world at the same time.

Tompkins County, Ithaca, Coy Glen

Hemlock, 6 samples *AD 1652 -1978B*

These samples were collected in 1968 and 1978 to look for any record in the tree-rings of a catastrophic flood that occurred in this glen in 1937. The 1968 samples come from 2 trees that were rooted in the nearly vertical cliff face on the glen escarpment. The “J” hook at the base of their trunks formed as the tree produced compression rings to keep its trunk in a vertical position. Their relative ring widths were very narrow for 3-5 years after 1937, opposite to those in the same years from the 1978 chronology (Figure 4.6). The 1978 samples were cored from trees with no

"J" hook, either at the top of the escarpment or growing in the talus at its base. The longest sample was cored from a log lying in the creek bed to determine whether the tree fell during that flood, but it has a bark date of 1973.

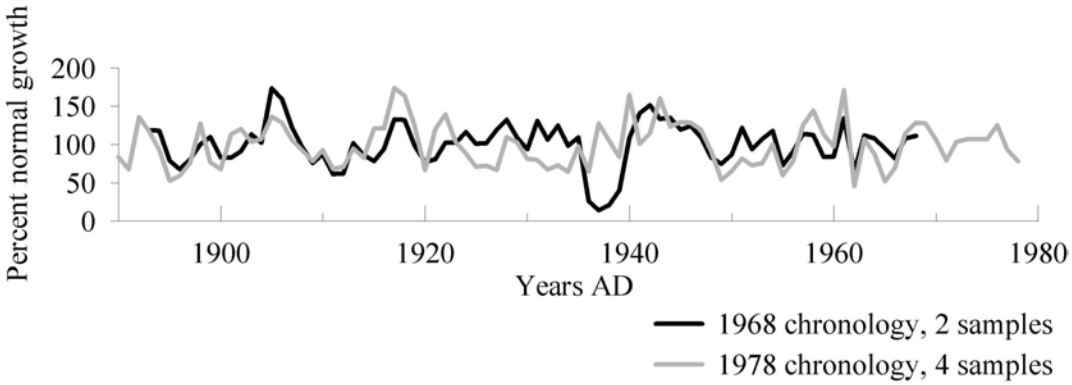

Figure 4.6. The two Coy Glen hemlock chronologies. The 1968 chronology was built with samples from trees that had been nearly toppled by a flood in 1937 in the Glen. They did not grow normal sized rings for the following 3-5 years. The complete 1978 chronology is shown in Figure 4.10.

Chemung County, Pine Valley, Chemung Mastodon site

Hemlock, 10 samples	*AD 1889 - 2003B*

Dutchess County, Hyde Park, Hyde Park Mastodon site

Pine, 11 samples	*AD 1938±p-2003B*

Wyoming County, North Java, Moffett Mastodon site

White pine (Pinus strobus), 3 samples	*AD 1956p-2003B*
Jack pine (Pinus banksiana), 3 samples	*AD 1959p-2003B*
White spruce (Picea glauca), 6 samples	*AD 1956p-2003B*

Core samples from live trees at 3 mastodon excavation sites were collected for oxygen and carbon isotope analyses.[14] The samples' short length is immaterial for that purpose, and they are securely dated only because they were taken from standing

[14] Mullins, Burnett, Anderson, and Griggs, isotope analysis in progress 2005.

trees. The Chemung site hemlock chronology crossdates well with the Coy Glen chronology (Figure 4.7) and hemlock forest chronologies from the Catskills and northern Pennsylvania.

The collections illustrate the use of tree-rings in dendroecology, the study of examining how, and to what degree, environmental stress is recorded in ring growth.

Historic sites

Steuben County, Campbell/Corning, Wixson Road Log Cabin

Oak, 6 samples	*AD 1707±p-1848+v*
Pine, 1 sample	*AD 1749 p- 1848v*

This cabin is now part of the Benjamin Patterson Inn Museum of the Corning Painted Post Historical Society, at 59 West Pulteney Street, Corning, NY, but was built in Campbell, NY, sometime in the late 1850s. None of the oak samples have bark, and there are 0-6 sapwood rings due to the removal of sapwood from cabin logs for less susceptibility to decay (Figure 4.8). This oak chronology was constructed to establish the building date for the cabin's listing on the National Historic Register, and it crossdates very well with modern chronologies from Judy's Hill and the Fire Tower site[15] northeast of Clarion, PA (Figure 4.9), ending in 1848. Thus the felling date is around AD1855-1860. The pine sample was from one of the logs just below the roof. The pine sample crossdates very well with pine chronologies from the Longfellow site, Pennsylvania, and the Catskills[16] as well as with the floorboard and railroad support beams from Houghton, NY (Figure 4.10).

[15] ITRDB, collected by E.R. Cook.
[16] E.R. Cook, ITRDB.

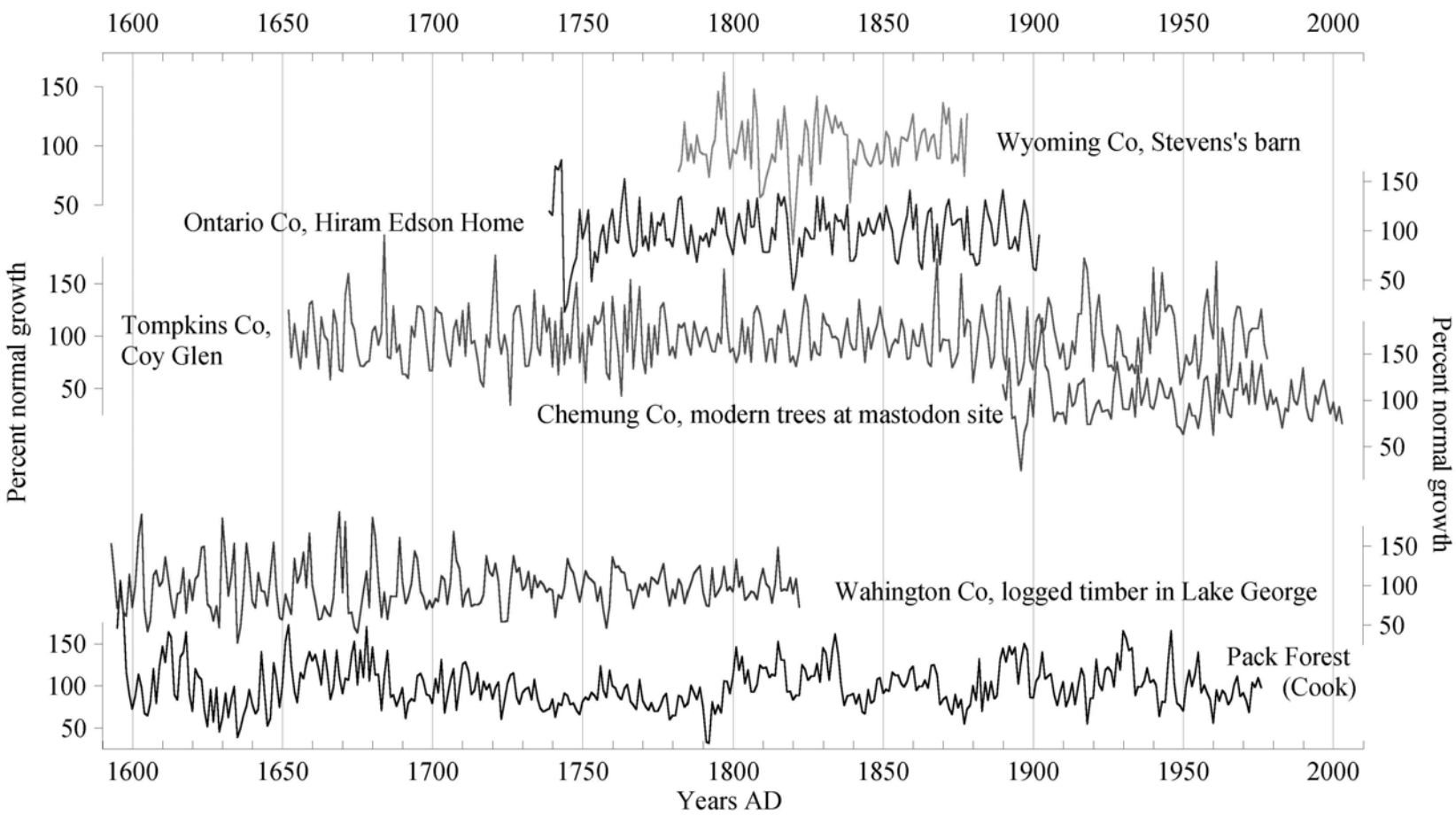

Figure 4.7. Hemlock chronologies and samples from Coy Glen, Stevens's Barn, Edson Home, Chemung site modern samples, and the Lake George log sample with the Park Forest chronology (Cook, ITRDB) for comparison.

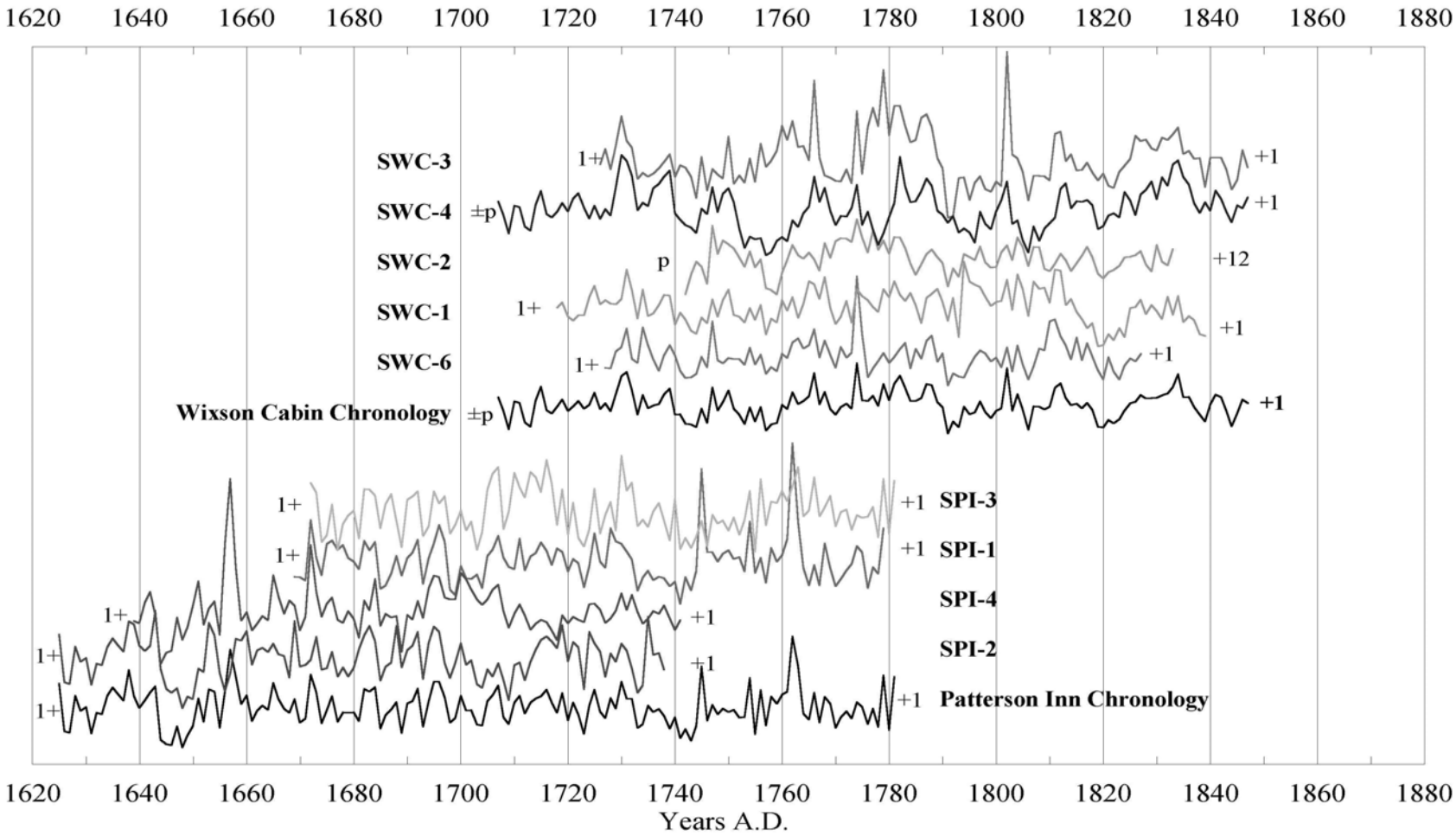

Figure 4.8. The oak samples from two Steuben County historic buildings and their chronologies

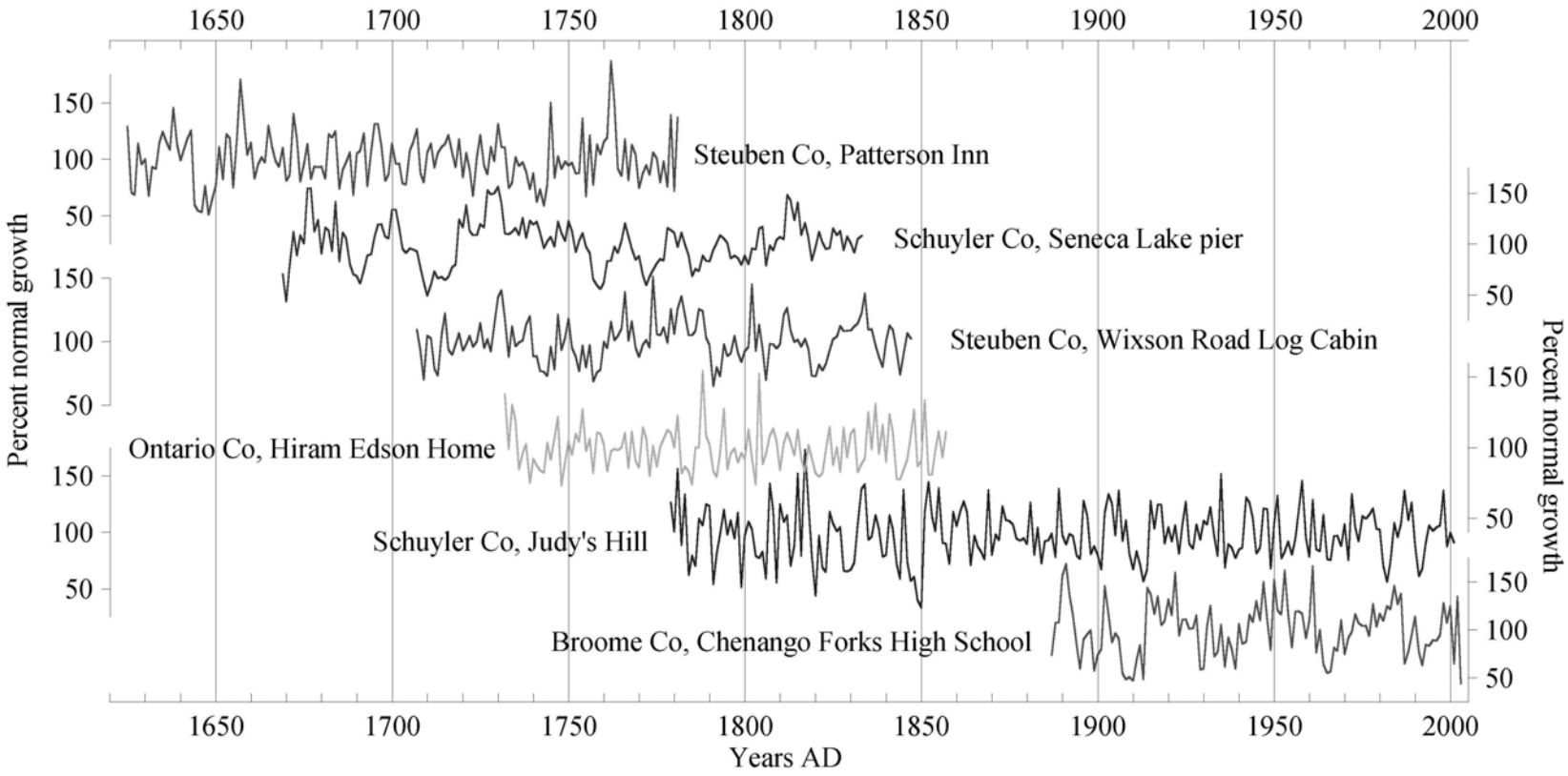

Figure 4.9. The modern and historic oak chronologies and samples. The position of the historic chronologies is determined by statistical and visual "crossdating," which involves matching patterns. These certainly do not look as similar as do the samples from one site (in Figure 4.8), but crossdating with established forest oak chronologies (Cook ITRDB) confirmed the dates shown here.

Steuben County, Corning, Benjamin Patterson Inn Museum

Oak, 4 samples *AD 1624 -1782+vv*

The Inn was built in 1796 and is well documented in the town's historical records. Four posts were cored to help establish the date of the Wixson Road Cabin (Figure 4.8). All the posts were squared with no sapwood remaining, and thus the end of this chronology is only a *terminus post quem* date. However, this chronology extends the area's oak chronology back 24 years (Figure 4.9), crossdating securely with the oak chronologies from Wixson Road log cabin and the Fire Tower site near Clarion, Pennsylvania.

Schuyler County, Hector, Seneca Lake pier posts

Oak, 3 samples *AD 1668p-1834+v*

This pier was originally built for barges transporting goods up and down Seneca Lake in the first half of the 19th century. The three oak samples have ring patterns remarkably similar to each other, but due to the ~8m length of the posts, and the closeness of their pith dates, they must be from separate trees in one grove. Their chronology significantly crossdates with the oak chronologies of Judy's Hill and Fire Tower, PA, but with a difference in ring patterns due either to different oak species or to the influence of the Finger Lakes and local topography on the variability of the climate patterns around the lakes (Figure 4.9).

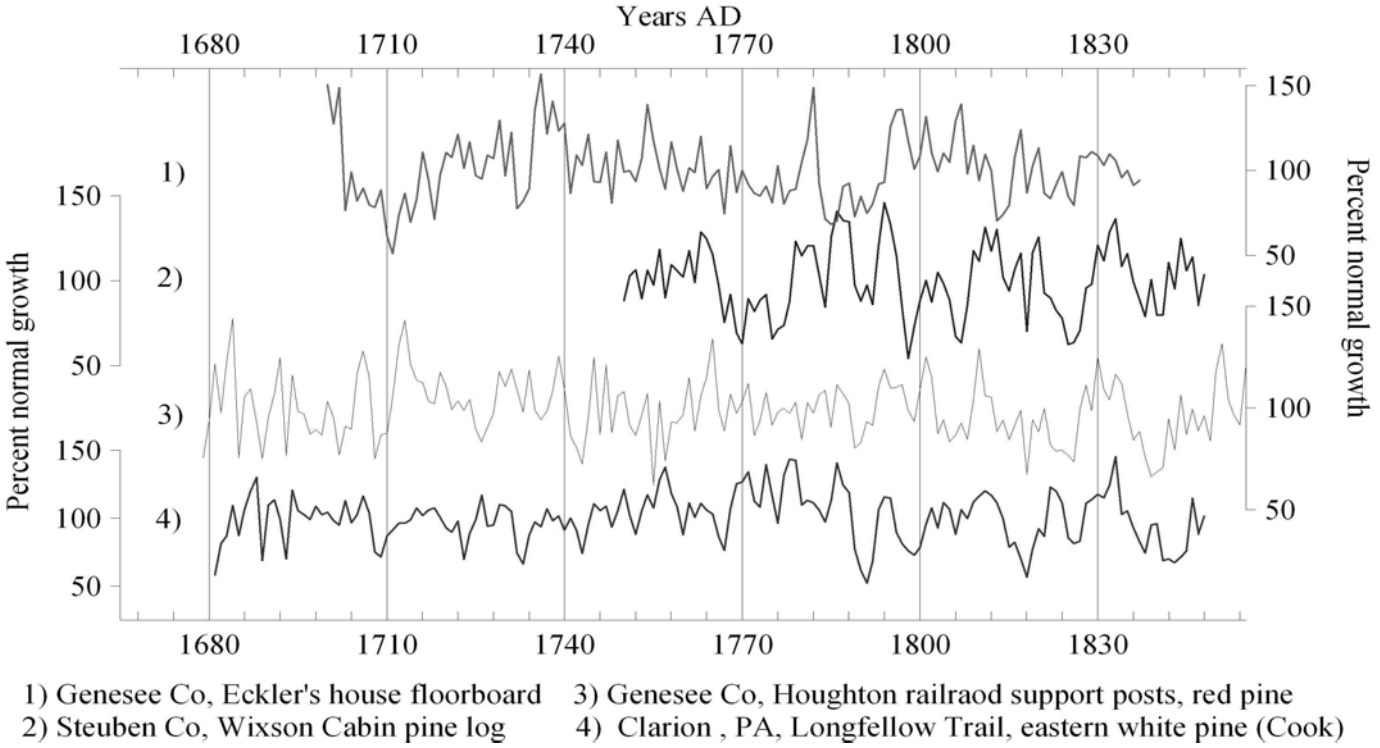

Figure 4.10. The pine chronology and samples with the Longfellow Trail chronology (Cook, ITRDB). The visual fit is a good indicator of the tentative nature of these dates. More pine samples are needed for a securer fit of the single samples.

Ontario County, Phelps, Hiram Edson Home, Adventist Heritage Site

Hemlock, attic floorboard, 1 sample *AD 1737-1903+vv*

Pine, clapboard and main floorboard, 2 samples *(AD 1816-1907+vv tentative)*

Oak, scab, 1 sample *AD 1731-1867+vv*

Elm, support beams, 2 samples

Beech, support beams, 2 samples, too few rings

Larch, first floor post and roof support beam, 2 samples

The number of species used in this building is remarkable. At least two more species, hop hornbeam and basswood, were used along with the beech in the basement beams, the earliest known part of the building. I was not able to date the initial construction due to the small ring count in the beech logs, but it is known that Edson lived on this property in the first half of the 19th century. There were at least two building repair and addition phases after initial construction. One is indicated by the end dates of the pine floorboard (1870) and oak scab (1867), and the other by the pine clapboard and hemlock floorboard end dates (1907 and 1903, respectively). The oak sample is shown in Figure 4.9 and the hemlock sample in Figure 4.7 with the other historic and modern chronologies from their respective genera. None of the dates are bark dates, and all are *terminus post quem*. The oak felling date is at least 10 years after 1867 since there are no sapwood rings included in the sample.

Wyoming County, Attica, Stevens's barn

Hemlock, 1 sample *AD 1781p-1879+v*

Pine, 1 sample with too few rings

The Stevens gave me these samples from their barn with a 1910 building date at the 2005 Preservation Conference of the Landmark Society of Western New York. The pine sample has less than 50 rings, so it cannot be dated. The hemlock sample, a

squared board 30 cm wide by 7 cm thick, securely crossdates with the modern hemlock chronologies from Coy Glen, the Catskills, and northern Pennsylvania, and the hemlock sample from the Edson Home (Figure 4.7). The end date is 31 years before the given building date, thus about 30 rings were removed if this tree was cut down in 1909-1910. However, the numbers of rings on opposite radii are only different by one year. The matching ring numbers are a good argument that very few rings were removed, since the removal of the same number of rings from each side of the pith is less probable than the use of as much of a log as possible. The cross-section of the sample shows that it is a squared section from the center of a log, possibly with only the very outer rings removed for squaring. There are three possibilities indicated by the board's end date: that the extra rings were indeed removed in the process of building in1910; that the barn, or a part of it, was originally built in the 1880s and rebuilt or expanded in 1910 with the date recorded at that point; or that this board or support plank was reused from a previous building. In any case, the rings in this sample date from AD 1781-1879, and the tree was felled sometime after 1879.

Washington County, Lake George, sent by Ron DeWitt of Ballston Spa, NY

Hemlock, 1 sample *1592p-1823+v*

This sample is from a logged hemlock that was transported down to Lake George where it got waterlogged and sank. The log contains a logger's stamped identification number. Logging was known to have occurred in the area in 1918-1919, and it was thought that this log was from those dates. However, its measurements crossdate securely with the Pack Forest hemlock chronology (43.55ºN, 73.8ºW)[17] with the partial outside ring dating to AD 1823, nearly a century earlier (Figure 4.7). There are up to 5 years' difference in the outer rings' dates around the circumference,

[17] E.R. Cook, ITRDB website.

and a few more rings may have been worn away during transport, but probably not over 10. A logging date of anywhere between 1823 and 1833 is indicated by this sample.

Allegany County, Houghton, Don and Lois Eckler's Genesee River property

Eastern white pine (Pinus strobus), squared floorboard *AD 1698±p-1837+vv*

Red pine (Pinus resinosa), 4 railroad support beams *AD 1680p –1849+W*

The extension of the Eckler's house in 2001, allowed Don to saw off the end of a floorboard for possible dating. The original building date is 1845, so the end date of the sample at 1837 is quite satisfactory as a *terminus post quem* date.

The railroad track that ran along the west riverbank of the Genesee River in Houghton was built in the mid-1800s by the Genesee Valley Railroad Company, replacing a canal used for transportation from Rochester to Olean, NY, in the early 1800s.[18] Of the 4 samples from the railroad support beams, two are from the same tree and have an end date of 1821 with no bark or waney edge. The other two both end in 1849 with waney edges, and indicate the date of their felling for the building of the railroad at that location. The species is red pine, *Pinus resinosa*, identifiable by its very strong smell, which gives the wood good resistance to insect and fungal infections and decomposition. Creosote was not used until 1865.[19] The pine railroad beam chronology crossdates securely with pine chronologies from northern Pennsylvania[20] (Figure 4.10).

[18] See website http://www.letchworthparkhistory.com/gvcanal.html. The railroad company was eventually bought out by the Western New York and Pennsylvania Railroad Company.
[19] D.A. Webb, no date, http://www.rta.org/pdf/sec4.PDF
[20] E.R. Cook, ITRDB.

The pine of the floorboard and the pine sample of the Wixson Road Log Cabin (discussed above) are *Pinus stobus*, white pine. The floorboard sample does not crossdate well with the RR chronology, but it does securely crossdate with the Wixson Cabin sample and the Longfellow Trail pine chronology (Figure 4.10).

Regional Chronologies of the Modern and Historic Sites

The dates indicated below do not include the dates of the partial rings added on to the site chronologies above.

Oak (*Quercus* spp. L.) N=380 AD 1625 to 2004

Composed of the 4 chronologies from Judy's Hill, Wixson Road Log Cabin, Ben Patterson Inn, and the Seneca Lake pier, and one sample each from the Chenango Forks High School and the Hiram Edson Building. Twenty samples total.

Eastern hemlock (*Tsuga canadensis)* N=411 AD 1593 to 2003

Includes modern and historic chronologies from the Gilbert mastodon site, Coy Glen, and 1 sample each from Steven's barn, Lake George, and the Hiram Edson Building. Twenty samples total.

Pine (*Pinus* spp.) – tentative only N=168 AD 1681 to 1848

The historic chronology is composed of the Houghton railroad beam chronology plus the two samples from the Eckler's house and the Wixson Road Log Cabin, six samples total. This is currently only a tentative regional chronology due to the low number of samples and the problems with crossdating different pine species. This problem is evident in Figure 4.10, but the averaging of the three data sets

enhances the regional pine chronology's crossdating with the Longfellow pine chronology. More samples are needed for splitting up the pines by species into at least two chronologies for the secure dating of other pine samples.

B. Subfossil Wood Sites

The chronologies developed from the sites below (also in Table 4.1) are all floating chronologies, some dated with calibrated radiocarbon dates which give a calibrated date with one standard deviation of ±*n* years. The dates below are given in both calibrated years BP and the corresponding BC/AD years (0 Cal BP = AD 1950). Figure 4.11 shows the placement in time of the dated chronologies and samples and Table 4.2 lists the radiocarbon dates. Table 4.3 lists the chronologies that have yet to be dated plus the dates that each species migrated back into New York State following the retreat of the Laurentide ice sheet, beginning ~16,000-17,000 years ago.

For radiocarbon dating, selected samples are generally part of a floating chronology, or from a structure or excavation stratum whose absolute date is of particular importance (an absolute date has an error range of ±*n* years indicating the 1-sigma level of the accuracy in the radiocarbon date). Segments are taken from each selected sample that have known ring placement in the chronology (*e.g.* the 11th to 20th rings in the sample). The number of rings included in the segments varies depending on the widths of the included rings and the size of the sample. Radiocarbon dates are measured by the ratio of the amount of radioactive to non-radioactive carbon in the segment, which indicates how much radioactive decay has occurred in the wood.[21] That measurement is converted to how many radiocarbon years have passed since

[21] A ring contains the ratio of the carbon isotopes (^{14}C, ^{13}C, and ^{12}C) that is in the atmosphere in its growth year. After the growth year the 14-carbon atoms decay into 14-nitrogen atoms over time, and the amounts of ^{13}C and ^{12}C remain the same. Thus the current amount of the ^{14}C in a sample relative to the sample's total carbon weight indicates how long ago that ring was formed. The half-life of ^{14}C is 5,730 ±40 years. Bradley 1999.

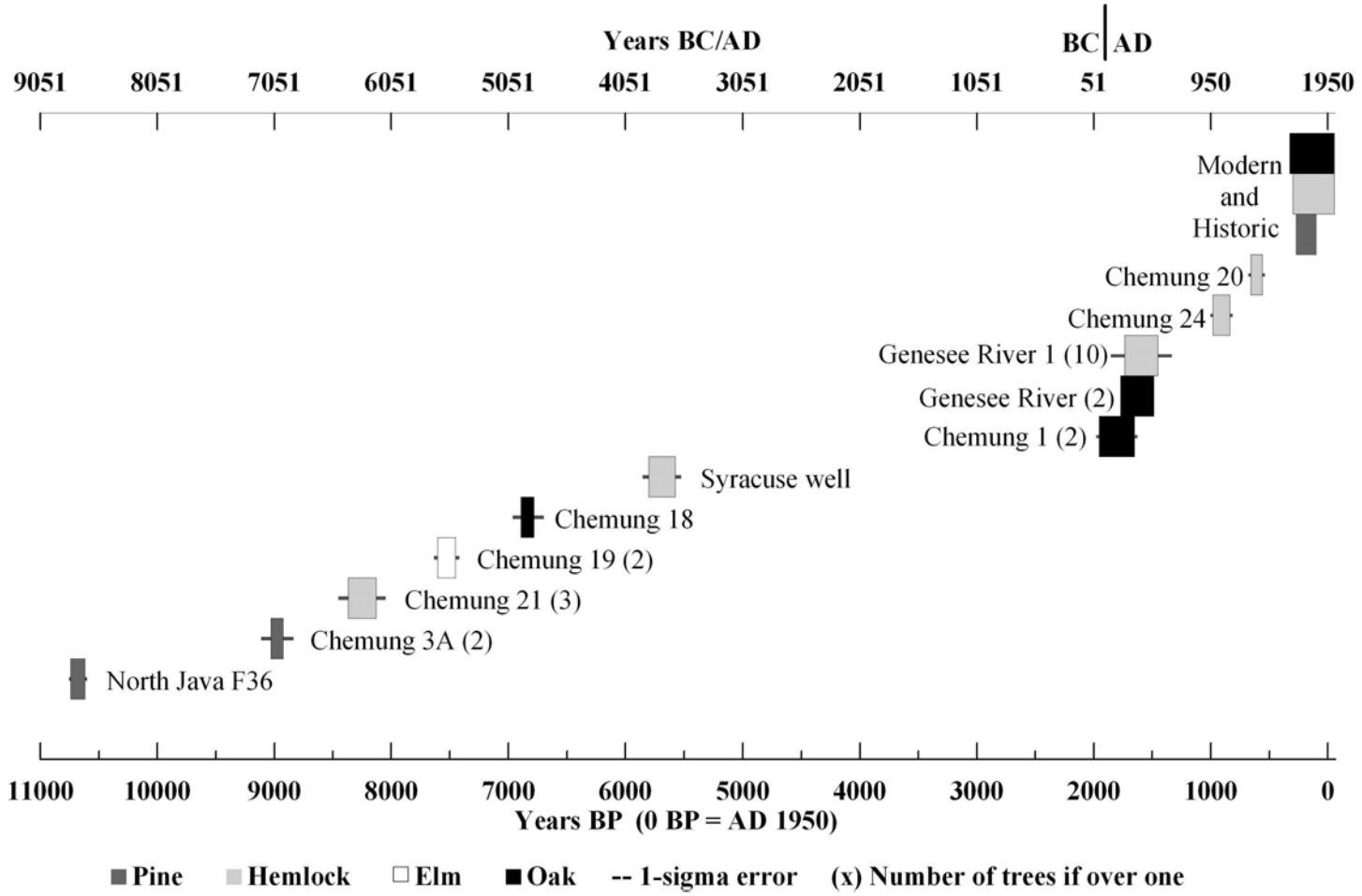

Figure 4.11. The placement of the Holocene subfossil samples and chronologies that have been radiocarbon-dated, or that crossdate with samples that are radiocarbon-dated. The error bars indicate tha range that the dates may represent and the width of the bars is the length of the sample or chronology.

Table 4.2. The radiocarbon dates of selected subfossil wood samples. The calibrated years are also indicated by the samples' location on the timescale in Figure 11, except for the HTN-1 sample, positioned 80 years earlier due to its crossdating with more securely dated samples (see text). Hd = Heidelberg Laboratory, AA= Arizona AMS Laboratory, and Beta = Beta Analytic Laboratory.

Lab and Analysis No	Site-Sample No.	Genus	First ring	Last ring	C14 Age	ΔC13	Calibrated Dates
Hd-22775	NY-WMM-F36	*Pinus*	pith	9	9509±29	-26.73	8791-8672 ±15 BC
Hd-22772	NY-WMM-F36	*Pinus*	110	119	9367±23	-24.15	
Hd-21416	NY-CHE-3A	*Pinus*	84	103	8028±60	-24.23	7079-6975 ±85 BC
Hd-21418	NY-CHE-21	*Tsuga*	25	44	7388±51	-25.38	6325-6181 ±80 BC
Hd-21413	NY-CHE-19	*Ulmus*	1	20	6729±40	-25.96	5656-5502 ±30 BC
Hd-21420	NY-CHE-18	*Quercus*	68	77	5993±56	-26.78	4943-4831 ±80 BC
AA-3810	NY-OKS-1	*Tsuga*	unknown		4958±47	-25.00	3851-3629 ±50 BC
Hd-20752	NY-CHE-1	*Quercus*	81	90	1929±30	-26.34	6 BC- 296 ±25 AD
Hd-20754	NY-CHE-1	*Quercus*	268	277	1726±24	-24.83	
Beta-52528	NY-HTN-1	*Tsuga*	unknown		1510±50	-25.00	394-580 ±105 AD
Hd-21396	NY-CHE-24	*Tsuga*	21	40	1059±24	-25.02	966-1110 ±21 AD
Hd-21414	NY-CHE-20	*Tsuga*	61	95	635±28	-26.07	1291-1387 ±20 AD

Table 4.3. The floating chronologies of wood samples from the subfossil sites that are still to be radiocarbon-dated.

Floating Chronologies	Length
Hemlock	
Wyoming Co, Moffett site	
WMM-11,F10,G2,G8	233
WMM-2, G13, B16	156
WMM-G1 and 37	162
WMM-3 and 8	195
WMM-15,45,G12	129
WMM-F26,F31,F34, 25	134
WMM-10 and G30	127
Chemung & Tompkins Cos., Chemung and Michigan Hollow sites	
CHE-3D, 12, 36, 41, and MHR-6	236
Pine	
Chemung Co, Gilbert site	
CHE 5-8-10	171
Elm	
Wyoming Co, Moffett site	
WMM-29&43&44 and 28	184
WMM-G17, G25	122
WMM-6&F25, F3, F4, F7, G26, G27&G28,G31	325
Chemung Co, Gilbert site	
CHE-14&42 and 31	118
Ash	
Wyoming Co, Moffett site	
WMM-F2&F6&42, F1	150
WMM-F11, 36	114
WMM-G16,F16	196
WMM-G14, 5	130

those rings were formed. The radiocarbon age ±error from each segment are calibrated via a current calibration curve[22] (Figure 4.12A) that adjusts the radiocarbon age by variations in the amount of ^{14}C in the atmosphere over time. The relative date of each segment's middle ring in the floating chronology is then assigned the

[22] INTCAL 2004 used here for calibrating the radiocarbon dates.

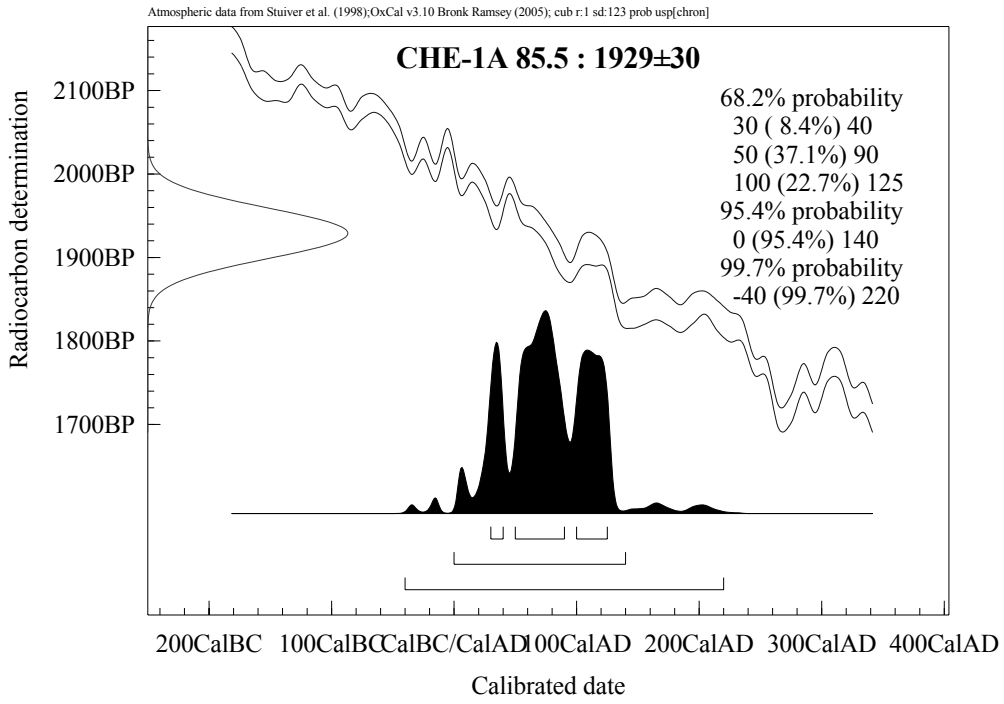

A.

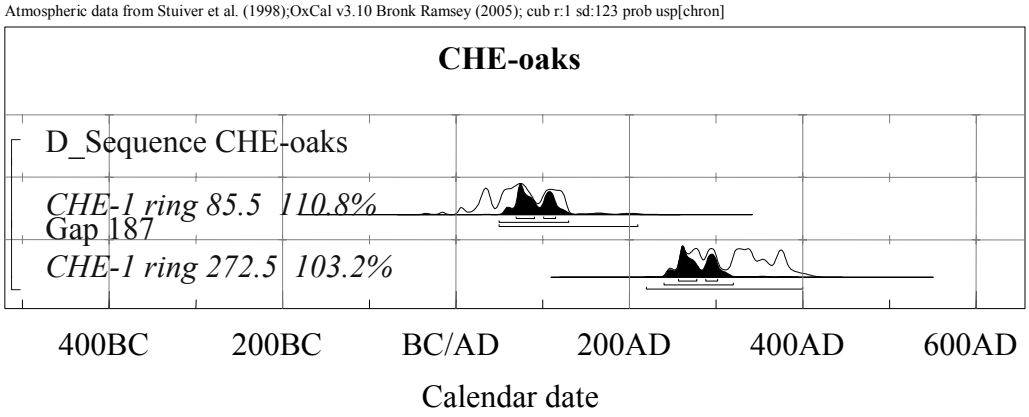

B.

Figure 4.12. **A.** The calibration of one radiocarbon value provides the calibrated ranges of dates for ring 86 at various levels of probability (68.2% = ±1 standard deviation, 95.4% = ±2 standard deviations, *etc.*). The 95.4% range gives the value AD 70 ±70 years, which is a very wide range of dates for a wood segment that only contains 10 rings. **B.** With the addition of another radiocarbon date from a segment whose center ring is ring 273, and knowing that there is a gap of 187 rings between the centers of the two segments (= 273-86), the spread of the possible calibrated dates for this sample is reduced to the darkened areas to the right of each segment's name. The most probable date for ring 86 is now AD 80 ±11 years at the 1-sigma level, with a smaller chance that it might be at AD 108 ±7 years.

calibrated date and the rest of the relative years are converted to the appropriate calibrated dates. If more than one segment from a floating chronology is radiocarbon-dated, then a "wiggle-match" is used for a more accurate date. The "wiggle" is composed of the radiocarbon ages assigned to the center rings of the measured segments plus the known number of rings between those center rings. This string of data allows a closer match to the wiggles in the calibration curve (Figure 4.12B), thus a more precise date with a lower value of ±*n* years. Of the subfossil wood chronologies, currently only two chronologies have more than one radiocarbon date, and those are the two chronologies with error values of less than 20 years (Table 4.2). The other calibrated error values range from ±40 to ±150 years.

Allegany County, Houghton, Don and Lois Eckler, Genesee Riverbed

Hemlock, 10 samples	*1739p- 1453B±105 Cal BP*	*AD 211-497±105*
Oak, 2 samples	*1773p- 1487vv±25 Cal BP*	*AD 177-463±25*

Over the last 20 years, the relatively flat level of alluvial sediments that the Eckler's house sits on, about 8m above the current riverbed, has been rapidly reducing in size from over two acres to about one acre by the undercutting of a meander in the Genesee River. Over this period, the Ecklers noticed logs being uncovered in the riverbed. The ten sampled hemlocks died within seven years of each other, probably due to another undercut from a similar meander causing the collapse that laid the trees across the river about 1500 years ago. They do not appear to have been transported at all, but the branches and most of the bark were worn off due to the water action. Their ring patterns indicate that there had been a few years of declining growth, then two hemlocks died in AD 490±105, probably upon their fall into the river. After the fall, the other eight hemlocks continued to grow with wider ring widths due to a release in competition before they also died in the next two to seven years.

One of the oaks and an underlying beech log probably died a decade or so earlier. The oak chronology matches very well with the hemlock chronology, with its last existing sapwood ring 27 years before that of the earliest bark date of the hemlocks. Three sapwood rings are still present on one small section of the oak's circumference, indicating that the actual end date of the tree's life is most probably from 10 to 20 years before the first hemlocks died. Thirty sapwood rings would be needed for the oak to have fallen at the same time as the first hemlocks, and thirty is high for the 10-20 sapwood ring count found in most oaks collected in the area. The oak and perhaps the beech may have fallen first, perhaps beginning a continuing saga of the collapse of and undercut riverbank over the next 20 to 40 years. The excellent preservation of the wood indicates that at some point in time, probably not very long after all these trees were felled, a major deposition occurred that buried the logs, perhaps from a local slump or from the transport of a large volume of sediment from upstream. This deposit could have been the cause of the death of the last few trees in this chronology. The approximately 8m of alluvial sediment above the logs is a mute testament to the continuing deposition of sediments in the river valley in the last 1500 years.

The ring measurements of another oak log, downstream and below the level of the other logs, possibly crossdates with the later oak sample but only with an overlap of 43 rings. The oak chronology crossdates tentatively with the Chemung Site's oak chronology (discussed below), and that is from where the radiocarbon date is assigned to this chronology. This site's oak chronology also crossdates well with its hemlock chronology, especially in the more mature years of hemlock ring growth, and we have also dated the hemlock chronology according to the oak chronologies' date, and that date is within the hemlock radiocarbon date's calibration error of ±105.

Chemung, Pine City, Gilbert Mastodon site, post-mastodon layers

Hemlock, 1 sample	*659p- 563vv ±20 Cal BP*	*AD 1291-1387±20*
Hemlock, 1 sample	*984p- 840vv ±21 Cal BP*	*AD 966-1110±21*
Oak, 2 samples	*1956p-1654+W ±25 Cal BP*	*6 BC - AD 296±25*
Oak, 1 sample	*6893p-6781B ±80 Cal BP*	*4943-4831 ± 80 BC*
Elm, 2 samples	*7606 -7452v ±80 Cal BP*	*5656-5502 ± 80 BC*
Hemlock, 2 samples	*8371p-8131vv ±80 Cal BP*	*6436-6197 ±150 BC*
Pine, 2 samples	*9029p-8925vv±85 Cal BP*	*7079-6975 ± 85 BC*

The amount and quality of well-preserved wood and other plant macrofossils in the sediment of this kettle pond at the time of excavation are of particular note. The needles appeared to have just fallen from a tree, were still a vibrant green color, and the wood contained tints of dark red and gold. All the vibrant colors faded within an hour of its exposure to air. Six large logs of around 0.5m in diameter were uncovered in the sediment above the mastodon level and thus from a post-mastodon date. Sections of were chain-sawed from all of them for dendrochronological analysis and radiocarbon dates for that layer. The mastodon level was composed mainly of mastodon dung, other organic material, and some gravel, and was approximately one to two meters deep and directly above a cobbled gravel layer and, below that, the glacial clay. Here wood segments were rarely over 0.2 m in diameter, and most were of branches less than 0.1 m in diameter. Bioturbation was evident from the small hemlock, elm, and early oak samples found down in the mastodon matrix, some in close proximity to the mastodon bone, because all those species migrated into the area at least one thousand years after the mastodons had become extinct.[23] Of the hundreds of wood samples collected from the matrix, 36 samples have enough rings for dendrochronological analysis, and 33 of them are of Holocene species. Of the total 39

[23] Jacobson et al., 1987; Webb 1993.

Holocene samples, seven were chosen for radiocarbon dates (Table 4.2), depending on their species, level, and relationship to the mastodon bones at the site. Included are one of the two oak logs found above the mastodon level, one each of elm and oak segments found within the matrix, and one pine and three hemlock segments found directly with the mastodon bones. Of the three hemlock samples, one is from ~2,000 years after the mastodon bone date, and the other two from over 9,000 years post-mastodon. The elm sample was taken from a large segment lying vertically but upside-down with a branching 'Y" sticking down into the clay. Its position was probably the result of a dead tree breaking up and this segment falling from enough height to give it the force to penetrate down through the matrix and into the glacial clay.

Table 4.3 lists the floating chronologies built of Holocene samples that have yet to be dated. Included are 3 chronologies built of samples from this site, one each of hemlock, pine, and elm. The floating hemlock chronology also crossdates securely with one hemlock sample from the Michigan Hollow site.

Onondaga County, Syracuse, well dug at south end of Onondaga Lake

Hemlock, 1 sample *5801p-5579++Cal BP ±50* *3851-3629 ±50 BC*

This wood was found at about 10m depth in a well being dug in the salt flats at the south end of Onondaga Lake. It was collected by, and radiocarbon dated for, William Kappel of the United States Geological Service. This hemlock's date is of particular interest since the hemlock population declined around 5460±150 Cal BP according to pollen records.[24] The decline is thought to be due to a disease specific to hemlock[25] and/or a dryer climate phase beginning at that time, since hemlocks grow best in a cool and moist environment.[26]

[24] Webb et al., 1993.
[25] Davis 1981; Bennett and Fuller 2002.
[26] Harlow and Harrar 1979.

Chemung, Horseheads, Bowman's Quarry, edge of current pond

Oak, 1 sample *N = p+130vv* *Unknown date*

This quarry has great potential for future collection. It is located to the south of the Valley Heads Moraine. In the 1970s a geological advisor to the owner of the quarry wrote an article about how the excavation was halted in at least one direction by extensive amounts of cedar buried at a certain level that was hard for the equipment to dig through.[27] I doubt that the wood is cedar[28] but need to have a sample for species identification. Collection of at least some of this wood may enable me to build a chronology that dates back to the first onset of the ice sheet at that site.[29]

Tioga, Berkshire, David Rabenstein's farm on Wilson Creek

Hemlock, 6 samples, with no secure crossdating *Maximum ring count = 211*

Tompkins, Danby, Michigan Hollow Creek bed

Hemlock, 5 samples *Maximum ring count = 116*

These two sets of mainly hemlock samples were collected from two creek beds at approximately the same latitude, both in the Valley Heads Moraine and draining to the south. Wilson Creek lies in a wider alluvial plain than the Michigan Hollow Creek. One of the Michigan Hollow samples securely crossdates with one of the Chemung site's floating hemlock chronology.

---

[27] Chiment, personal communication 2001.

[28] The comment that subfossil wood is cedar occurs quite often. I find that the comment is generally due to a reddish color in the wood, in most cases a result of the composition of the deposited mineral sediments and the amount of time since the wood was deposited. In an aquatic environment leaching of the minerals occurs with the onset of fossilization (mineral replacement) over time. Cedar has been found only at two of the subfossil wood sites, and only with small ring counts.

[29] Luckman 1996.

Dutchess County, Hyde Park, Lozier mastodon site

Oak, 1 sample *N=182*

Here the mastodon was found in a small oxbow pond that was originally a meander of the nearby Fall Kill (creek). Very few wood subfossils were found due to the higher stream flow of the creek and the relative low topography of the area. This oak sample is the only Holocene sample with sufficient ring count for analysis and was found in a stratum of the pond sediment above the mastodon layer. It does not currently crossdate with any other subfossil wood oak chronology in the area.

Wyoming County, North Java, Moffett mastodon site

Pine, 1 sample	*10,740p-10,621vv±15 Cal BP*	*8790p-8671vv±15 BC*
Hemlock, 45 samples	*7 floating chronologies, maximum length =235 rings*	
Elm, 31 samples	*3 floating chronologies, maximum length =324 rings*	
Ash, 28 samples	*4 floating chronologies, max length = 196 rings*	
Beech and maple, 13 samples	*Currently not measured*	

The excavation of the sediment from this pond was almost completely finished before we were notified about the mastodon bones. The wood was collected as part of a recovery from the excavated sediment mounds around the pond. Only the pine log was still *in situ* when sampled. All of the wood has been preserved remarkably well by the pond's highly alkalinic sediment. Of the 153 samples collected for dendrochronology, 34 are of samples of the Late Pleistocene cooler climate species, including spruce and larch and are discussed elsewhere.[30] One sample of pine plus approximately equal amounts of hemlock, elm, and ash, make up the bulk of the rest of the samples. Forty-five samples are of hemlock, and of those, 39 have been measured and six have too few rings. Seven chronologies have been constructed as

[30] Griggs and Kromer 2006 in review.

listed in Table 4.3, and one example is shown in Figure 4.13A. At least two species of elm (*Ulmus americana* L. and *U. rubra* Mühl. and/or *U. thomasii* Sarg.) are represented here, and also two species of ash (*Fraxinus nigra* Marsh. and *F. americana* L.). Four elm and three ash floating chronologies have been built (Table 4.3). Figure 4.13B and C show examples of each of the species' chronologies.

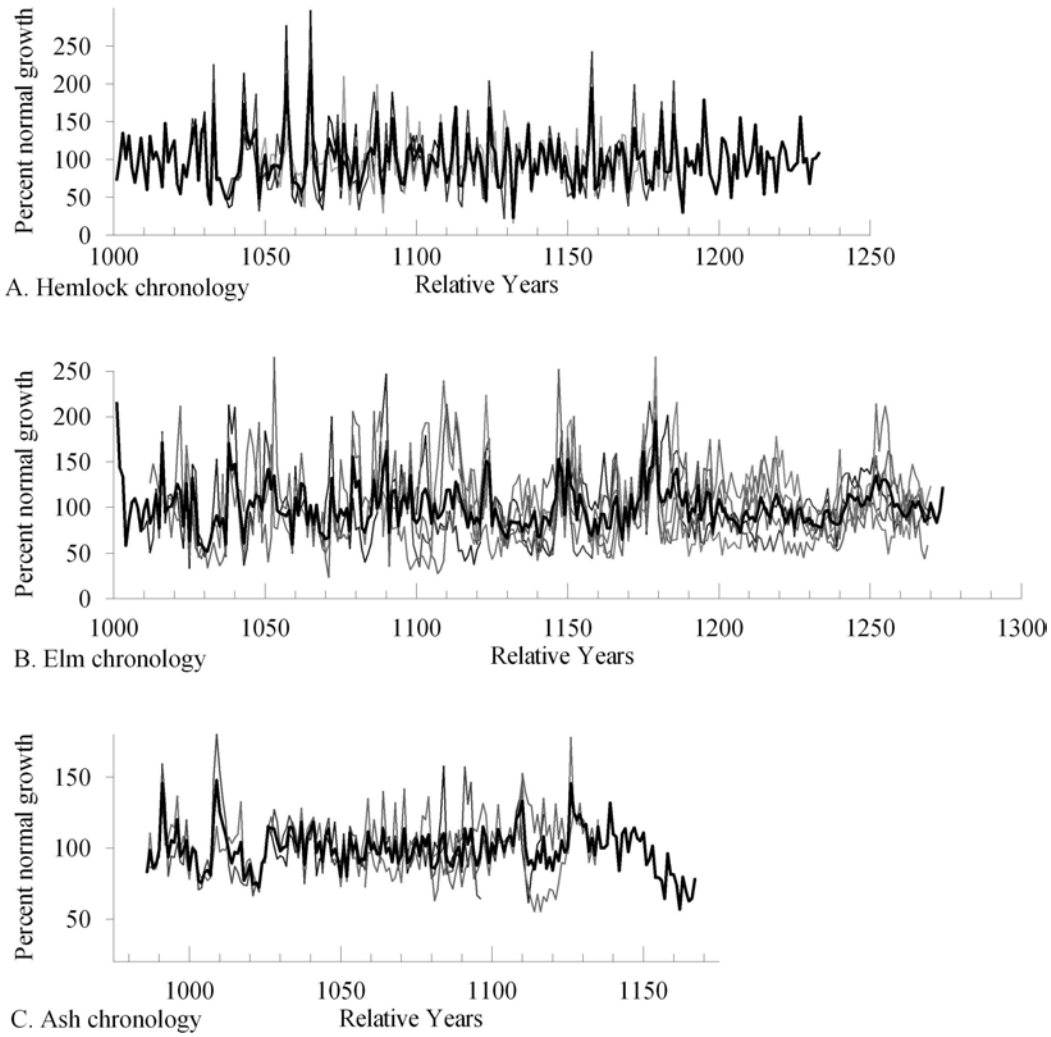

Figure 4.13. Examples of chronologies of subfossil wood from the three genera indicated. All samples have still to be radiocarbon-dated.

The pine sample has been radiocarbon-dated (Table 4.2 and Figure 4.11). Dates are needed for the floating chronologies. This will further illustrate the species' migration into western New York plus any changes in climate over time.

CONCLUSIONS

The results of matching historic tree-ring chronologies with the modern forest chronologies in upstate New York show that oak and hemlock chronologies both crossdate well throughout the region, and that any buildings constructed from local wood with over 50 rings are datable to at least a *terminus post quem* date. More pine samples need to be collected for species-specific, robust chronologies. Ash and elm and the other species of small sample numbers also need future research and the establishment of a modern chronology.

The chronology construction and exploratory climate analyses of the New York State wood samples indicate that long-term changes in the environment over the Holocene period in New York State are recorded in the species represented and possibly in their tree-ring patterns. The samples and their chronologies are a complement to the pollen record,[31] allowing a glimpse in many windows of time back over the last 11,000 years and extending back into the Pleistocene with the mastodon site samples. Pleistocene through Holocene wood is present in New York State, waiting to be collected for an accurate reconstruction of past climates and environments for a better assessment of today's climate change and the future.

[31] Jackson et al., 1997.

REFERENCES

Bennett, K. D., and J. L. Fuller. 2002. Determining the age of the mid-Holocene *Tsuga canadensis* (hemlock) decline, eastern North America. *The Holocene* 12(4): 421-429.

Bradley, R. S. 1995. *Paleoclimatology*, 2nd ed. (International Geophysics Series, Vol. 68.) San Diego: Academic Press.

Buckley, B. M., R. J. S. Wilson, P. E. Kelly, D. E. Larson, and E. R. Cook. 2004. Inferred summer precipitation for southern Ontario back to AD 610, as reconstructed from ring widths of *Thuja occidentalis. Canadian Journal of Forest Research* 34:2541-2553.

Burnett, A. W., M. E. Kirby, H. T. Mullins, and W. P. Patterson. 2003. Increasing Great Lake–Effect Snowfall during the Twentieth Century: A Regional Response to Global Warming? *Journal of Climate* 16: 3535-3542.

Cook, E. R., and G. C. Jacoby Jr. 1977. Tree-ring–drought relationship in the Hudson Valley, New York. *Science* 198:399-401.

Cook, E. R., and G. C. Jacoby Jr. 1979. Evidence for quasi-periodic July drought in the Hudson Valley, New York. *Nature* 282:390-392.

Cook, E. R., and L. A. Kairiukstis, eds. 1990. *Methods of Dendrochronology*. Dordrecht: Kluwer Academic Publishers.

Davis, M. B. 981. Outbreaks of forest pathogens in Quaternary history. *Proceedings of the IV International Palynological Conference* (Lucknow, India, 1976-77) 3: 216-228.

Davis, M. B. 1993. Holocene vegetational history of the eastern United States. In *Late-Quaternary Environments of the United States*, Volume 2: The Holocene, ed. H. E. Wright, 166-181. University of Minnesota Press.

Griggs, C. B., and B. Kromer. In review 2006. Wood macrofossils from three mastodon sites in Upstate New York: a preliminary report. *Palaeontographica Americana.*

Harlow, W. M., E. S. Harrar, and F. M. White. 1979. Textbook of Dendrology, 6th Ed. New York: McGraw-Hill.

Jackson, S. T., J. T. Overpeck, T. Webb III, S. E. Keattch, and K. H. Anderson. 1997. Mapped plant-macrofossil and pollen records of Late Quaternary vegetation change in eastern North America. *Quaternary Science Reviews* 16:1-70.

Larson, D. W., and P. E. Kelly. 1991. The extent of old-growth *Thuja occidentalis* on cliffs of the Niagara Escarpment. *Canadian Journal of Botany* 69:1628-1636.

Luckman, B. 1996. Reconciling the glacial and dendrochronological records for the last millennium in the Canadian Rockies. In *Climatic Variations and Forcing Mechanisms of the Last 2000 Years,* eds. P. D. Jones, R. S. Bradley, and J. Jouzel, 85-108. Proceedings of the NATO Advanced Research Workshop, Il Ciocco, Italy, October 3-7, 1994 (NATO ASI Series I: Global Environmental Change, vol 41) Berlin, Heidelberg: Springer-Verlag.

Kelly, P. E., and D. W. Larson. 1997. Dendroecological analysis of the population dynamics of an old-growth forest on cliff-faces of the Niagara Escarpment, *Canadian Journal of Ecology* 85:467-478.

Panshin, A. J., and C. de Zeeuw. 1970. *Textbook of Wood Technology,* Vol. 1, 3rd ed. New York: McGraw-Hill.

Stokes, M. A., and T. L. Smiley. 1968. *An Introduction to Tree-ring Dating.* Chicago: University of Chicago Press.

Webb, T., III, P. J. Bartlein, S. P. Harrison, and K. H. Anderson. 1993. Vegetation, lake levels, and climate in eastern North America for the past 18,000 years. In *Global Climates Since the Last Glacial Maximum,* eds. H. E. Wright, et al., 415-467. Minneapolis: University of Minnesota Press.

Wilson, R. J. S., J. Esper, and B. H. Luckman. 2004. Utilising historical tree-ring data for dendroclimatology: A case study from the Bavarian Forest, Germany. *Dendrochronologia* 21(2): 53-68.

Yarnal, B. 1994. *Synoptic Climatology in Environmental Analysis: A Primer*. New York: Wiley.